JNC TJ7400 2003-007

東濃地域を対象とした地球化学モデルの構築

（核燃料サイクル開発機構　契約業務報告書）

2003年3月

三菱商事株式会社

〒319-1184 茨城県那珂郡東海村村松 4 番地 49
核燃料サイクル開発機構
技術展開部 技術協力課
電話：029-282-1122
ファックス：029-282-7980
電子メール：jserv@jnc.go.jp

東濃地域を対象とした地球化学モデルの構築

要旨

Randolph C. Arthur※

本報告書は，平成14年度に実施された地下水の地球化学モデル構築に関する研究成果をまとめたものである。核燃料サイクル開発機構 東濃地科学センターでは，これまでに取得した瑞浪層群および基盤の花崗岩中の地下水の化学データを用いて，地下水の地球化学概念モデルを構築している。このモデルは，岩盤中における化学反応を解釈する上で有用なモデルではあるが，地下水流動と水－岩石反応の現象を両方組み合わせた理解の観点では十分とは言えない。そのため，地下水中の化学反応を正確に表現できる地球化学モデルの構築を目的として，本業務では，以下の３項目について検討を行った。

・東濃地域における既往分析データの品質の評価

・地下水の地球化学特性の把握

・Eh と pH およびCO_2分圧などの相関性

地下水の既往分析データは，採水法・試料保存方法・分析方法や，試錐孔掘削・水理試験・採水機器に起因する問題等によって，原位置の地下水を代表していない可能性があり，品質の評価を行う必要がある。陽イオンの総量と陰イオンの総量を用いたチャージバランスの計算は，分析データの品質評価を行う上で重要な指標となる。多くの試料はチャージバランスのずれが，0±5 %の許容範囲内にあるが，この範囲を超えている試料もある。この理由としては，以下の３つが考えられる。

①分析誤差（特にアルカリ度）

②保存・分析中に試料中のCO_2が増減することによる無機炭素濃度の変化

③硫化物イオンなどがアルカリ度に与える影響

地下水はトリリニアダイヤグラムを用いた水質分類によって，以下の３つの地下水に分類される。

①沖積層と瀬戸層群（堆積岩）中の浅部の地下水

②瑞浪層群（堆積岩）中の深部の地下水

③土岐花崗岩中の深部の地下水

東濃地域の地下水の pH と CO_2 の分圧は，相関性が高く，単純化されたカルサイトの緩衝モデルで説明できる。

本報告書は，三菱商事株式会社が核燃料サイクル開発機構との契約により実施した業務「超深層研究所計画　地球化学研究における瑞浪市有地を対象とした地球化学モデルの構築」に関するものである。

機構担当課室：東濃地科学センター　瑞浪超深地層研究所　研究グループ

※MONITOR SCIENTIFIC LLC

March, 2003

Geochemical modelling of groundwater chemistry in the Tono area.

Abstract

Randolph C. Arthur※

This report summarizes the research result about geochemical modelling of the groundwater during H14 financial year. JNC-TGC have built the geochemical conceptual models of groundwater by using the chemical data of the groundwater of the Mizunami group and Toki granite. Although this models are extremely useful as interpretive tools, they lack the quantitative basis necessary to evaluate coupled processes of fluid-flow and water-rock interaction driving the chemical evolution of groundwater systems.

In this research, the following three items have been considered for the purpose of construction of the geochemical model which can express the chemical reaction in groundwater correctly.

- Evaluation of the quality of the previous analytical data in the Tono region
- Grasp of the chemical character of groundwaters
- Consideration about the influence between Eh, pH and $CO_2(g)$ parameter, and which the change has

Evaluation of the quality of the previous analytical data are important because deficiencies in sampling technique, sample-preservation procedures or analytical method may adversely affect the overall quality of groundwater chemical and isotopic analysis. In addition, the effects of borehole drilling and logging, hydraulic testing, inappropriate sampling strategies or inadequate sampling tools may perturb groundwater compositions to such an extent that they are unrepresentative of in-situ conditions. The quality of a water analysis is indicated by its charge balance. The charge balance of many of the analysis lies within the strictly acceptable range of 0 ± 5 %, but charg imbalances exceeding these limits are calculated for many other samples. These reasons are examined in the following.

- Analytical errors (e.q., of alkalinity)
- Errors arising from the use of IC values that are unrepresentative because CO_2 was gained by or lost from the sample during storage and (or) analysis
- Errors arising from the invalid assumption that non-carbonate contributions to the alkalinity of Tono groundwater are always negligible

Chemical character of groundwaters are defined in three geologic domains.

- Shallow groundwaters in alluvium and in sedimentary formations of Seto group.
- Deeper groundwater in sedimentary formations of the underlying Mizunami group
- Groundwaters in Toki granite

The pH of Tono groundwaters is strongly correlated with variations in the partial pressure of $CO_2(g)$. It appears that much of the covariance in the pH and $P_{CO2(g)}$ data can be explained using a highly simplified model of buffering by calcite. It suggests that this highly simplified buffer model adequately captures much of the complex evolutionary processes controlling pH, $P_{CO2(g)}$ and Ca variations in the granite groundwaters. This conclution also appears to be valid for many of the deep groundwaters in sedimentary formations of Mizunami group.

This report is related with the work "Mizunami Underground Research Laboratory Construction of the geochemical model for the MIU construction site in geochemistry research" was performed by Mitsubishi Corporation under construct with Japan Nuclear Cycle Development Institute.

JNC Liaison : Underground Reseach Group, Mizunami Underground Research Laboratory,
Tono Geoscience Center
※MONITOR SCIENTIFIC LLC

Table of Contents

1 Introduction

Data characterizing the chemistry of stream waters, soil solutions and groundwaters in the Tono region of Gifu Prefecture have been collected during the past several decades as a result of numerous surface-based investigations carried out by JNC-TGC. These data have been used to develop qualitative conceptual models of hydrochemical conditions in the Tono area. The models invoke various heterogeneous reactions to explain trends in groundwater chemistry with increasing residence time of the fluids in sedimentary formations of the Mizunami group and basement Toki granite.

Although the qualitative models are extremely useful as interpretive tools, they lack the quantitative basis necessary to evaluate coupled processes of fluid-flow and water-rock interaction driving the chemical evolution of groundwater systems. The models therefore cannot be used to predict spatial and temporal variations in groundwater chemistry that are needed to: 1) develop a 3-dimensional understanding of the chemical evolution of Tono groundwaters, and 2) assess changes in groundwater chemistry resulting from "external" disturbances such as borehole drilling and shaft sinking.

For this reason, a study was intitiated in FY02 with the long-term goal of developing a quantitative geochemical modeling approach that can be used to help improve our understanding of groundwater evolution in the Tono area, and to evaluate the effects of human-induced disturbances on groundwater chemistry. As a first step toward achieving this goal, the work carried out during FY02 attempts to establish quantitative constraints on the modeling approach that are consistent with empirical observations of hydrochemical conditions in the Tono region, and with conceptual models of:

- the groundwater flow system and its possible transients,
- processes leading to dilution or mixing of different groundwater types, and
- mass-transfer processes among the minerals and aqueous solutions comprising the hydrologic system.

The constraints established in this initial study will provide important guidance for the future development of groundwater evolution models that are specifically appropriate for the Tono region.

Three tasks were set up in FY02 to help achieve these objectives. The regional hydrochemical database for the Tono area developed by Iwatsuki *et al.* (2001) was first updated and critically evaluated. Results of this work are summarized below in Section 2. The second task includes an examination of empircal trends among the chemical and isotopic parameters comprising the regional hydrochemical database. Results of this work are summarized in Section 3. The third task involves an initial evaluation of geochemical models that are consistent with the identified empirical trends. Work on this task during FY02 has focussed on two critically important

physico-chemical parameters, Eh and pH, and includes an examination of mineral indicators of Eh-pH conditions in paleo-groundwaters of the Tono region. Results are discussed in Section 4.

2 Regional hydrochemical database

The primary analytical data characterizing the chemistry of groundwaters from the Tono region are critically evaluated in this section. Such evaluations are important because deficiencies in sampling technique, sample-preservation procedures or analytical methods may adversely affect the overall quality[1] of groundwater chemical and isotopic analyses (*e. g.*, Hem, 1985; Nordstrom *et al.*, 1989; Laaksoharju, 1999). In addition, the effects of borehole drilling and logging, hydraulic testing, inappropriate sampling strategies or inadequate sampling tools may perturb groundwater compositions to such an extent that they are unrepresentative of *in-situ* conditions (*e.g.*, Wittwer, 1986; Nordstrom *et al.*, 1990; Smellie and Laaksoharju, 1992; Lampén and Snellman, 1993; Pitkänen *et al.*, 1996; 1999; 2001; McEwan and Äikäs, 2000). An evaluation of the quality and representativeness of groundwater chemistry data is essential because conceptual hydrochemical models based on inaccurate or unrepresentative data are certain to be a source of confusion at best, and, at worst, may lead to conclusions that are seriously misleading.

The available groundwater data for the Tono region are discussed in Section 2.1. The quality of the analyses is critically evaluated in Section 2.2.

2.1 Groundwater chemical and isotopic data

The data evaluated below are taken from chemical analyses compiled by Iwatsuki *et al.* (2001a). This database includes 330 analyses of rainwater, surface waters and shallow and deep groundwaters from within and around the Tono mine, and from a larger area that encompasses the mine and which roughly coincides with the boundaries of JNC's regional hydrogeological conceptual model (Koide *et al.*, 1996; Saegusa *et al.*, 1997; JNC 2000). The data were collected over a period of more than 15 years in studies having varied purposes ranging from reconnaissance uranium-exploration surveys to detailed borehole studies of the region's geology, hydrogeology and geochemistry. Primary data sources include borehole reports, journal articles and unpublished technical reports and notes (see Iwatsuki *et al.*, 2001a).

A subset of the analyses compiled by Iwatsuki *et al.* (2001a) was selected for detailed evaluation. The selected data are from relatively recent studies, and are restricted to:

- groundwater samples from shallow, open boreholes in Quaternary alluvium and surface exposures of the Seto group, Mizunami group and weathered Toki granite,
- deep groundwaters sampled at discrete intervals between inflatable packers in boreholes penetrating sedimentary formations of the Mizunami group, and
- deep groundwaters collected in the same manner from boreholes in the Toki granite.

[1] Analytical quality is a measure of the overall accuracy of a water analysis.

The shallow groundwaters were collected in a series of related studies referred to as the MC-series borehole investigations. The deeper groundwaters were obtained from several different investigations, including the TH-, AN-, KNA-, TFA- and DH-series borehole investigations. Other groundwaters were sampled from boreholes drilled into the lower Toki formation from galleries and drifts in the Tono mine. The selected data altogether comprise 137 groundwater analyses plus 25 analyses of drilling fluids. Borehole locations are shown in Figures 2.1_1 (MC-, AN- and DH-series), 2.1_2 (TH-series) and 2.1_3 (KNA-series).

Chemical analyses of the selected water samples are given in Table 2.1_1. Sample numbers are taken in most cases from Iwatsuki *et al.* (2001a). Sample numbers beginning with "dh" (DH-series sample) or "df" (drilling fluid), or ending with a, b, c...*etc.*, are designated in the present study. All sampling depths noted in the table are measured from the top of the borehole. Temperatures are those measured at the time of sampling, inferred from borehole temperature logs or estimated on the basis of temperatures measured in other boreholes at similar depths. Many original references to the data in Table 2.1_1 report concentrations of HCO_3^- and CO_3^{2-} calculated from the measured alkalinity, pH and temperature. The alkalinities were, however, not reported. For reasons discussed in the following section, the HCO_3^- and CO_3^{2-} concentrations for these analyses are noted in Table 2.1_1, and corresponding alkalinities are back calculated from these concentrations. It is important to emphasize that these calculated values represent total alkalinity and may differ significantly from carbonate alkalinity.

Selected isotopic, chemical and sampling-related properties of the groundwaters in Table 2.1_1 are summarized in Table 2.1_2. Yusa *et al.* (1993), Iwatsuki and Yoshida (1999), Iwatsuki *et al.* (2000), Iwatsuki *et al.* (2001b) and Iwatsuki *et al.* (2002) have used these data to establish constraints on groundwater sources and processes controlling their hydrochemical evolution. The data are used in the present study mainly as objective criteria that can be used to help assess the representativeness of the groundwater samples.

Groundwater sampling methods and analytical techniques are noted in Table 2.1_3. Several different types of sampling methods have been used in the regional borehole investigations. Iwatuski *et al.* (2001a) provide an overview of the sampling apparatus and procedures used in these investigations. Important details, such as the pumping rate, total amount of water extracted prior to sampling, and sample filtration and preservation procedures are generally provided in the corresponding detailed borehole reports (see Iwatsuki *et al.*, 2001a). In some cases, however, such information is either lacking or is not readily available.

2.2 Analytical quality

The quality of a water analysis is indicated by its charge balance (cb), which can be calculated using the data in Table 2.1_1 and the equation:

$$\text{cb}\,(\%) = \frac{\Sigma cations - \Sigma anions}{\Sigma cations + \Sigma anions} \times 100, \qquad (2.2.1)$$

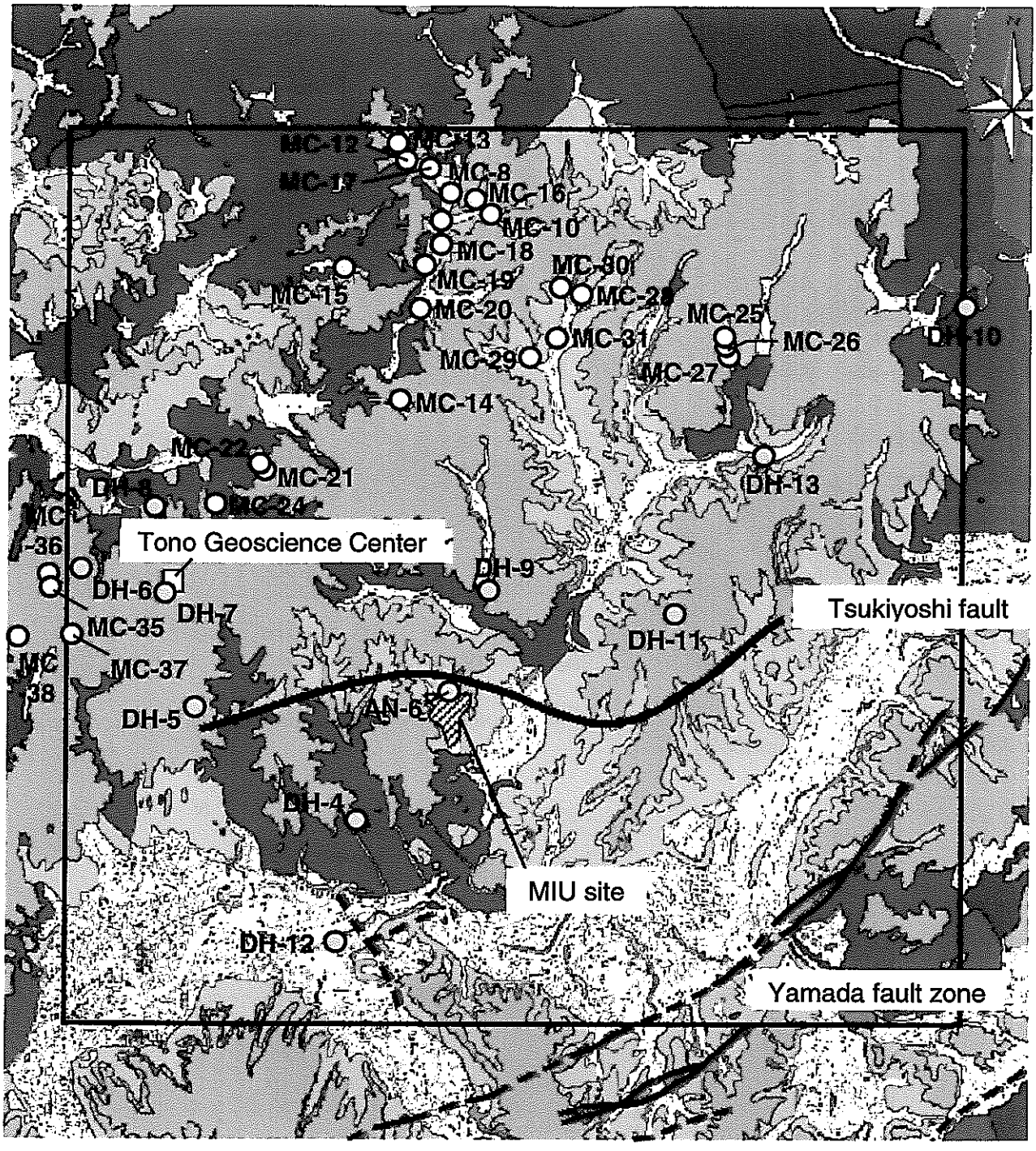

Figure 2.1_1: Geological map of the Tono region showing the locations of MC-series boreholes (white symbols), and AN- and DH-series boreholes (yellow symbols). The map's legend is identical to that in Figure 2.1_2. The square outline represents the boundaries of JNC's regional hydrogeological model. Each boundary represents a distance of 10 km. Regional groundwater flow is from high ground in the N-NE toward the discharge zone in the south represented by the Toki River.

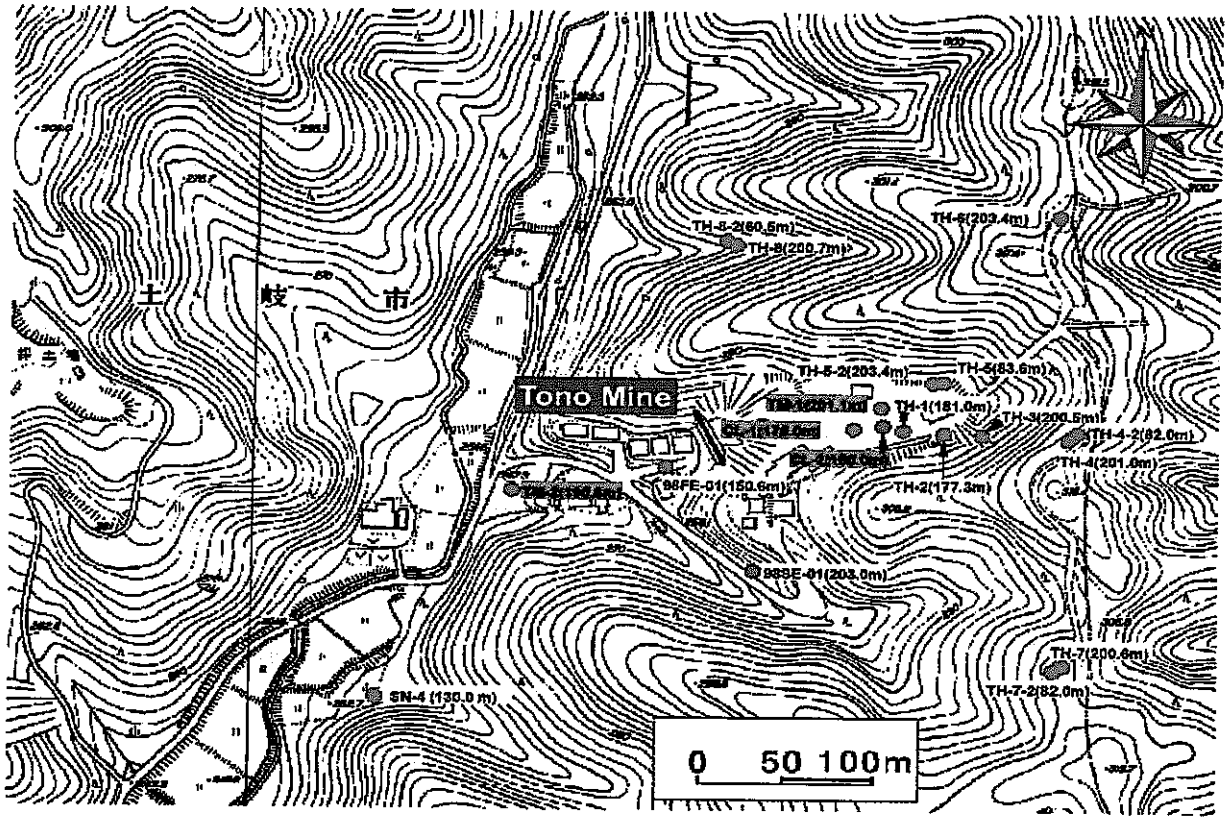

Figure 2.1_2: Topograhic map of the region around the Tono mine showing the locations of TH-series boreholes (red symbols).

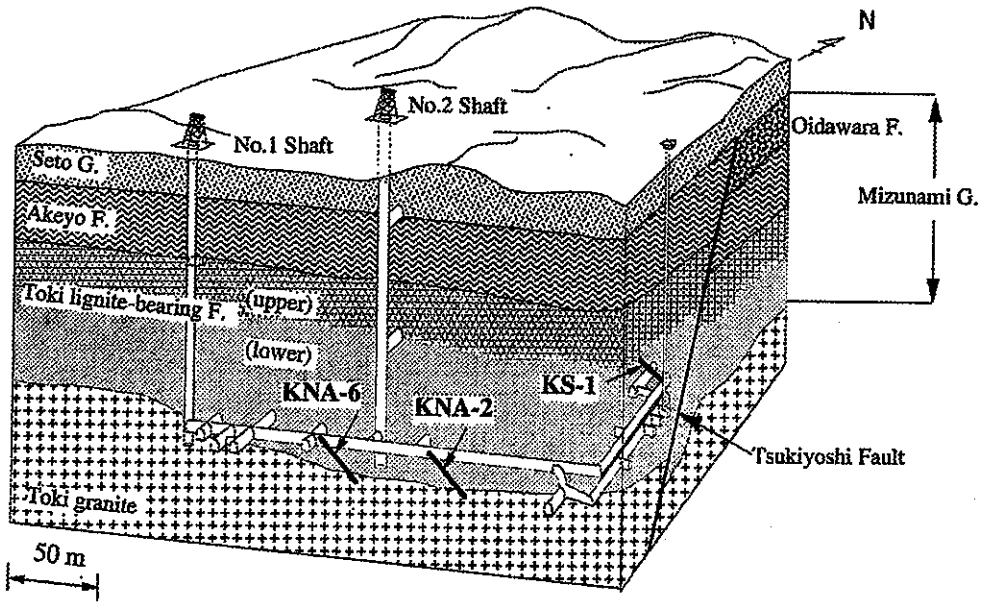

Figure 2.1_3: Schematic diagram of the Tono mine showing locations and orientations of boreholes KNA-6 and KNA-2 and KS-1.

Table 2.1_1. Chemistry of groundwaters and drilling fluids*.

No.	loc.	Depth (mbgl) min	Depth (mbgl) max	Elev. masl	Temp. °C	pH	Eh mV	cond. µS/cm	Na^+ ppm	K^+ ppm	Ca^{2+} ppm	Mg^{2+} ppm	Sr^{2+} ppm	TC ppm	IC ppm	HCO_3^- ppm	CO_3^{2-} ppm	alk.[1] meq/l	SO_4^{2-} ppm	HS^- ppm	F^- ppm	Cl^- ppm	NO_2^- ppm	NO_3^- ppm	NH_4^+ ppm	PO_4^{3-} ppm	Si ppm	Al ppm	ΣFe ppm	Fe^{2+} ppm	c.b. %
OIDAWARA FORMATION																															
13	TH-6	68	247	246	16.3	7.8		171	27.9	2.2	7.5	0.4	0.04			85.0		1.39	12.2	0.4	0.7	3.0	0.11	0.23		0.11	28.8	<0.02	0.09	<0.02	-1.9
14	TH-8	29		247		7.7		165	30.5	2.0	7.4	0.5	0.05			108.0		1.77	0.3	<0.1	1.0	1	<0.02	<0.02		0.12	31.3	<0.02	<0.02	<0.02	-0.4
94	TH-8	29		247	11.7	7.8			30.8	1.9	7.1	0.5		21.1				1.77	0.3		0.8	1.1		0.16	0.02						
95	TH-6	68		247	13.0	7.8			27.1	1.8	6.9	0.4		16.7				1.40	9.2		0.8	2.6		0.12	0.04						
dh11c	DH-11	132	135	208	19.1	9.0	-323	295	67.3	1.7	2.8	0.2	0.01	38.5	32.3			2.54	4.2	<0.1	1.0	2.5	<0.02	<0.02		0.23	2.3	0.06	0.21	0.05	1.2
AKEYO FORMATION																															
15	TH-1	34		253	13.7	7.6		147	18.0	1.6	12.1	1.1	0.09			84.0		1.38	4.2	<0.1	0.2	1.0	<0.02	<0.02		0.51	36.0	<0.02	0.07	<0.02	2.7
16	TH-2	33		257		7.2		130	13.7	1.5	12.1	1.3	<0.01			70.0		1.15	4.9	<0.1	0.2	0.9	<0.02	<0.02		0.25	36.3	<0.02	0.58	<0.02	8.3
17	TH-3	47		252	16.7	7.5		143	16.3	1.1	12.5	1.2	0.06			88.0		1.44	5.8	<0.1	0.2	1.9	<0.02	<0.02		0.53	36.3	<0.02	0.04	<0.02	-2.5
18	TH-4	61		249	15.8	7.6		180	32.3	1.3	6.6	0.5	0.02			105.0		1.72	5.4	25.7	0.3	2.8	<0.02	<0.02		0.19	32.3	<0.02	<0.02	<0.02	-13.1
19	TH-6	104		211	18.1	8.8		223	42.7	1.1	4.7	0.1	0.03			73.0	8.0	1.47	35.0	16.5	2.5	3.7	<0.02	<0.02		0.04	17.4	<0.02	0.06	0.03	-16.5
20	TH-8	64		212	16.6	8.1		232	44.7	1.6	5.0	0.1	0.02			143.0		2.34	1.2	<0.1	1.9	1.3	<0.02	<0.02		<0.02	28.4	<0.02	<0.02	<0.02	-5.5
97	TH-8	64		212	11.9	8.0			47.7	1.2	4.5	0.2		27.7				2.43	0.4		1.0	1.3		<0.03	0.06						
21	AN-6	14		240		7.7		219	29.7	0.8	4.6	0.2	0			94.0		1.54	1.6	<0.1	0.2	0.9	0.1	0.09		0.40	19.3	<0.02	<0.02	<0.02	0.0
96	AN-6	14		240	14.0	7.7			43.7	1.1	6.3	0.4		27.4				2.32	2.6		0.7	1.3		0.18	0.02						
UPPER TOKI FORMATION																															
22	TH-1	71		216	15.7	8.0		257	50.5	1.8	4.3	0.2	0.02			134.0		2.20	10.7	<0.1	2.9	3.3	<0.02	<0.02		0.45	26.7	<0.02	0.09	<0.02	-3.4
23	TH-2	75		215		8.2		311	65.0	1.4	5.2	0.2	0.02			181.0		2.97	1.1	0.2	2.8	1.1	<0.02	<0.02		0.78	24.6	<0.02	<0.02	<0.02	-1.1
24	TH-3	86		213	17.1	8.4		271	62.0	1.3	4.1	0.2	0.01			159.0		2.61	1.3	30.1	4.8	1.5	<0.02	<0.02		<0.02	29.7	<0.02	<0.02	<0.02	-13.7
25	TH-4	83		227	16.1	7.6		230	46.7	1.4	3.6	0.2	0.01			130.0		2.13	4.7	<0.1	1.5	3.7	<0.02	0.09		<0.02	26.3	<0.02	<0.02	<0.02	-0.8
26	TH-6	132		183	18.6	8.7		370	73.0	1.6	6.2	0.1	0.03			127.0	7.0	2.31	51.0	37.4	2.8	8.4	<0.02	<0.02		<0.02	15.0	<0.02	0.04	<0.02	-16.3
27	TH-8	91		185		7.6		213	13.3	1.0	1.8	0.1	0.03			34.0		0.56	4.8	<0.1	0.8	1.9	<0.02	<0.02		<0.02	4.9	<0.02	<0.02	<0.02	-1.3
152	DH-13	0	21	278	17.2	7.5	-11	258	19.9	0.7	27.3	0.6	<0.03	27.5	23.5			1.86	18.4	<0.1	0.3	1.6	<0.02	<0.03	<0.02		15.5	<0.01	0.18	0.14	0.6
LOWER TOKI FORMATION																															
28	TH-1	138		148	18.4	9.5		181	38.7	0.3	1.5	0.03	<0.01			51.0		0.84	12.2	0.9	3.0	1.9	<0.02	<0.02		0.04	12.9	<0.02	<0.02	<0.02	3.3
29	TH-2	110		180		8.6		210	45.0	0.5	1.9	0.04	<0.01			106.0		1.74	9.7	<0.1	2.7	2.0	<0.02	<0.02		0.14	9.6	<0.02	<0.02	<0.02	-3.2
30	TH-3	124		174	18.0	8.8		200	40.7	0.4	1.5	0.03	<0.01			79.0		1.29	17.1	25.7	3.1	3.9	<0.02	<0.02		0.11	14.1	<0.02	<0.02	<0.02	-21.0
31	TH-4	152		158		9.0		272	55.3	0.4	2.9	0.03	<0.01			67.0		1.10	29.8	<0.1	3.5	4.2	<0.02	<0.02		<0.02	10.6	<0.02	<0.02	<0.02	9.0
98	TH-4	152		158	12.8	9.0			56.5	0.3	2.6	<0.02		17.5				1.74	38.8		3.7	4.6		<0.03	0.02						-6.4
32	TH-6	153		160	19.1	9.0		237	45.0	0.4	2.1	0.02	0.04			50.0	10.0	1.15	41.0	15.1	4.2	4.3	<0.02	<0.02		<0.02	6.4	<0.02	<0.02	<0.02	-14.4
33	TH-8	121		155		7.9		145	21.3	0.3	1.1	0.04	<0.01			53.0		0.87	3.6	0.16	0.9	0.9	<0.02	<0.02		1.29	6.7	<0.02	<0.02	<0.02	-1.7
41						8.6	-300		35.0									1.47			3.0								<0.10		
1	KNA-6.			143		9.5		202	45.5	0.4	1.7	0.03	<0.01	22.8	17.9				0.9	<0.05	4.6	1.0	<0.02	0.04		<0.02	7.4	<0.10	0.04	<0.05	-1.6
2	KNA-6			136		9.2	-360	180	42.5	0.3	2.3	0.02	<0.01	23.4	21.6				0.1		4.3	0.9	<0.02	<0.02		<0.02	7.5	<0.10	<0.02	<0.05	-7.8
2a	KNA-6			136		9.4		167	46.5	0.2	1.9	0.02	<0.01	20.7	20.4				0.2		4.4	0.7	<0.02	<0.02		<0.02	8.1	<0.10	<0.02		-3.9
46	KNA-2	153			18.5	9.2	-300	168	45.0	0.3	2.0	0.02				79.0	8.0	1.56	1.3		4.1	1.1					8.1	<0.02		<0.02	4.5
52	TFA-1					8.1			49.9	<1.0	0.8	0.3	0.02	22.4	13.4	79.0		1.29	7.4		12.0	6.3	1.24	1.84			6.9	0.23	<0.02		2.1
53	TFA-1					8.0			31.9	<1.0	0.3	0.3	0.01	17.7	8.6	48.3		0.79	10.4		5.1	2.6	0.40	0.67			6.1	0.12	<0.02		5.0
54	TFA-1					7.5			62.9	<1.7	1.4	0.6	0.02	12.8	6.4	30.6		0.5	97.5		4.3	3.7	0.19	<0.20			5.8	0.16	<0.03		-0.2
150	DH-12	158	164	-23	27.1	9.7	-42	407	72.5	0.4	2.1	<0.2	<0.3	12.2	7.4			1.10	<0.4	<0.1	14.8	53.3	<0.20	<0.30	<0.2		7.0	<0.10	<0.05	<0.05	0.2
TONO MINE (LOWER TOKI FORMATION)																															
57	gallery A+C				15.2	7.0		159	15.1	2.9	8.7	1.5				32.9		0.54	32.6		0.1	2.3				0.10	12.5		0.0		4.0
58	gallery B				15.7	8.5		250	38.3	5.8	11.6	1.0				140.0		2.29	5.3		0.4	1.0				0.36	15.5		0.16		-1.1
61	20m S. gallery drop				16.4	8.4		222	49.1	0.4	3.3	0.04				113.0		1.85	1.0		6.4	0.6					6.3		0.0		1.5
62	30m S. gallery drop					8.7			50.9	0.4	2.5	0.03				104.0	1.2	1.74	3.3		6.5	0.6					6.5		0.02		4.8
64	main gallery, 65 m boring				18.2	9.3		232	43.8	0.2	1.8	0.02				86.9	8.9	1.72	0.1		3.7	0.6					7.8		0.01		-1.0
66	main gallery, 70 m boring				19.1	9.2		202	42.7	0.3	2.8	0.03				91.5	6.6	1.72	0.1		3.6	0.6					7.9		0.00		-1.1
67	main gallery, 95m boring				19.5	9.2		199	38.7	0.2	3.1	0.05				87.2	6.0	1.63	0.4		3.6	0.8					8.2		0.01		-3.6
68	main gallery, 95m boring				19.0	9.2		197	40.3	0.3	3.1	0.04				87.6	6.5	1.66	0.3		3.7	0.7					8.2		0.02		-1.8
70	main gallery, 120m boring				18.6	9.0		191	34.0	0.4	6.1	0.12				93.4	2.0	1.60	0.1		4.0	0.7					8.8		0.01		-4.1
72	north gallery, end				17.1	9.4		217	47.1	0.5	1.6	0.01				75.0	13.2	1.67	0.4		6.4	0.8					9.0		0.00		0.8
74	under gallery, higashidobira bor.				15.6	9.6		232	49.8	0.2	1.5	0.02				76.9	14.4	1.74	0.3		6.8	0.7					6.4		0.01		-0.1
77	under gallery, Tsukiyoshi f. drop				15.4	8.3		256	54.2	0.3	2.1	0.03				130.0		2.13	5.5		4.1	1.1					7.3		0.01		-0.5
78	under gallery, Tsukiyoshi f. pool				11.0	9.5		260	57.4	0.7	3.2	0.08				95.8	13.2	2.01	9.5		4.3	1.0					7.5		0.05		2.2
99	T08;Main drift 70m from #1shaft				18.5	9.1			41.4	0.2	2.1	<0.02		19.2				1.85	0.5		3.8	1.2		<0.03	0.04						
100	T09 (KNA-2) 9.0				18.8	9.1			39.3	0.2	2.5	<0.02		18.6				1.76	0.3		3.7	1.1		<0.03	0.05						
101	T10: main drift 120m from #1S				18.3	8.9			34.3	0.3	6.1	0.11		18.5				1.74	0.2		3.8	1.1		<0.03	0.06						
102	T11 (KS1)				18.1	9.1			44.6	0.3	1.3	<0.02		18.1				1.82	1.0		5.9	1.0		0.05	0.00						
103	T12 (KNA 1)				18.6	9.1			39.9	0.2	1.9	0.04		18.1				1.73	<0.1		3.9	0.9		<0.03	0.05						

No.	loc.	Depth (mbgl) min	Depth (mbgl) max	Elev. masl	Temp. °C	pH	Eh mV	cond. µS/cm	Na^+ ppm	K^+ ppm	Ca^{2+} ppm	Mg^{2+} ppm	Sr^{2+} ppm	TC ppm	IC ppm	HCO_3^- ppm	CO_3^{2-} ppm	alk.[1] meq/l	SO_4^{2-} ppm	HS^- ppm	F^- ppm	Cl^- ppm	NO_2^- ppm	NO_3^- ppm	NH_4^+ ppm	PO_4^{3-} ppm	Si ppm	Al ppm	ΣFe ppm	Fe^{2+} ppm	c.b. %
104	T13 (lower drift)				17.6	9.4			48.0	0.2	1.1	<0.02		18.3				1.89	<0.1		7.5	0.9		<0.03	0.06						
TOKI GRANITE																															
3	KNA-6			121		8.2	0	180	29.3	0.4	12.3	0.2	0.08	24.5	23.4				0.2	<0.05	3.8	1.1	<0.02	<0.02	<0.01	<0.02	10.7	<0.1	<0.02	<0.05	-6.6
3a	KNA-6			121		8.5		155	31.5	0.5	11.7	0.2	0.08	20.1	19.9				0.1		3.7	0.6	<0.02	<0.02		<0.02	10.9	<0.1	<0.02		1.6
34	TH-1	166		120	18.9	7.9		145	36.3	0.9	7.0	0.3	0.02			119.0		1.95	14.7		1.6	2.5	<0.02	<0.02		0.16	9.6	<0.02	<0.02	<0.02	-8.9
35	TH-6	178		135	19.4	7.8		319	46.0	1.3	15.1	0.4	0.05			75.0		1.23	82.0		1.4	12.1	0.04	<0.02		<0.02	5.6	<0.02	<0.02	<0.02	-7.4
105	TH-8	160		116	10.9	7.9			23.6	1.2	16.4	0.5		20.4				1.74	4.2		2.8	1.5		0.05	0.05						-0.1
51	DH-3	0		356	18.0	6.2			12.3	10.1	1.4	0.2	0.01		7.1				2.9		0.6	1.4					1.6	<0.02	0.06		27.0
6	DH-3	207	219	150	15.0	9.7		131	8.2	3.5	16.0	0.1	0.12	14.0	12.0				2.3		2.0	2.3	<0.02	<0.02		<0.02	8.2	<0.1	<0.02	<0.05	-17.8
7	DH-3	325	332	31	15.0	8.9		125	11.6	0.9	12.2	0.1	0.12	11.8	9.2				6.7		4.1	3.7	<0.02	<0.02		0.04	13.8	<0.01			-8.9
8	DH-3	487	498	-130	22.4	9.7			19.5	1.6	9.6	0.03	0.10	15.8	7.9				12.7		3.5	4.2	<0.02	<0.02		0.08	2.5	<0.01	0.03	<0.05	-4.4
9	DH-3	601	613	-245	25.5	9.6		168	36.5	1.2	4.1	0.03	0.04	16.0	13.6				9.1		10.9	3.5	<0.02	<0.02		0.17	5.6	<0.01	0.02	<0.05	-15.8
10	DH-3	791	798	-434	27.8	9.0		188	36.0	1.2	4.7	0.2	0.04	19.3	16.2				6.8		8.9	3.9	<0.02	<0.02		0.11	4.1	<0.01	<0.02	<0.05	-9.4
11	DH-3	829	837	-473	30.0	9.3		202	39.5	0.8	3.7	0.1	0.03	14.0	13.5				6.2		9.7	3.1	<0.02	<0.02		<0.02	5.5	<0.01	<0.02	<0.05	-4.7
5	DH-4	186	189	81	13.0	6.8	49	172	13.3	6.1	17.6	1.9	0.11			88.5			0.1	<0.05	5.0	2.7	<0.02	0.02		<0.02	5.6	<0.01	9.34	9.34	17.6
106	DH-5	324	331	-13	19.3	7.8	-16	159	10.3	3.0	19.0	0.8	0.15	16.2	14.5				7.8		2.5	1.4	0.01	0.01	0.01	0.10	19.6	0.01	0.41	0.24	1.7
107	DH-6	733	740	-414	25.5	8.9	-303	148	21.4	0.6	3.2	0.1		14.1	12.4			0.70	5.5		4.1	3.4			0.3		8.6	0.04	0.18	0.2	-17.7
dh7d	DH-7	438	445	-98		8.9		98	7.7	1.6	11.9	0.7						0.73	5.6		0.8	4.3		<0.1			4.5		<0.01		
dh7e	DH-7	479	486	-139		10.3		133	13.3	2.5	13.7	0.2						0.89	6.8		2.4	4.5		<0.1			9.7		<0.01		
dh7f	DH-7	479	488	-139		9.9		134	18.6	2.4	9.3	0.03						0.83	5.7		3.8	3.9		<0.1			13.0		<0.05		
108	DH-7	561	567	-220	26.2	10.1	-400	179	25.4	2.3	5.4	0.3	0.08	20.8	18.4			1.51	4.6		2.1	4.4	0.01	0.01	22.9	0.09	1.9	0.19	8.9	8.5	-35.6
dh7g	DH-7	561	567	-220		10.4		192	20.4	3.7	13.0	0.01						1.25	6.5		5.3	4.2		<0.1			24.3		<0.01		
dh7h	DH-7	561	567	-220		10.1		131	19.0	2.4	10.6	0.01						0.83	6.3		4.8	3.5		<0.1			20.1		<0.1		
dh7l	DH-7	598	605	-258		10.8		250	27.2	3.4	20.3	0.01						1.49	4.5		6.4	5.9		<0.1			22.3		0.04		
dh7i	DH-7	598	605	-258		10.8		202	28.8	2.8	18.2	<0.01						1.26	4.2		7.1	5.7		<0.1			20.8		<0.05		
dh7k	DH-7	660	667	-320		10.1		153	18.6	1.6	13.5	0.3						0.97	5.0		4.4	4.2		<0.1			12.6		0.01		
dh7l	DH-7	660	667	-320		9.6		175	30.8	1.0	10.2	0.01						1.01	4.6		7.8	2.8		0.2			13.2		<0.1		
dh7m	DH-7	736	742	-395		11.1		323	40.7	5.7	20.0	0.02						2.08	6.0		6.3	6.4		0.4			27.7		0.03		
dh7n	DH-7	736	742	-395		11.2		307	45.6	4.6	18.8	0.02						1.96	2.8		8.7	6.1		<0.1			27.6		<0.1		
109	DH-7	834	840	-493	29.3	9.6	-373	298	31.3	9.1	3.2	0.6	0.06	21.6	20.3			1.65	5.6		10.0	3.1	0.1	0.05	3.0	0.04	8.5	1.2	7.2	6.9	-27.4
dh7o	DH-7	834	840	-493		10.7		237	40.6	1.9	8.2	0.04						1.48	4.2		9.2	4.3		<0.1			17.1		0.02		
110	DH-7	880	887	-540	30.9	9.4	-355	297	48.0	22.0	5.4	0.7	0.06	24.8	22.0			1.79	5.4		8.6	5.1	0.09	0.03	4.6	0.33	14.7	4.3	7.5	8.8	0.5
dh7p	DH-7	880	887	-540		10.5		235	46.0	4.2	9.7	0.1						1.63	2.8		10.2	6.5		<0.1			29.8		0.87		
dh7q	DH-7	880	887	-540		10.7		249	49.0	3.7	10.0	0.07						1.55	2.0		10.2	5.8		<0.1			22.4		0.60		
111	DH-8	642	648	-372	27.3	9.0	-353	195	23.2	5.1	2.8	0.04	0.18	15.0	14.2			1.11	n.d.		3.2	3.8	0.01	n.d.	0.2	0.01	13.6	0.68	0.03	0.03	-14.4
112	DH-8	694	700	-424	28.2	8.5	-274	187	22.1	0.5	6.9	0.09	0.25	18.1	17.2			1.36	4.2		3.6	3.8	0.09	0.01	1.4	<0.01	17.0	0.05	0.19	0.17	-18.1
113	DH-8	746	752	-476	29.3	8.4	-298	207	28.0	4.5	1.0	0.09	0.23	17.3	16.3			1.32	3.7		4.4	3.9	0.01	n.d.	1.1		16.7	0.32	0.18	0.21	-14.0
114	DH-8	869	876	-600	31.8	8.8	-305	327	39.1	11.0	4.3	0.7	0.18	15.7	15.1			1.32	3.1		11.2	19.2	.	0.01	1.1		12.8	0.98	0.07	0.08	-7.8
115	DH-8	975	982	-705	33.7	8.8	-364	262	25.8	0.9	6.8	0.7	0.16	15.9	15.0			1.26	1.7		6.8	6.4	.		0.3	0.01	14.5	0.08	0.19	0.2	-13.2
dh9a	DH-9	228	235	47	20.9	8.4	-277	169	24.0	7.3	12.0	0.4	0.09	27.0	18.0			1.44	1.8	<0.1	4.4	2.9	<0.05	<0.05	0.56	<0.01	16.0	0.05	0.12	<0.05	0
dh9b	DH-9	313	319	-37	22.1	8.5	-319	165	20.0	6.6	12.0	0.4	0.11	39.0	14.0			1.17	1.8	<0.1	2.7	2.2	<0.05	<0.05	2.9	<0.01	16.0	0.06	0.46	<0.05	11.7
dh9c	DH-9	957	964	-682	35.9	8.3	-250	196	15.0	4.0	14.0	0.7	0.11	80.0	15.0			1.38	3.1	<0.1	3.3	1.8	<0.05	<0.05	0.6	<0.01	24.0	0.05	0.53	<0.05	-0.3
dh10a	DH-10	47	62	429		7.5		94	5.7	2.1	9.7	0.5	0.03					0.64	1.4		1.2	2.4		<0.03			11.3	0.05	0.03	<0.05	
dh10b	DH-10	47	122	429		7.4		76	5.6	2.0	8.8	0.4	0.02					0.59	1.4		1.2	1.9		<0.03			11.4	0.04	0.03	<0.05	
dh10c	DH-10	334	342	142	18.3	8.5	-254	155	12.9	1.6	18.2	0.3	0.08	10.2	9.8			0.96	15.6	<0.1	3.3	6.9	<0.02	<0.02		<0.01	13.7		0.06	<0.05	-0.9
dh11a	DH-11	393	468	-53		7.4		200	38.2	5.3	6.5	0.05	0.07					1.36	5.5	<0.1	7.9	6.0		<0.02			6.3	0.29	0.43		
dh11b	DH-11	932	1008	-592		7.6		215	38.0	6.9	7.6	0.06	0.08					1.48	6.4	<0.1	8.0	5.4		<0.02			4.1	0.15	0.09		
151	DH-12	172	280	-34	25.6	9.3	-26	358	55.2	<0.2	6.5	<0.2	<0.30	6.6	6.4			0.68	<0.4	<0.1	12.5	52.6	<0.2	<0.3	<0.2		6.9	<0.1	<0.05	<0.05	-2.2
154	DH-12	279	345	-142	22.4	9.2	-32	504	71.7	0.4	13.1	<0.2	<0.30	5.7	4.9			0.52	<0.4		10.0	99.9	<0.2	<0.3	<0.2		6.7	<0.1	<0.05	<0.05	-1.5
155	DH-12	346	387	-209	25.2	8.9	-84	630	81.5	0.9	25.6	<0.2	<0.30	4.4	3.8			0.43	<0.4	<0.1	9.8	137.0	<0.2	<0.3	<0.2		7.3	<0.1	<0.05	<0.05	0.6
156	DH-12	389	430	-252	25.7	8.9	-24	777	94.9	0.9	32.4	<0.2	<0.30	4.3	3.1			0.37	<0.4	<0.1	9.4	175.0	<0.2	<0.3	<0.2		6.7	<0.1	<0.05	<0.05	-0.1
157	DH-12	431	473	-294	26.5	9.2	-20	423	66.0	0.4	10.4	<0.2	<0.30	6.3	5.4			0.63	<0.4	<0.1	12.8	72.1	<0.2	<0.3	<0.2		6.5	<0.1	<0.05	<0.05	1.4
153	DH-13	61	74	217	20.6	8.1	58	201	16.1	0.9	22.2	0.7	<0.30	19.1	18.7			1.50	6.9	<0.1	2.9	1.6	<0.2	<0.3	<0.2		12.9	<0.1	<0.05	<0.05	-0.2
158	DH-13	408	442	-131	18.4	8.4	-12	193	15.4	1.1	20.6	0.5	<0.30	19.0	17.2			1.40	5.5	<0.1	3.1	1.4	<0.2	<0.3	<0.2		10.6	<0.1	<0.05	<0.05	-0.6
SHALLOW GROUNDWATER (SHALLOW BOREHOLES IN QUATERNARY ALLUVIUM/SETO GROUP)																															
MC-8		0	21			6.0		49	4.8	1.7	4.0	0.4	0.05	13.2	12.6				7.2		0.03	1.2	<0.02	<0.02	<0.2	<0.02	22.7	<0.1	<0.02		0.0
MC-9		0	41			7.3		99	12.8	1.6	9.5	1.1	0.07	7.2	6.5				5.7		0.2	1.5	0.04	1.8	b.d.	0.04	22.3	<0.1	<0.02		25.8
MC-10		0	31			6.6		44	5.8	2.0	3.3	0.4	0.02						2.6		0.1	0.7	<0.02	<0.02	b.d.	<0.02	25.6	<0.1	0.04		
MC-12		0	31			6.6		63	9.5	5.3	3.1	0.5	0.02	6.4	4.0				2.4		0.10	5.1	<0.02	<0.02	<0.2	<0.02	7.2	<0.1	0.04		23.6
MC-13		0	31			6.3		38	5.2	1.8	1.5	0.2	0.01	4.8	4.5				4.7		0.1	3.3	<0.02	0.20	<0.2	<0.02	14.4	<0.1.	<0.02		0.1
MC-14		0	31			6.3		37	4.7	1.9	2.2	0.5	0.02	14.1	13.6				1.9		0.1	0.7	<0.02	0.04	<0.2	<0.02	13.6	<0.1	<0.02		-7.1
MC-15		0	50			6.8		114	10.4	1.5	13.7	1.1	0.07	9.1	8.4				5.2		0.05	1.3	<0.02	<0.02	<0.2	<0.02	38.1	<0.1	0.36		26.6

No.	loc.	Depth (mbgl) min	Depth (mbgl) max	Elev. masl	Temp. °C	pH	Eh mV	cond. µS/cm	Na^+ ppm	K^+ ppm	Ca^{2+} ppm	Mg^{2+} ppm	Sr^{2+} ppm	TC ppm	IC ppm	HCO_3^- ppm	CO_3^{2-} ppm	alk.[1] meq/l	SO_4^{2-} ppm	HS^- ppm	F^- ppm	Cl^- ppm	NO_2^- ppm	NO_3^- ppm	NH_4^+ ppm	PO_4^{3-} ppm	Si ppm	Al ppm	ΣFe ppm	Fe^{2+} ppm	c.b. %
MC-16		0	62			5.8		55	4.7	1.3	6.0	0.4	0.03	6.4	5.4				7.6		0.03	2.3	<0.02	0.29	<0.2	<0.02	11.4	<0.1	<0.02		15.7
MC-17		0	31			6.4		79	6.3	2.7	6.7	1.0	0.10	9.5	8.8				18.9		0.2	1.1	<0.02	<0.02	<0.2	<0.02	20.2	<0.1	<0.02		-1.8
MC-18		0	31			6.4		59	4.8	1.4	5.1	0.6	0.04	42.5	39.4				4.8		0.07	1.3	<0.02	0.59	<0.2	2.06	22.4	<0.1	0.02		-22.6
MC-19		0	30			6.1		222	8.0	8.2	26.1	4.2	0.23	9.5	8.4				19.1		0.08	6.1	<0.02	0.02	<0.2	<0.02	18.7	<0.1	<0.02		36.2
MC-20		0	41			5.7		58	4.6	2.1	3.6	0.7	0.03	3.0	2.5				2.7		0.07	3.3	<0.02	7.99	<0.2	<0.02	16.0	<0.1	<0.02		29.8
MC-21		0	21			5.4		18	1.7	1.3	0.8	0.2	0.01	5.7	5.4				1.1		0.03	1.4	<0.02	<0.02	<0.2	<0.02	7.3	<0.1	0.28	0.21	6.8
MC-22		0	21			5.3		18	1.6	1.3	0.6	0.3	<0.01						1.5		0.02	1.5	<0.02	0.02	<0.2	<0.02	5.4	<0.1	0.03		
MC-24		0	21			7.5		100	3.5	1.8	15.2	1.5	0.18	6.3	5.8				3.9		0.37	1.0	<0.02	<0.02	<0.2	<0.02	9.4	<0.1.	<0.02		28.9
MC-25		0	31			6.3		35	4.1	1.2	2.5	0.3	0.02	5.5	4.8				1.2		0.05	0.7	<0.02	<0.02	<0.2	0.26	15.3	<0.1	<0.02		12.8
MC-26		0	20			6.1		31	3.3	1.2	1.9	0.2	0.02	7.2	6.7				0.8		0.03	0.7	<0.02	0.13	<0.2	0.19	12.9	<0.1	<0.02		4.7
MC-27		0	20			6.2		30	3.5	1.1	2.1	0.3	0.02	35.7	33.5				1.1		0.03	0.9	<0.02	0.03	<0.2	0.26	13.3	<0.1	<0.02		-17.3
MC-28		0	41			7.1		229	26.5	1.4	25.4	1.2	0.08	35.3	32.6				21.0		0.20	2.5	<0.02	0.02	<0.2	0.08	17.8	<0.1	0.05		-4.0
MC-29		0	41			6.7		209	21.5	1.7	24.9	3.2	0.09	13.6	12.6				4.7		0.03	3.0	<0.02	<0.02	<0.2	<0.02	22.9	<0.1	0.67		39.9
MC-30		0	41			6.5		104	20.0	1.5	11.8	1.5	0.03	14.8	13.6				9.7		0.08	2.0	<0.02	0.04	<0.2	<0.02	18.3	<0.1	0.04		20.6
MC-31		0	60			6.6		143	9.5	1.7	18.0	2.1	0.09	2.8	2.7				24.1		0.05	4.1	<0.02	0.08	<0.2	<0.02	13.9	<0.1	<0.02		31.4
MC-32		0	40			6.6		19	2.2	0.4	1.3	0.3	0.01	8.5	7.6				0.4		0.08	0.5	<0.02	0.06	<0.2	<0.02	7.5	<0.1	<0.02		-20.2
MC-33		0	32			6.0		55	4.6	1.6	3.2	0.9	0.03	9.4	8.9				0.5		0.02	4.7	0.08	6.96	<0.2	<0.02	7.7	<0.1	<0.02		6.5
MC-34		0	52			6.3		34	2.8	1.0	1.9	0.7	0.02	11.2	10.9				0.4		0.03	0.7	<0.02	0.68	<0.2	<0.02	7.0	<0.1	<0.02		-7.6
MC-35		0	51			7.1		89	3.8	2.0	12.0	2.5	0.07	9.5	8.9				6.1		0.26	0.7	<0.02	<0.02	<0.2	<0.02	17.0	<0.1	0.12		12.3
MC-36		0	51			6.6		62	2.6	3.3	3.2	1.5	0.02	8.7	8.2				3.7		0.21	1.9	<0.02	0.03	<0.2	<0.02	14.7	<0.1	<0.02		-4.8
MC-37		0	51			5.6		19	1.4	0.8	0.5	0.2	<0.01	4.7	4.0				0.7		0.02	0.8	<0.02	0.03	<0.2	<0.02	5.7	<0.1	<0.02		4.9
MC-38		0	51			6.1		18	1.2	2.2	0.4	0.2	<0.01						0.5		0.02	1.6	<0.02	0.03	<0.2	<0.02	8.2	<0.1	<0.02		
DRILLING FLUIDS																															
dftfa	TFA-1					7.1			0.2	0.6	1.3	<0.1	0.01		2.3				1.8		0.1	0.1	0.04	0.39			5.8	<0.02	<0.01		
dftfa	TFA-1					7.4			<0.02	<0.5	6.9	<0.1	0.02		4.5				1.9		0.1	0.1	0.52	0.29			6.0	<0.02	<0.01		
df5	DH-5								10.2	1.5	8.5	0.4	0.06	9.0	8.0				5.1		2.7	1.0		0.03	0.03	0.02	23.0	0.03	1.23	0.93	
df6-8	DH-6,7,8					6.8			27.4	0.5	7.6	0.1	0.21	18.0	17.1			1.22	4.0		6.2	2.6	<0.02	<0.02	<0.02	<0.02	14.3	0.05	0.02	0.03	2.1
df9	DH-9								29.0	0.3	14.5	0.05	0.20	17.0	17.0			1.38	3.5		8.7	2.3	<0.05	<0.05	<0.05	<0.01	31.0	0.02	<0.01	<0.05	
df101	DH-10,11					6.4		46	6.2	0.6	3.8	0.3	0.02	7.2	7.6			0.39	2.4		1.3	0.9	<0.02	<0.02		<0.01	11.0	0.05	0.02	<0.05	2.8
df12a	DH-12 (100m)				25.4	9.3		163	23.6	2.4	4.8	<0.2	<0.3	16.9	8.9			0.87	18.7		1.0	2.6		<0.3			11.1	<0.1	<0.05		-7.7
df12b	DH-12 (161m)					9.2		252	51.8	1.0	4.0	<0.2	<0.3	20.4	15.6			1.20	43.5		1.8	4.5		<0.3			4.6	<0.1	0.07		-2.9
df12c	DH-12 (200m)				24.2	9.3		291	54.8	1.7	3.1	<0.2	<0.3	15.9	10.5			1.06	13.6		9.2	31.7		<0.3			4.7	<0.1	<0.05		-2.7
df12d	DH-12 (300m)				21.1	9.7		424	69.2	3.2	9.8	<0.2	<0.3	5.8	4.7			0.70	1.0		9.9	84.0		<0.3			4.8	<0.1	0.10		0.6
df12e	DH-12 (400m)				21.8	9.7		433	68.5	0.9	11.4	<0.2	<0.3	5.8	4.3			0.64	<0.4		10.7	84.9		<0.3			6.2	<0.1	<0.05		-2.1
df12f	DH-12 (500m)				21.8	9.5		423	67.4	1.0	11.2	<0.2	<0.3	6.2	4.9			0.63	<0.4		10.6	84.8		<0.3			6.5	<0.1	<0.05		-0.9
df12g	DH-12 (600m)				22.0	10.7		484	62.7	1.0	10.4	<0.2	<0.3	5.1	4.6			0.78	0.9		11.2	69.8		<0.3			6.5	<0.1	<0.05		-11.7
df12h	DH-12 (700m)				23.2	9.4		406	63.2	1.1	10.7	<0.2	<0.3	6.0	5.1			0.62	<0.4		11.2	79.0		<0.3			6.2	<0.1	0.05		-1.8
df13a	DH-13 (48m)				25.8	9.7		110	12.1	1.0	7.5	<0.2	<0.3	11.5	6.4			0.70	7.5		0.5	2.0		<0.3			9.3	<0.1	<0.05		-17.6
df13b	DH-13 (100m)				22.9	8.7		117	8.4	3.9	11.5	0.4	<0.3	15.7	10.8			0.92	3.3		0.4	2.9		<0.3			6.3	<0.1	<0.05		-2.8
df13c	DH-13 (200m)				17.9	9.5		173	18.5	20.8	3.5	<0.2	<0.3	34.7	13.3			1.32	5.5		1.7	2.7		<0.3			2.2	<0.1	<0.05		-2.9
df13d	DH-13 (300m)				13.9	8.9		112	10.1	11.5	6.0	0.7	<0.3	15.0	10.4			0.90	2.2		0.8	1.7		<0.3			3.5	<0.1	<0.05		1.8
df13e	DH-13 (400m)				12.1	8.8		98	9.7	5.3	6.9	0.4	<0.3	11.8	8.6			0.78	2.1		1.4	2.0		<0.3			4.4	<0.1	<0.05		0.4
df13f	DH-13 (500m)				12.1	10.9		301	35.0	12.5	6.9	<0.2	<0.3	11.0	5.8			1.72	7.5		6.4	4.1		<0.3			17.7	<0.1	<0.05		-8.8
df13g	DH-13 (600m)				11.0	10.0		225	31.0	10.6	4.0	<0.2	<0.3	15.4	10.7			1.36	5.0		6.4	4.6		<0.3			5.2	<0.1	0.08		-2.3
df13h	DH-13 (700m)				11.7	9.8		225	32.2	12.6	5.4	<0.2	<0.3	18.7	14.4			1.45	5.7		6.2	4.5		<0.3			4.5	<0.1	<0.05		-4.6
df13i	DH-13 (800m)				11.1	9.3		231	29.8	11.6	4.2	<0.2	<0.3	21.1	15.9			1.40	5.4		6.6	4.4		<0.3			3.4	<0.1	<0.05		-7.1
df13j	DH-13 (900m)				10.1	8.8		218	31.7	10.7	6.7	<0.2	<0.3	19.7	18.1			1.45	4.1		6.3	4.1		<0.3			3.3	<0.1	<0.05		-2.6
df13k	DH-13 (1000m)				14.4	8.9		199	30.9	10.7	6.1	<0.2	<0.3	17.6	16.7			1.38	3.6		6.5	4.6		<0.3			3.3	<0.1	0.05		-2.2

*Parameter values suggesting that the sample may not be representative of *in-situ* conditions are highlighted in yellow - highlighted sample numbers indicate that the sample may have been contaminated (Iwatsuki *et al.*, 2000a). Abbreviations are as follows: No. – sample number; loc. – borehole location (see Figs. 2.1_1 – 2.1_3); mbgl – meters below ground level; masl – meters above sea level.

Table 2.1_2. Chemical and isotopic parameters of groundwaters and drilling fluids*.

Sample No.	Pump-out vol./time l/hr	Sample vol./time l/hr	δD ‰ SMOW	$\delta^{18}O$ ‰ SMOW	$\delta^{13}C$ ‰	$\delta^{34}S$ ‰	C-14 activity % MC	C-14 age y B.P.	Tritium T.U.	U ppb	Th ppb	$O_2(aq)$ ppm	$H_2(aq)$ ppm	$CH_4(aq)$ ppb	TOC ppm	Sicc
OIDAWARA FORMATION																
13			-53.7	-8.4	-18.5		35.4		1	<0.05						-0.90
14			-57.2	-8.6	-15.9		35.2		1	<0.05						-0.88
94			-55.8	-8.5	-15.4		31.4		1							-0.93
95			-53.8	-8.4	-18.5		35.4		1							-0.96
dh11c									1.2						6.2	0.11
AKEYO FORMATION																
15			-52.6	-8.4					0	0.40						-0.91
16			-53.7	-8.4					0	0.82						-1.30
17			-53.5	-8.4	-20.1		31.0		0	0.21						-0.99
18			-53.8	-8.3	-17.4		28.8		0	0.15						-1.29
19			-58.3	-8.7	-12.3		30.5		0	0.29						-0.49
20			-56.5	-8.5	-14.3		40.7		3	0.33						-0.60
97			-54.2	-8.6	-15.2		49.6		5							-0.82
21			-53.5	-8.4	-20.7		66.4		0	0.20						-1.14
96			-52.8	-8.4	-20.7		66.4		2							-0.93
UPPER TOKI FORMATION																
22			-55.7	-8.5					0	1.3						-0.80
23			-55.9	-8.8	-7.8				0	4.8						-0.34
24			-59.2	-8.8	-5.2		32.8		0	0.08						-0.48
25			-58.2	-8.4	-10.9		27.2		0	0.11						-1.26
26			-58.8	-9.1	-13.4		27.0		0	0.37						-0.30
27			-56.2	-8.3	-11.7		24.0		2	<0.05						-2.06
152			-49.5	-8.0					2.3						4.0	-0.51
LOWER TOKI FORMATION																
28			-55.6	-8.6	-16.1				0	28.0						-0.16
29			-57.3	-8.8					0	8.4						-0.62
30			-58.7	-8.5	-12.6		26.5		0	0.39						-1.13
31			-57.5	-8.6	-10.3		18.1		0	1.8						-0.12
98			-55.4	-8.7	-13.9		21.7		2							-0.29
32			-58.1	-8.4	-15.1		12.0		0	1.0						-0.84
33			-57.1	-8.4	-15.8		5.6		2	0.16						-1.81
41			-55.0	-8.5					<3	0.1 – 1.0						
1			-59.4	-9.0					<0.3	2.3 – 2.8	0.2	b.d.[1]	0.12	b.d.	4.9	0.07
2			-57.7	-8.5			22.1		<0.3	0.04 - 0.06	0.004				1.8	-0.003
2a															0.3	
46			-54.0	-8.6	-17.6		11.0		0	0.15						-0.06
52			-56.0	-8.9											9.0	-1.59
53			-59.0	-9.1											9.1	-2.38
54															6.4	-2.42
150			-59.1	-9.0					<0.3						4.8	0.07
TONO MINE (LOWER TOKI FORMATION)																
67										0.01						0.11
77										2.0						-0.79
99			-52.8	-8.6	-17.7											
100			-54.8	-8.5	-17.6		10.8		0							
101			-54.3	-8.6	-17.6											
102			-57.5	-8.9	-14.0		6.7		0							
103			-53.6	-8.8	-17.0		7.8									
104			-55.4	-8.7	-18.5				0							
TOKI GRANITE																
3			-59.2	-8.7	-17.3		22.0		<0.3	0.04 - 0.11					1.1	-0.18
3a															0.2	

Sample No.	Pump-out vol./time l/hr	Sample vol./time l/hr	δD ‰ SMOW	$\delta^{18}O$ ‰ SMOW	$\delta^{13}C$ ‰	$\delta^{34}S$ ‰	C-14 activity % MC	C-14 age y B.P.	Tritium T.U.	U ppb	Th ppb	$O_2(aq)$ ppm	$H_2(aq)$ ppm	$CH_4(aq)$ ppb	TOC ppm	*SIcc*
34			-52.0	-8.2	-16.9				1	21.0						-0.75
35			-55.7	-8.5	-14.1		9.6		2							-0.89
105			-53.7	-8.6	-17.8		28.7		1							-0.51
51			-51.7	-8.1	-21.2											-3.41
6			-53.7	-8.2		12.4	99.0		2.9						2.0	0.88
7			-53.6	-8.3	-17.3	16.9	65.8		2.8						2.6	0.03
8				-8.5		5.5									7.9	0.66
9				-8.3	-17.1	4.5			2						2.4	0.32
10				-7.9		30.0			3						3.1	0.09
11			-53.2	-8.5	-20.3	21.3			2.6						0.5	0.25
5			-52.5	-8.0					4.6	0.07	0.01		21.0			-1.46
106			-56.7	-8.2	-17.5	10.7	45.5	6330	3.1						1.7	-0.50
107	355/108	11/4	-52.0	-8.2	-16.3		37.5	7880	2.1	4.4	0.07	b.d.	b.d.	10.0	1.7	-0.38
dh7d									2.2							0.21
dh7e									4.5							0.85
dh7f									1.4							0.63
108	292/155	12/3	-53.0	-8.0	-16.9		50.6	5480	2.3	0.21	0.04	b.d.	b.d.	10.0	2.4	0.77
dh7g									2.1							0.07
dh7h									1.0							0.43
dh7i									<0.9							0.80
dh7j									1.0							0.73
dh7k									4.0							0.91
dh7l									<0.5							0.77
dh7m									4.7							
dh7n									1.2							
109	228/97	12/7	-58.0	-8.5	-15.9		22.5	12000	3.4	0.4	0.43	b.d.	b.d.	20.0	1.3	0.32
dh7o									4.3							0.49
110	199/83	12/39	-54.0	-8.2	-15.5		39.0	7570	2.1	0.28	0.13	b.d.	b.d.	10.0	2.8	0.67
dh7p									6.8							0.67
dh7q									0.9							0.78
111	421/119	12/4	-54.0	-8.5	-17.8		36.7	8060	1.1	0.46		b.d.	b.d	20.0	0.8	-0.23
112	227/55	13/4	-54.0	-8.4	-17.9		31.3	9330	1.8	1.7		b.d	b.d	10.0	0.9	-0.21
113	573/118	13/4	-55.0	-8.4	-18.0		27.2	10470	3.7	2.1		b.d	b.d	20.0	1.0	-1.12
114	872/238	13/5	-56.0	-8.6	-14.5		18.8	13440	<1	2.0		b.d	b.d	5.0	0.6	-0.12
115	490/176	13/5	-58.0	-8.6	-16.9		29.9	9690	<1	0.77		b.d	b.d	10.0	0.9	0.09
dh9a															9.0	0.00
dh9b			-57.3	-8.8	-20.3		56.1		<1						25.0	0.13
dh9c			-59.0	-8.9	-21.2		45.0		4.8						65.0	0.10
dh10a			-54.1	-8.7					4.5							-1.33
dh10b			-52.5	-8.7					3.4							-1.50
dh10c									1.8						0.4	-0.03
dh11a			-46.9	-7.0					<2.3							-1.20
dh11b			-51.3	-7.9					3.7							-2.64
151			-56.7	-8.8					<0.3						0.2	0.18
154			-56.6	-8.7					<0.3						0.8	0.22
155			-56.1	-8.9					<0.3						0.6	0.15
156			-56.5	-8.8					<0.3						0.6	0.15
157			-56.9	-9.0					<0.3						0.9	0.23
153			-51.6	-8.3					0.38						0.4	-0.02
158			-50.6	-7.9					1.1						1.8	0.17
SHALLOW GROUNDWATER (QUATERNARY ALLUVIUM/ SETO GROUP)																
MC-8					-20.3		95.6		4.5						0.6	-3.55
MC-9															0.7	-1.39
MC-12					-20.4		105.7		4.6						1.4	-2.81
MC-13															0.3	-3.92

Sample No.	Pump-out vol./time l/hr	Sample vol./time l/hr	δD ‰ SMOW	$\delta^{18}O$ ‰ SMOW	$\delta^{13}C$ ‰	$\delta^{34}S$ ‰	C-14 activity % MC	C-14 age y B.P.	Tritium T.U.	U ppb	Th ppb	$O_2(aq)$ ppm	$H_2(aq)$ ppm	$CH_4(aq)$ ppb	TOC ppm	*Slcc*
MC-14															0.5	-3.46
MC-15					-14.2		100.1		4.4						0.7	-1.68
MC-16															1.0	-3.52
MC-17															0.7	-2.90
MC-18															3.1	-2.91
MC-19					-18.1		104.4		3.6						1.1	-1.96
MC-20															0.5	-3.84
MC-21					-17.2				3.9						0.3	-5.22
MC-24															0.5	-1.00
MC-25															0.7	-3.43
MC-26					-21.7		103.6		8.4						0.5	-3.83
MC-27															2.2	-3.66
MC-28															2.7	-0.90
MC-29															1.0	-1.24
MC-30					-18.4		101.3		4.5						1.2	-1.97
MC-31															0.1	-1.86
MC-32															0.9	-3.65
MC-33					-19.6				5.2						0.5	-3.58
MC-34															0.3	-3.58
MC-35															0.6	-1.53
MC-36															0.5	-2.98
MC-37															0.7	-5.40
DRILLING FLUIDS																
df5			-55.5	-8.0	-15.1			2710	7.5						1.0	
df6-8			-57.0	-8.4	-13.7		23.6	11590	2.7			1.2	b.d.	20.0	0.9	
df9			-56.3	-9.2	-17.7		14.4		1.5						0	
df1011									4.6			3.7	<0.002	<0.002	0	
df12a			-49.6	-8.0					3.6						8.0	0.11
df12b			-49.7	-8.0					3.0						4.8	0.19
df12c			-54.9	-8.8					0.83						5.4	-0.01
df12d			-55.7	-9.0					<0.35						1.1	0.50
df12e			-57.1	-9.0					<0.35						1.3	0.50
df12f			-57.3	-9.0					<0.35						1.3	0.35
df12g															0.5	-0.07
df12h															0.9	0.23
df13a			-48.9	-8.0					3.0						5.1	0.42
df13b			-48.3	-8.0					3.3						4.9	0.08
df13c			-48.1	-7.9					3.3						21.4	0.27
df13d			-49.0	-8.0					3.5						4.6	-0.11
df13e			-48.8	-8.2					3.3						3.2	-0.26
df13f			-52.9	-8.6					<0.28						5.2	0.86
df13g			-53.8	-8.6					0.48						4.7	0.53
df13h			-52.5	-8.5					0.56						4.3	0.60
df13i			-53.5	-8.6					0.47						5.2	0.12
df13j			-53.0	-8.5					0.79						1.6	-0.05
df13k			-52.4	-8.5					0.83						0.9	0.04

*- Parameter values suggesting that the sample may not be representative of *in-situ* conditions are highlighted in yellow - highlighted sample numbers indicate that the sample may have been contaminated (Iwatsuki *et al.*, 2000a). 1- below detection

Table 2.1_3. Summary of borehole sampling and groundwater analytical methods*.

No.	loc.	Date	Sample method	pH	Eh	cond.	Na^+	K^+	Ca^{2+}	Mg^{2+}	Sr^{2+}	SO_4^{2-}	F^-	Cl^-	NO_2^-	NO_3^-	NH_4^+	PO_4^{3-}	Si	Al	ΣFe	Fe^{2+}
OIDAWARA FORMATION																						
13	TH-6		MP	PM		PM	AAS	AAS	ICP	ICP	ICP	IC	IC	IC	IC	IC	IC	IC	ICP	ICP	ICP	CA
14	TH-8		MP	PM		PM	AAS	AAS	ICP	ICP	ICP	IC	IC	IC	IC	IC	IC	IC	ICP	ICP	ICP	CA
94	TH-8		MP	PM			AAS	AAS	ICP	ICP		IC	IC	IC		IC	IC					
95	TH-6		MP	PM			AAS	AAS	ICP	ICP		IC	IC	IC		IC	IC					
dh11c	DH-11	1999.12.15	1000GS	DCP	DCP	DCP	AAS	AAS	ICP	ICP	ICP	IC	IC	IC	IC	IC		CA	ICP	ICP	ICP	CA
AKEYO FORMATION																						
15	TH-1		MP	PM		PM	AAS	AAS	ICP	ICP	ICP	IC	IC	IC	IC	IC		IC	ICP	ICP	ICP	CA
16	TH-2		MP	PM		PM	AAS	AAS	ICP	ICP	ICP	IC	IC	IC	IC	IC		IC	ICP	ICP	ICP	CA
17	TH-3		MP	PM		PM	AAS	AAS	ICP	ICP	ICP	IC	IC	IC	IC	IC		IC	ICP	ICP	ICP	CA
18	TH-4		MP	PM		PM	AAS	AAS	ICP	ICP	ICP	IC	IC	IC	IC	IC		IC	ICP	ICP	ICP	CA
19	TH-6		MP	PM		PM	AAS	AAS	ICP	ICP	ICP	IC	IC	IC	IC	IC		IC	ICP	ICP	ICP	CA
20	TH-8		MP	PM		PM	AAS	AAS	ICP	ICP	ICP	IC	IC	IC	IC	IC		IC	ICP	ICP	ICP	CA
97	TH-8		MP	PM			AAS	AAS	ICP	ICP		IC	IC	IC		IC	IC					
21	AN-6		MP	PM		PM	AAS	AAS	ICP	ICP	ICP	IC	IC	IC	IC	IC		IC	ICP	ICP	ICP	CA
96	AN-6		MP	PM			AAS	AAS	ICP	ICP		IC	IC	IC		IC	IC					
UPPER TOKI FORMATION																						
22	TH-1		MP	PM		PM	AAS	AAS	ICP	ICP	ICP	IC	IC	IC	IC	IC		IC	ICP	ICP	ICP	CA
23	TH-2		MP	PM		PM	AAS	AAS	ICP	ICP	ICP	IC	IC	IC	IC	IC		IC	ICP	ICP	ICP	CA
24	TH-3		MP	PM		PM	AAS	AAS	ICP	ICP	ICP	IC	IC	IC	IC	IC		IC	ICP	ICP	ICP	CA
25	TH-4		MP	PM		PM	AAS	AAS	ICP	ICP	ICP	IC	IC	IC	IC	IC		IC	ICP	ICP	ICP	CA
26	TH-6		MP	PM		PM	AAS	AAS	ICP	ICP	ICP	IC	IC	IC	IC	IC		IC	ICP	ICP	ICP	CA
27	TH-8		MP	PM		PM	AAS	AAS	ICP	ICP	ICP	IC	IC	IC	IC	IC		IC	ICP	ICP	ICP	CA
152	DH-13	2000.7.27	1000PT	HMS	HMS	HMS	IC	IC	IC	IC	IC	IC	IC	IC	IC	IC	IC		CA	CA	CA	CA
LOWER TOKI FORMATION																						
28	TH-1		MP	PM		PM	AAS	AAS	ICP	ICP	ICP	IC	IC	IC	IC	IC		IC	ICP	ICP	ICP	CA
29	TH-2		MP	PM		PM	AAS	AAS	ICP	ICP	ICP	IC	IC	IC	IC	IC		IC	ICP	ICP	ICP	CA
30	TH-3		MP	PM		PM	AAS	AAS	ICP	ICP	ICP	IC	IC	IC	IC	IC		IC	ICP	ICP	ICP	CA
31	TH-4		MP	PM		PM	AAS	AAS	ICP	ICP	ICP	IC	IC	IC	IC	IC		IC	ICP	ICP	ICP	CA
98	TH-4		MP	PM		PM	AAS	AAS	ICP	ICP	ICP	IC	IC	IC	IC	IC		IC	ICP	ICP	ICP	CA
32	TH-6		MP	PM		PM	AAS	AAS	ICP	ICP	ICP	IC	IC	IC	IC	IC		IC	ICP	ICP	ICP	CA
33	TH-8		MP	PM		PM	AAS	AAS	ICP	ICP	ICP	IC	IC	IC	IC	IC		IC	ICP	ICP	ICP	CA
41				HMS	HMS								IC								ICP	
1	KNA-6		PS			HMS	AAS	AAS	ICP	ICP	ICP	IC	IC	IC	IC	IC		IC	ICP	ICP	ICP	CA
2	KNA-6		PS	HMS	HMS	HMS	AAS	AAS	ICP	ICP	ICP	IC	IC	IC	IC	IC		IC	ICP	ICP	ICP	CA
2a	KNA-6		PS																			
46	KNA-2		PS	HMS	HMS	HMS	AAS	AAS	ICP	ICP		IC	IC	IC					ICP	ICP		CA
52	TFA-1		Squeezing	PM			ICP	ICP	ICP	ICP	ICP	IC	ISE	IC	IC	IC			ICP	ICP	ICP	
53	TFA-1		Squeezing	PM			ICP	ICP	ICP	ICP	ICP	IC	ISE	IC	IC	IC			ICP	ICP	ICP	
54	TFA-1		Squeezing	PM			ICP	ICP	ICP	ICP	ICP	IC	ISE	IC	IC	IC			ICP	ICP	ICP	
150	DH-12		1000PT	HMS	HMS	HMS	IC	IC	IC	IC	IC	IC	IC	IC	IC	IC	IC		CA	CA	CA	CA
TOKI GRANITE																						
3	KNA-6		PS	HMS	HMS	HMS	AAS	AAS	ICP	ICP	ICP	IC	IC	IC	IC	IC	IC	IC	ICP	ICP	ICP	CA
3a	KNA-6	1997.12.18	PS																			
34	TH-1		MP	PM		PM	AAS	AAS	ICP	ICP	ICP	IC	IC	IC	IC	IC	IC	IC	ICP	ICP	ICP	CA
35	TH-6		MP	PM		PM	AAS	AAS	ICP	ICP	ICP	IC	IC	IC	IC	IC	IC	IC	ICP	ICP	ICP	CA
105	TH-8		MP	PM		PM	AAS	AAS	ICP	ICP		IC	IC	IC		IC	IC					
51	DH-3		MP	PM		PM	AAS	AAS	ICP	ICP	ICP	IC	IC	IC			IC		ICP	ICP	ICP	
6	DH-3		MP	PM		PM	AAS	AAS	ICP	ICP	ICP	IC	IC	IC	IC	IC	IC	IC	ICP	ICP	ICP	CA
7	DH-3		MP	PM		PM	AAS	AAS	ICP	ICP	ICP	IC	IC	IC	IC	IC	IC	IC	ICP	ICP		
8	DH-3		MP	PM		PM	AAS	AAS	ICP	ICP	ICP	IC	IC	IC	IC	IC		IC	ICP	ICP	ICP	CA
10	DH-3		MP	PM		PM	AAS	AAS	ICP	ICP	ICP	IC	IC	IC	IC	IC		IC	ICP	ICP	ICP	CA
11	DH-3		MP	PM		PM	AAS	AAS	ICP	ICP	ICP	IC	IC	IC	IC	IC		IC	ICP	ICP	ICP	CA
5	DH-4	1995.4.18	PS	PM		PM	AAS	AAS	ICP	ICP	ICP	IC	IC	IC	IC	IC		IC	ICP	ICP	ICP	CA
106	DH-5	1997.8.6-21	1000GS	DCP	DCP	DCP	AAS	AAS	ICP	ICP	ICP	IC	IC	IC	IC,CA	IC,CA	CA	CA	ICP	ICP	ICP	CA
107	DH-6	1997.12.19-22	1000GS	DCP	DCP	DCP	AAS	AAS	ICP	ICP	AAS	IC	IC	IC	CA	CA	CA	CA	CA,ICP	ICP	ICP	CA

No.	loc.	Date	Sample method	pH	Eh	cond.	Na^+	K^+	Ca^{2+}	Mg^{2+}	Sr^{2+}	SO_4^{2-}	F^-	Cl^-	NO_2^-	NO_3^-	NH_4^+	PO_4^{3-}	Si	Al	ΣFe	Fe^{2+}
dh7d	DH-7	1999.5	MP	PM		PM	AAS	AAS	AAS	AAS		IC	IC	IC		IC			AAS		AAS	
dh7e	DH-7	1999.6	MP	PM		PM	AAS	AAS	AAS	AAS		IC	IC	IC		IC			AAS		AAS	
dh7f	DH-7	2000.7	MP	PM		PM	AAS	AAS	AAS	AAS		IC	IC	IC		IC			AAS		AAS	
108	DH-7	1998.4.20-22	1000GS	DCP	DCP	DCP	AAS	AAS	ICP	ICP	AAS	IC	IC	IC	CA	CA	CA	CA	CA,ICP	ICP	ICP	CA
dh7g	DH-7	1999.7	MP	PM		PM	AAS	AAS	ICP	AAS		IC	IC	IC		IC			AAS		AAS	
dh7h	DH-7	2000.8	MP	PM		PM	AAS	AAS	AAS	AAS		IC	IC	IC		IC			AAS		AAS	
dh7l	DH-7	1999.8	MP	PM		PM	AAS	AAS	AAS	AAS		IC	IC	IC		IC			AAS		AAS	
dh7j	DH-7	2000.9	MP	PM		PM	AAS	AAS	AAS	AAS		IC	IC	IC		IC			AAS		AAS	
dh7k	DH-7	1999.9	MP	PM		PM	AAS	AAS	AAS	AAS		IC	IC	IC		IC			AAS		AAS	
dh7l	DH-7	2000.10	MP	PM		PM	AAS	AAS	AAS	AAS		IC	IC	IC		IC			AAS		AAS	
dh7m	DH-7	1999.10	MP	PM		PM	AAS	AAS	AAS	AAS		IC	IC	IC		IC			AAS		AAS	
dh7n	DH-7	200.11	MP	PM		PM	AAS	AAS	AAS	AAS		IC	IC	IC		IC			AAS		AAS	
109	DH-7	1998.4.2-9	1000GS	DCP	DCP	DCP	AAS	AAS	ICP	ICP	AAS	IC	IC	IC	CA	CA	CA	CA	CA,ICP	ICP	ICP	CA
dh7o	DH-7	1999.11	MP	PM		PM	AAS	AAS	AAS	AAS		IC	IC	IC		IC			AAS		AAS	
110	DH-7	1998.3.11-19	1000GS	DCP	DCP	DCP	AAS	AAS	ICP	ICP	AAS	IC	IC	IC	CA	CA	CA	CA	CA,ICP	ICP	ICP	CA
dh7p	DH-7	1999.12	MP	PM		PM	AAS	AAS	AAS	AAS		IC	IC	IC		IC			AAS		AAS	
dh7q	DH-7	2000.12	MP	PM		PM	AAS	AAS	AAS	AAS		IC	IC	IC		IC			AAS		AAS	
111	DH-8	1998.3.16-27	1000GS	DCP	DCP	DCP	AAS	AAS	ICP	ICP	AAS	IC	IC	IC	CA	CA	CA	CA	CA,ICP	ICP	ICP	CA
112	DH-8	1998.4.2-5	1000GS	DCP	DCP	DCP	AAS	AAS	ICP	ICP	AAS	IC	IC	IC	CA	CA	CA	CA	CA,ICP	ICP	ICP	CA
113	DH-8	1998.4.13-16	1000GS	DCP	DCP	DCP	AAS	AAS	ICP	ICP	AAS	IC	IC	IC	CA	CA	CA	CA	CA,ICP	ICP	ICP	CA
114	DH-8	1998.4.29-5.3	1000GS	DCP	DCP	DCP	AAS	AAS	ICP	ICP	AAS	IC	IC	IC	CA	CA	CA	CA	CA,ICP	ICP	ICP	CA
115	DH-8	1998.5.14-18	1000GS	DCP	DCP	DCP	AAS	AAS	ICP	ICP	AAS	IC	IC	IC	CA	CA	CA	CA	CA,ICP	ICP	ICP	CA
dh9a	DH-9	1998.11.26-27	1000GS	DCP	DCP	DCP	AAS	AAS	ICP	ICP	ICP	IC	IC	IC	CA	CA	CA	CA	ICP	ICP	ICP	CA
dh9b	DH-9	1998.12.10-12	1000GS	DCP	DCP	DCP	AAS	AAS	ICP	ICP	ICP	IC	IC	IC	CA	CA	CA	CA	ICP	ICP	ICP	CA
dh9c	DH-9	1999.1.26-30	1000GS	DCP	DCP	DCP	AAS	AAS	ICP	ICP	ICP	IC	IC	IC	CA	CA	CA	CA	ICP	ICP	ICP	CA
dh10a	DH-10	1999.11,10-12	1000GS	DCP	DCP	DCP	AAS	AAS	ICP	ICP	ICP	IC	IC	IC	IC	IC		CA	ICP		ICP	CA
dh10b	DH-10		1000PT	PM		PM	AAS	AAS	ICP	ICP	ICP	IC	IC	IC		IC			ICP	ICP	ICP	CA
dh10c	DH-10		1000PT	PM		PM	AAS	AAS	ICP	ICP	ICP	IC	IC	IC		IC			ICP	ICP	ICP	CA
dh11a	DH-11		1000PT	PM		PM	AAS	AAS	ICP	ICP	ICP	IC	IC	IC		IC			ICP	ICP	ICP	
dh11b	DH-11		1000PT	PM		PM	AAS	AAS	ICP	ICP	ICP	IC	IC	IC		IC			ICP	ICP	ICP	
151	DH-12	2000.8.27	1000PT	HMS	HMS	HMS	IC	IC	IC	IC	IC	IC	IC	IC	IC	IC	IC		CA	CA	CA	CA
154	DH-12	2000.12.27	1000PT	HMS	HMS	HMS	IC	IC	IC	IC	IC	IC	IC	IC	IC	IC	IC		CA	CA	CA	CA
155	DH-12	2000.12.19	1000PT	HMS	HMS	HMS	IC	IC	IC	IC	IC	IC	IC	IC	IC	IC	IC		CA	CA	CA	CA
156	DH-12	2000.12.7	1000PT	HMS	HMS	HMS	IC	IC	IC	IC	IC	IC	IC	IC	IC	IC	IC		CA	CA	CA	CA
157	DH-12	2000.11.22	1000PT	HMS	HMS	HMS	IC	IC	IC	IC	IC	IC	IC	IC	IC	IC	IC		CA	CA	CA	CA
153	DH-13	2000.9.1	1000PT	HMS	HMS	HMS	IC	IC	IC	IC	IC	IC	IC	IC	IC	IC	IC		CA	CA	CA	CA
158	DH-13	2000.12.19	1000PT	HMS	HMS	HMS	IC	IC	IC	IC	IC	IC	IC	IC	IC	IC	IC		CA	CA	CA	CA
MIU-4-1	MIU-4	2000.8.13	1000PT	HMS	HMS	HMS	IC	IC	IC	IC	IC	IC	IC	IC	IC	IC	IC		CA	CA	CA	CA
MIU-4-2	MIU-4	2000.12.2	1000PT	HMS	HMS	HMS	IC	IC	IC	IC	IC	IC	IC	IC	IC	IC	IC		CA	CA	CA	CA
MIU-4-3	MIU-4	2001.7.2	1000PT	HMS	HMS	HMS	IC	IC	IC	IC	IC	IC	IC	IC	IC	IC	IC		CA	CA	CA	CA
MIU-4-4	MIU-4		1000PT	HMS	HMS	HMS	IC	IC	IC	IC	IC	IC	IC	IC	IC	IC	IC		CA	CA	CA	CA
SHALLOW GROUND WATER																						
MC-8			NK	PM		PM	AAS	AAS	ICP	ICP		IC	IC	IC	IC	IC	IC	IC	ICP	ICP	ICP	
MC-9			NK	PM		PM	AAS	AAS	ICP	ICP		IC	IC	IC	IC	IC	IC	IC	ICP	ICP	ICP	
MC-10			NK	PM		PM	AAS	AAS	ICP	ICP		IC	IC	IC	IC	IC	IC	IC	ICP	ICP	ICP	
MC-12			NK	PM		PM	AAS	AAS	ICP	ICP		IC	IC	IC	IC	IC	IC	IC	ICP	ICP	ICP	
MC-13			NK	PM		PM	AAS	AAS	ICP	ICP		IC	IC	IC	IC	IC	IC	IC	ICP	ICP	ICP	
MC-14			NK	PM		PM	AAS	AAS	ICP	ICP		IC	IC	IC	IC	IC	IC	IC	ICP	ICP	ICP	
MC-15			NK	PM		PM	AAS	AAS	ICP	ICP		IC	IC	IC	IC	IC	IC	IC	ICP	ICP	ICP	
MC-16			NK	PM		PM	AAS	AAS	ICP	ICP		IC	IC	IC	IC	IC	IC	IC	ICP	ICP	ICP	
MC-17			NK	PM		PM	AAS	AAS	ICP	ICP		IC	IC	IC	IC	IC	IC	IC	ICP	ICP	ICP	
MC-18			NK	PM		PM	AAS	AAS	ICP	ICP		IC	IC	IC	IC	IC	IC	IC	ICP	ICP	ICP	
MC-19			NK	PM		PM	AAS	AAS	ICP	ICP		IC	IC	IC	IC	IC	IC	IC	ICP	ICP	ICP	
MC-20			NK	PM		PM	AAS	AAS	ICP	ICP		IC	IC	IC	IC	IC	IC	IC	ICP	ICP	ICP	
MC-21			NK	PM		PM	AAS	AAS	ICP	ICP		IC	IC	IC	IC	IC	IC	IC	ICP	ICP	ICP	
MC-22			NK	PM		PM	AAS	AAS	ICP	ICP		IC	IC	IC	IC	IC	IC	IC	ICP	ICP	ICP	
MC-24			NK	PM		PM	AAS	AAS	ICP	ICP		IC	IC	IC	IC	IC	IC	IC	ICP	ICP	ICP	

No.	loc.	Date	Sample method	pH	Eh	cond.	Na^+	K^+	Ca^{2+}	Mg^{2+}	Sr^{2+}	SO_4^{2-}	F^-	Cl^-	NO_2^-	NO_3^-	NH_4^+	PO_4^{3-}	Si	Al	ΣFe	Fe^{2+}
MC-25			NK	PM		PM	AAS	AAS	ICP	ICP		IC	IC	IC	IC	IC	IC	IC	ICP	ICP	ICP	
MC-26			NK	PM		PM	AAS	AAS	ICP	ICP		IC	IC	IC	IC	IC	IC	IC	ICP	ICP	ICP	
MC-27			NK	PM		PM	AAS	AAS	ICP	ICP		IC	IC	IC	IC	IC	IC	IC	ICP	ICP	ICP	
MC-28			NK	PM		PM	AAS	AAS	ICP	ICP		IC	IC	IC	IC	IC	IC	IC	ICP	ICP	ICP	
MC-29			NK	PM		PM	AAS	AAS	ICP	ICP		IC	IC	IC	IC	IC	IC	IC	ICP	ICP	ICP	
MC-30			NK	PM		PM	AAS	AAS	ICP	ICP		IC	IC	IC	IC	IC	IC	IC	ICP	ICP	ICP	
MC-31			NK	PM		PM	AAS	AAS	ICP	ICP		IC	IC	IC	IC	IC	IC	IC	ICP	ICP	ICP	
MC-32			NK	PM		PM	AAS	AAS	ICP	ICP		IC	IC	IC	IC	IC	IC	IC	ICP	ICP	ICP	
MC-33			NK	PM		PM	AAS	AAS	ICP	ICP		IC	IC	IC	IC	IC	IC	IC	ICP	ICP	ICP	
MC-34			NK	PM		PM	AAS	AAS	ICP	ICP		IC	IC	IC	IC	IC	IC	IC	ICP	ICP	ICP	
MC-35			NK	PM		PM	AAS	AAS	ICP	ICP		IC	IC	IC	IC	IC	IC	IC	ICP	ICP	ICP	
MC-36			NK	PM		PM	AAS	AAS	ICP	ICP		IC	IC	IC	IC	IC	IC	IC	ICP	ICP	ICP	
MC-37			NK	PM		PM	AAS	AAS	ICP	ICP		IC	IC	IC	IC	IC	IC	IC	ICP	ICP	ICP	
MC-38			NK	PM		PM	AAS	AAS	ICP	ICP		IC	IC	IC	IC	IC	IC	IC	ICP	ICP	ICP	

*- Abbreviations:

General: No. – sample number; loc. – borehole location (see Figs. 2.1_1 – 2.1_3).

Sampling method: MP – multiple piezometer (MP) monitoring system; PS – packer type groundwater sampler; "squeezing" – porewater squeezed out of the drillcore by compression; 1000GS – deep groundwater sampling apparatus equipped with DCP (see below); 1000PT – deep groundwater sampling apparatus without DCP.

Analytical method: PM - portable meter; DCP – downhole chemical probe; HMS hydrochemical monitoing system; AAS – atomic absorption spectrometry; ICP – inductively coupled plasma light emission spectrometry; IC – ion chromatography; CA – colorimetry; ISE – ion-selective electrode; NK – not known.

where Σ *cations* and Σ *anions* refer to total concentrations (meq l^{-1}) of each element summed over all major cations and anions determined in the analysis. These quantities were calculated in the present evaluation for each analysis in Table 2.1_1 using the Geochemist's Workbench (GWB) geochemical modeling software package (Bethke, 1996), and a supporting thermodynamic database that was developed specifically for the TGRP (Iwatsuki *et al.*, 2000a). An acceptable charge balance, indicating that the analysis is of good quality, is generally taken to be in the range 0 ± 5 % (Friedman and Erdman, 1982). Charge imbalances as high as 0 ± 10 % may, however, be tolerable, particularly if the groundwaters are extremely dilute or highly saline (*e.g.*, Lampén and Snellman, 1993).

2.2.1 Analytical constraints on dissolved carbonate

Two different analytical techniques and several associated computational approaches have been used to determine the total carbonate concentrations listed in Table 2.1_1. The analytical methods include: 1) direct measurement of dissolved inorganic carbon (IC) by infrared absorption spectrometry (IR), and 2) indirect measurement by acidimetric titration (see Table 2.1_3). In this section we explain how these different analytical techniques and associated computations are accounted for in the charge-balance calculations.

Direct IR analyses were made for IC and for total dissolved carbon (organic carbon is determined by difference, see Table 2.1_2). Because the IR determinations provide a direct measure of IC, these analyses are taken at face value in the present study. To do this, the IC values in Table 2.1_1 (in ppm) are multiplied by a conversion factor of 5.08 (representing the ratio of the molecular weight of HCO_3^- to the atomic weight of C) to obtain the corresponding concentration of the GWB *basis* species[2] HCO_3^-. It is important to note that this approach is appropriate only if the redox potential of the groundwater is sufficiently oxidizing that the concentration of $CH_4(aq)$ is negligible. This is because $CH_4(aq)$ does not contribute to IC in an IR measurement, but significant concentrations of this species will be calculated by GWB if redox conditions are sufficiently reducing. Under such conditions it is necessary to decouple the CO_2 - CH_4 redox pair in the GWB calculations.

Several groundwater analyses in Table 2.1_1 include alkalinity measurements. Conceptually, the alkalinity of a solution is the amount of strong base that must be neutralized to reach a pH corresponding to a solution of pure $CO_2(aq)$ in water (*e.g.*, Butler, 1982; Fresenius *et al.* 1988). In practice, the alkalinity of a solution is determined by measuring the pH during titration of a sample with a strong acid. Alkalinity is thus the total amount of acid taken up by all solute species during the titration, and is usually expressed in terms of the equivalents of acid used as meq l^{-1} or meq kg^{-1}. Alkalinity titrations are presently carried out electrometrically to a specified pH between 4.3 and 4.8.

A point worth emphasizing for future reference is that the alkalinity is nearly equivalent to IC in most groundwaters if the pH is between about 6.5 and 10.5. Under such conditions the

[2] Wolery (1992) and Bethke (1996) provide succinct descriptions of the concept of a basis species and its (normally) direct correspondence to total dissolved elemental concentrations that are determined in a water analysis.

contribution to IC of the aqueous species $CO_2(aq)$ is negligible and the alkalinity, like IC, is then determined only by the concentrations of all other carbonate species (*i.e.*, HCO_3^-, CO_3^{2-}, and related ion pairs). Aqueous species other than carbonates may, however, contribute significantly to the alkalinity under certain conditions. For example, in reducing waters,

$NH_3(aq) + H^+ = NH_4^+$, and

$HS^- + H^+ = H_2S(aq)$

may be important reactions. In moderately alkaline waters under reducing or oxidizing conditions the reaction

$HSiO_3^- + H^+ = SiO_2(aq) + H_2O(l)$

and reactions with polymeric forms of silica contribute to alkalinity. Organic acids may also contribute substantially to the alkalinity of groundwaters containing high concentrations of dissolved organic carbon.

Three approaches are used to deal with alkalinity in the charge-balance calculations. First, if both IC and alkalinity measurements are available, IC is used to calculate the concentration of HCO_3^- following the procedure noted above. Converting both IC and alkalinity to units of meq l^{-1}, assuming as a first approximation that the amount of non-carbonate alkalinity is negligible, and comparing results provides a check on the internal consistency of the two analyses.

Second, as noted in Section 2.1, some of the original references to the data in Table 2.1_1 report only HCO_3^- and CO_3^{2-} concentrations calculated from measured alkalinities, pH and temperature. It was apparently assumed in these calculations that non-carbonate contributions to the alkalinity are negligible. In such cases, the concentrations of HCO_3^- and CO_3^{2-} are accepted provisionally, converted to units of meq kg^{-1}, and added together to give the concentration of the basis species HCO_3^-. The original alkalinity value is then back calculated from the reported concentrations of HCO_3^- and CO_3^{2-} to afford comparison with other alkalinities determined by titration.

Third, charge balances are not calculated if the analysis includes only an alkalinity measurement. This is necessary because GWB does not accept alkalinity as an input parameter, and pragmatic because there are relatively few such analyses in Table 2.1_1. A reconnaissance study to evaluate the internal consistency of analyses in which both alkalinity and IC were determined was carried out, however, using the PHREEQC geochemical modeling code (Parkhurst & Appelo, 1999), which accepts either alkalinity or IC as input constraints. Results are summarized in Section 2.2.3.

2.2.2 Results of charge-balance calculations

Charge balances calculated using GWB and Eqn. (2.2.1) are listed in the final column of Table 2.1_1, and are plotted versus the corresponding total ionic concentration of the water sample in Fig. 2.2.2_1. As can be seen, the charge balance of many of the analyses lies within the strictly

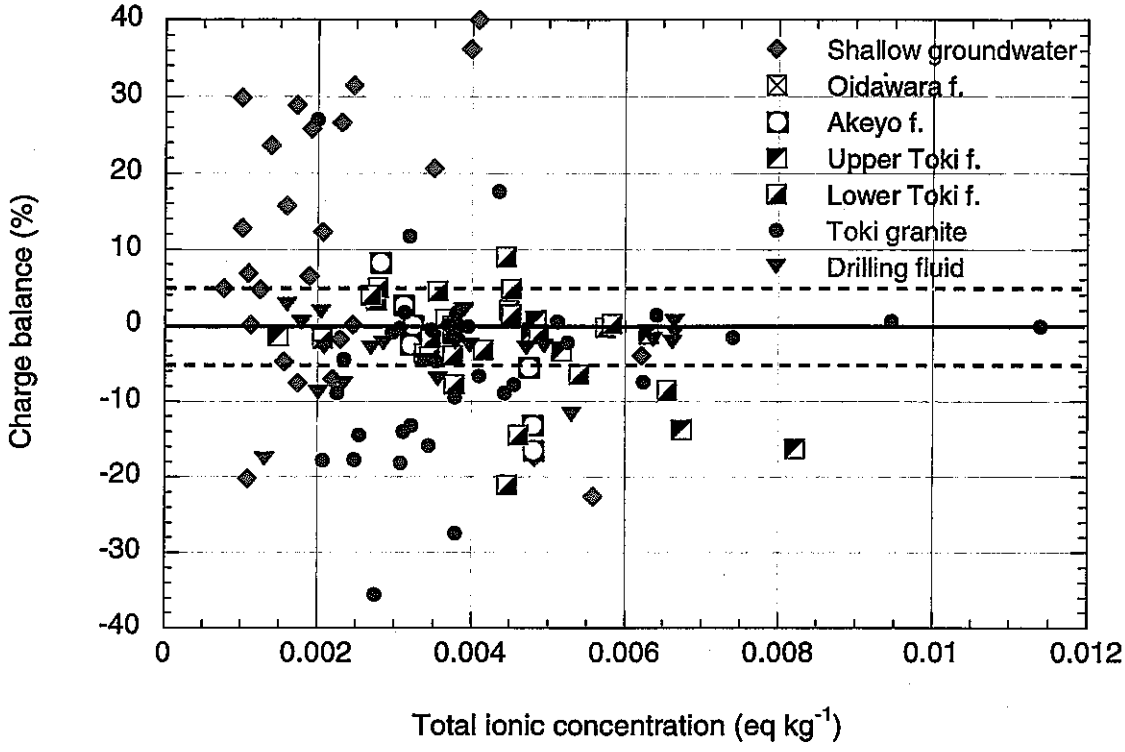

Figure 2.2.2_1. Charge balances plotted versus the total ionic concentration of water samples.

acceptable range of 0 ± 5 %, but charge imbalances exceeding these limits are calculated for many other samples. Most of the groundwaters are extremely dilute, and there appears to be a tendency for the magnitude of any charge imbalances to increase as total ionic concentration decreases. Most of the excessively positive charge imbalances are calculated for shallow groundwaters (MC-series, Table 2.1_1)[3]. Samples with large negative charge imbalances are mainly of deep groundwaters from the Toki granite.

2.2.3 Factors contributing to poor charge balances

There appear to be a number of reasons why the calculated charge imbalances for many of the Tono groundwaters lie significantly outside the acceptable range of 0 ± 5 %. These reasons are examined in the following paragraphs.

Inaccurate analyses of IC and (or) alkalinity. Analytical problems related to these parameters are revealed by internal inconsistencies between their reported values in a groundwater analysis that includes both types of measurement. To explore associated effects on calculated charge

[3] The three granite waters exhibiting charge balances greater than + 5 % are chemically similar to shallow groundwaters. One was sampled from within a few meters of the surface (DH-3; Sample 51) and has a high ^{14}C content (87 %MC; see Table 2.1_2), which suggests it was recently recharged from the surface. Another (Sample 5 from DH-4) contains a relatively high concentration of tritium (4.5 T.U.) similar to levels found in shallow groundwaters (Table 3.1_2), and the third (Sample dh9b) may have been contaminated with drilling fluid or shallow groundwater.

imbalances, it was decided to perform some test calculations with the PHREEQC code, which accepts either IC or alkalinity as input (as noted above, GWB does not accept the latter as input). The calculations are based on a limited set of data for samples from boreholes DH-3, DH-7, DH-12 and DH-13. The samples from DH-3 (Sample 51) and DH-7 (Samples 108 – 110) were chosen because they had some of the worst charge balances noted above (Table 2.1_1). The main conclusions from this evaluation are summarized in the following paragraphs.

The analyses of samples from DH-12 and DH-13 are internally consistent in that the charge balances calculated using either alkalinity or IC as input are below 2%. Samples 108, 109, and 51 from DH-7 and DH-3 do not have internally consistent analyses (*i.e.*, alkalinity is not consistent with IC) and illustrate a variety of causes for such inconsistencies.

The charge balances for Sample 109, from 837m depth in DH-7, are 4% when calculated from the analytical data and less than 1% when modeled using PHREEQC and alkalinity as input. This indicates internal consistency among the analytical data, including the alkalinity. However, in spite of the fact that the measured alkalinity and IC values are nearly the same, which commonly indicates consistency between the two, modeling with IC as input leads to a charge imbalance of –21%. This shows that the IC value is too high for consistency with the remainder of the analytical data. The excessive IC value may result from sample contamination by contact with air, or from inadequate filtering of particulates containing carbonate.

The ion balances for Sample 108, from 564m in DH-7, are poor no matter how they are calculated or modeled. The poor balances calculated from the analytical data and modeled using alkalinity as input are associated with the high NH_4^+ content reported for this sample. Acceptable charge balances can be reached assuming that the alkalinity reported does not include the alkalinity contribution from $NH_3(aq)$, which dominates over NH_4^+ at the high pH of this sample. This does not affect the charge imbalance modeled using IC, however. This imbalance, like that of Sample 109, can be attributed to too high a measured IC value. Adjusting IC for charge balance gives a modeled alkalinity similar to the sum of the measured alkalinity and $NH_3(aq)$ alkalinity. Thus, there appear to be two difficulties with the analytical data for this sample: (1) the measured IC is too high, and (2) the measured alkalinity is grossly inaccurate.

No alkalinity value is reported for Sample 51, from near the surface in DH-3. Assuming that alkalinity equals IC leads to a poor charge balance calculated from the analytical data and a worse balance from the modeling using PHREEQC and IC as input. The probable cause is that the reported IC is too low, perhaps due to CO_2 loss during sampling, storage or analysis. Such loss is not uncommon because of the high $P_{CO2(g)}$ values in waters with such low pH values.

Contamination by contact with air. A potential source of the inconsistencies between alkalinity and IC noted above may be losses or gains of $CO_2(g)$ from the sample by contact with ambient air. Such contamination is a common problem that may occur during storage if sample containers are inadequately sealed, and (or) during sampling and analysis (*e.g.*, Lampén and Snellman, 1993). Some of the poor charge balances shown in Fig. 2.2.2_1 appear to result from such contamination. This possibility is evaluated with reference to Fig. 2.2.3_1, where for each sample in Table 2.1_1 that includes an IC analysis, charge balances calculated using GWB are plotted versus the corresponding partial pressure of $CO_2(g)$.

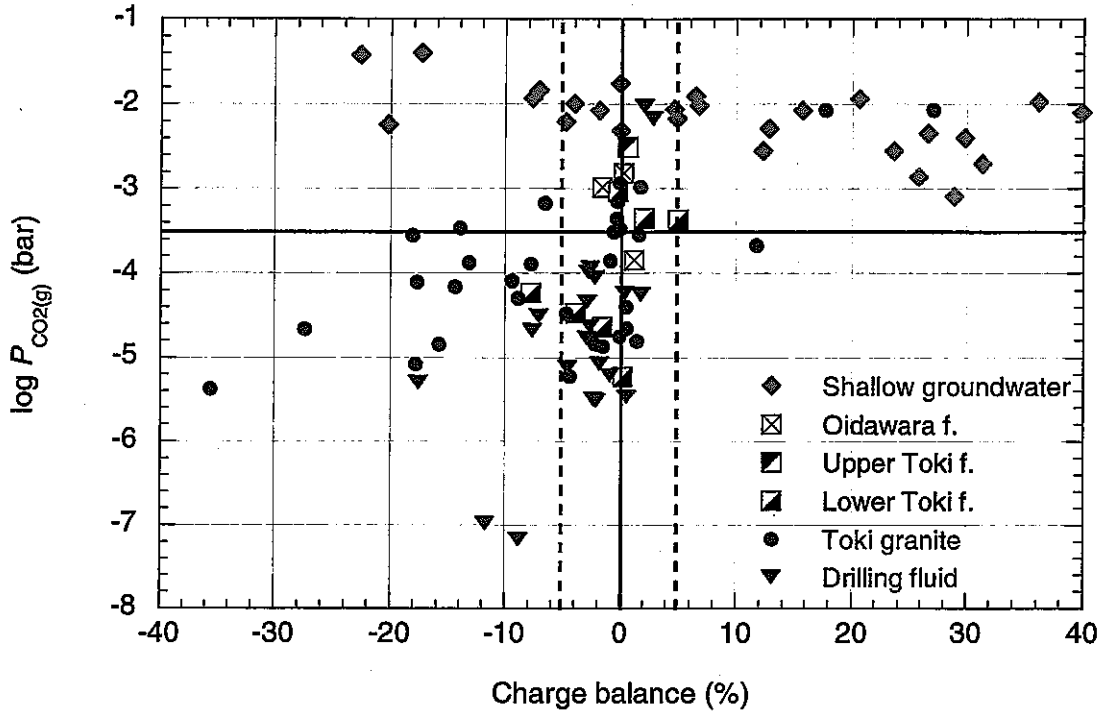

2.2.3_1. Plot showing calculated charge imbalances versus log $P_{CO2(g)}$.

The results shown in Fig. 2.2.3_1 are interpreted with two observations in mind. The first deals with the chemical potential controlling the tendency for $CO_2(g)$ to dissolve into or exsolve from a water sample. The horizontal line in the figure represents the approximate $CO_2(g)$ partial pressure of the ambient atmosphere at room temperature, 25 °C (*e.g.*, Langmuir, 1997). Thus, if the sample $P_{CO2(g)}$ is lower than that of the surrounding atmosphere, the potential exists for atmospheric $CO_2(g)$ to enter the sample and dissolve into the groundwater. Conversely, if the sample's $P_{CO2(g)}$ is greater than that of the ambient atmosphere, then $CO_2(g)$ may exsolve from the groundwater and escape to the atmosphere.

The second observation pertinent to the interpretation of Fig. 2.2.3_1 is that although $P_{CO2(g)}$ is calculated based on the groundwater's IC content, pH and temperature, these quantities were measured at different times on different splits of the same groundwater sample. The pH and temperature were measured in the field, but IC was analyzed later in the laboratory. Losses or gains of $CO_2(g)$ from a given sample cannot affect charge balance because the balance is maintained by changes in the concentrations of other anions and cations, including H^+. This is not the case, however, if the pH and IC measurements are made on different samples. Thus any loss of $CO_2(g)$ from the laboratory sample will result in a positive charge imbalance if the field pH is used in the calculation because the IC content of the sample is too low. Conversely, a gain of $CO_2(g)$ will result in a negative charge imbalance because the IC content is then too high.

Based on these two observations, the results shown in Fig. 2.2.3_1 are interpreted as follows. The solid vertical line in the figure represents an accurate groundwater analysis having no charge imbalance. This line and the atmospheric $P_{CO2(g)}$ line together divide the figure into quadrants. If

any $CO_2(g)$ was lost or gained from samples used in the laboratory IC measurements, the resultant charge imbalances should plot in the upper right or lower left quadrants, respectively. As can be seen, this is the case for most of the samples for which charge imbalances significantly exceed ± 5 %. Negative charge imbalances are calculated mainly for granite groundwaters where $CO_2(g)$ partial pressures are much lower than atmospheric, whereas positive balances are calculated for shallow groundwaters in which $P_{CO2(g)}$ values are as high as those typically found in soil waters (*e.g.*, Stumm and Morgan, 1996). This line of reasoning is not compatible with any charge imbalances plotting in the upper left or lower right quadrants of Fig. 2.2.3_1, and as can be seen such occurrences are limited to just three of the shallow groundwaters. It thus appears that the root cause of significant charge imbalances in many of the Tono groundwater samples is a loss or gain of CO_2 during sample storage and (or) analysis. Measuring IC and alkalinity as soon as possible after sampling, and isolating the samples as much as possible from contact with air during the measurements, can minimize such problems.

Non-carbonate contributions to alkalinity. Some of the poor charge balances shown in Fig. 2.2.2_1 may indicate that species other than carbonate are important sources of alkalinity in these groundwaters. As noted in Section 2.2.1, the reported concentrations of HCO_3^- and CO_3^{2-} in Table 2.1_1 are calculated from measured alkalinities, pH and temperature assuming that non-carbonate contributions to the alkalinity are negligible. In six of these samples, however, the groundwaters also contain high concentrations of HS^- (Samples 18, 19, 24, 26, 30 and 32; Table 2.1_1). Sulfide may be an important source of alkalinity as noted in Section 2.2.1. As can be seen in Fig. 2.2.3_2, large negative charge imbalances are calculated for these samples, but not for others in which HS^- concentrations are low. The negative charge imbalances thus appear to be the result of calculated HCO_3^- and CO_3^{2-} concentrations that are too high because they were incorrectly calculated by assuming that only these species contribute to the measured alkalinity.

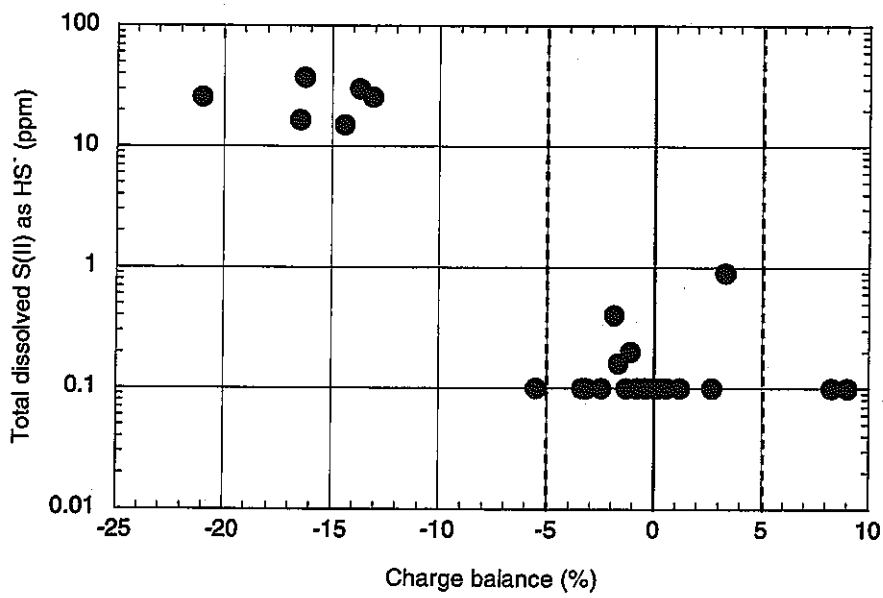

Figure 2.2.3_2. Relation between calculated charge imbalances and total dissolved sulfide [S(II)] concentrations in Tono groundwaters. Concentrations plotting at the detection limit (0.1 ppm) are maximum values.

In summary, a number of factors are apparently responsible for the poor charge balances shown in Table 2.1_1. They include: 1) analytical errors (*e.g.*, of alkalinity), 2) errors arising from the use of IC values that are unrepresentative because CO_2 was gained by or lost from the sample during storage and (or) analysis, and 3) errors arising from the invalid assumption that non-carbonate contributions to the alkalinity of Tono groundwaters are always negligible. As a result, nearly one in three of the groundwater analyses considered in this assessment suffer from charge imbalances that exceed the strictly acceptable range of 0 ± 5 %.

2.2.4 Correction of charge imbalances

The poor charge balances noted above must be dealt with before these analyses can be considered in the interpretations of regional groundwater chemistry discussed later (Sections 3 and 4). This is an important problem that can be resolved in one of four ways:

1. eliminate analyses for which the charge imbalance is unacceptable (*e.g.*, $> 0 \pm 5$ %),
2. do nothing, and instead carry any imbalances through calculations supporting the interpretations,
3. correct the imbalances in cases where they exceed the accepted range, or
4. correct all charge imbalances.

The first approach is unacceptable because a rather high percentage of the available analyses have marginal or poor charge balances. The second approach may be unnecessary because the causes of the charge imbalances are reasonably well understood in most cases, and might therefore be corrected. The latter of the remaining approaches is selected for detailed evaluation in this study. It is preferred over the penultimate approach because all the groundwater analyses are treated in a consistent manner, and because the correction procedure (see below) progressively minimizes differences between corrected and uncorrected compositions as the magnitude of the analytical charge imbalance decreases.

The correction procedure is based on the common geochemical modeling practice of adjusting the analyzed concentration of a major cation or anion until charge balance is achieved (*e.g.*, Wolery, 1992). Based on the discussion in Section 2.2.3, it appears that almost all of the poor charge balances result from inaccurate, unrepresentative or misinterpreted measurements of IC or alkalinity. The correction procedure therefore assumes that the water sample is perfectly charge balanced, and uses this constraint with GWB to calculate the corresponding concentration of the basis species HCO_3^-. Implicit in this approach is the key assumption that the values of all other parameters in the groundwater analysis are both accurate and representative.

The validity of this assumption is evaluated as follows. We first assume that the concentration of the basis species HCO_3^- is fixed by charge balance, as noted above, and then calculate the corresponding total alkalinity (T_{alk}) using the following equation

$$T_{alk} = \sum_i b_{alk,i} M_i ,$$

where $b_{alk,I}$ (equ. mol^{-1}) refers to the alkalinity factor for each species, i, and M_i stands for its molarity. The alkalinity factor represents the number of equivalents of acid consumed by the species on titration to the end-point pH. Values of $b_{alk,i}$ are taken from the thermodynamic database supporting the PHREEQC code (Parkhurst and Appelo, 1999). Molarities are calculated using GWB.

The accuracy of the correction procedure is assessed by comparison of calculated alkalinities with their analytical counterparts. Results are shown in Fig. 2.2.4_1, where the vertical error bars represent analytical precision (± 5%; Iwatsuki *et al.*, 2000a). Uncertainties in the charge-balance calculations are conservatively estimated to be at least as large as the corresponding analytical uncertainty. As can be seen, most of the calculated and analytical values agree within these uncertainty limits. This agreement provides confidence that the correction procedure is valid.

The agreement is not as good in many other cases, however. We believe the discrepancies result from analytical uncertainties that are greater than has been assumed here, but the evidence for this is not conclusive. Uncertainties increase in titrations of groundwaters containing high concentrations of organic acids, for example, because these acids become fully associated at pH values near the titration end-point. Tono groundwaters are generally low in organic carbon (Table 2.1_2), however, and TOC does not appear to be correlated with variations in alkalinity (Fig. 2.2.4_2). Uncertainties also increase if the groundwater sample is unfiltered, or improperly filtered, and if it contains significant amounts of particulate minerals or colloids. If so, calculated

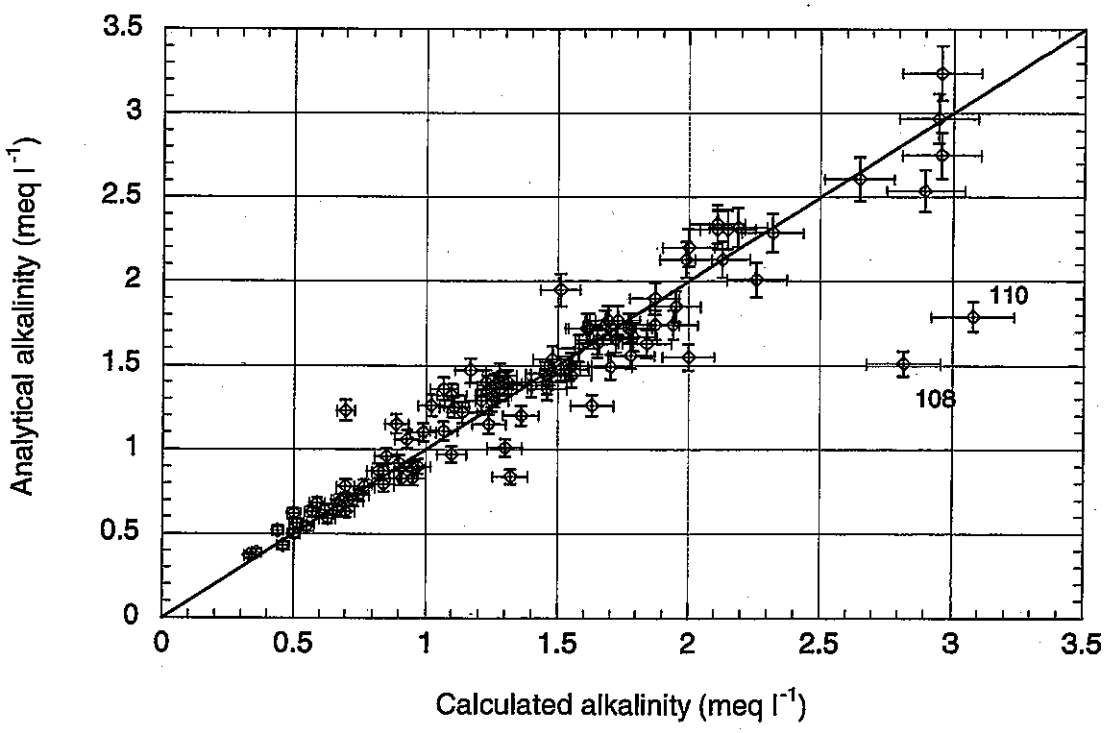

Figure 2.2.4_1. Comparison of analytical and calculated alkalinities. Numbers refer to sample numbers (see Table 2.1_1).

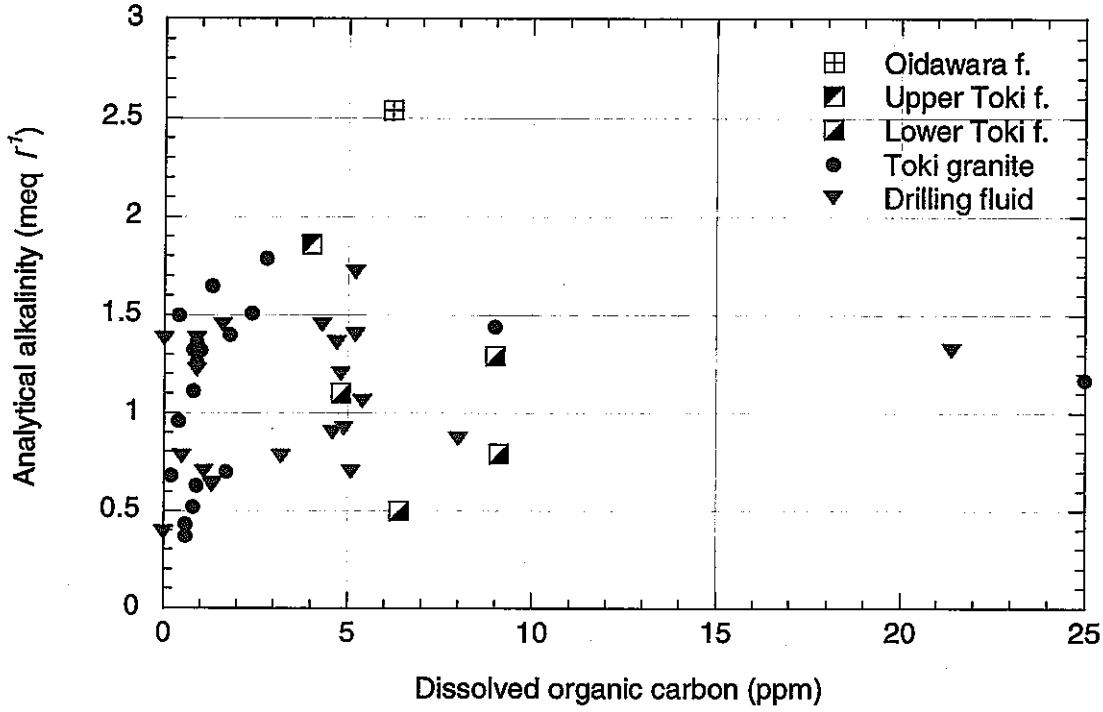

Figure 2.2.4_2. Plot showing relation between dissolved organic carbon and measured alkalinities in Tono groundwaters and drilling fluids.

alkalinities will be smaller than analyzed values. This could be the case for some samples, but as can be seen in Fig. 2.2.4_1 most of the discrepant data result from calculated alkalinities that are greater than their analytical counterparts. Two extreme such cases (Samples 108 and 110) almost certainly result from alkalinity measurements that are highly inaccurate. As noted in Section 2.2.3, the alkalinity determined for Sample 108 cannot possibly be correct because it is internally inconsistent with respect to both the sample's IC and NH_4^+ concentration. The accuracy of the analysis for Sample 110 is similarly suspect because, although it is internally consistent with respect to IC, the high pH and high $SiO_2(aq)$ and NH_4^+ content of this sample indicates that there must be a significant non-carbonate contribution to its measured alkalinity. There are thus sound, but not definitive, reasons to believe that uncertainties in at least some of the measured alkalinities are significantly greater than ± 5%. We therefore conclude provisionally that the discrepancies shown in Fig. 2.2.4_1 do not invalidate the charge-imbalance correction procedure.

The T_{alk} calculations are of considerable general interest because they indicate that the alkalinity of most Tono groundwaters is strongly influenced by non-carbonate sources. This is mainly because the groundwaters are often moderately alkaline (*i.e.*, pH greater than about 9) and contain high concentrations of dissolved silica. Under such conditions $HSiO_3^-$ is an important source of alkalinity. This species contributes up to 70 – 80% of T_{alk} in some of the granite groundwaters, for example. Other important sources of alkalinity (*i.e.*, > 10% of T_{alk}) include HS^-, as noted in Section 2.2.3, as well as $NaHSiO_3(aq)$, OH^- and $NH_3(aq)$. Tono groundwaters are thus unusual compared to most other deep groundwaters because their alkalinities include important, and in some cases dominant, contributions from non-carbonate sources.

The impact of corrections to the analytical charge imbalances can be assessed in terms of associated effects on the chemistry of the carbonate system, which is evaluated in further detail in Sections 3 and 4. Corrected and uncorrected dissolved carbonate concentrations are shown, for example, in Fig. 2.2.4_3. The corrected values for most shallow groundwaters are as much as three times higher than those measured by infrared spectrometry (*i.e.*, even excluding the three obvious outliers at IC > 0.002 mol kg^{-1}). The corrected concentrations for the deeper groundwaters tend to be smaller than their analytical counterparts by a factor of less than about 2.5. These differences are thus non-trivial in some cases.

Aqueous-speciation calculations using the corrected and uncorrected analyses also reveal corresponding differences in $P_{CO2(g)}$ (Fig. 2.2.4_4) and in the saturation index of calcite (*SIcc*, Fig. 2.2.4_5). The latter parameter provides a thermodynamic indication of whether the groundwater is equilibrated with calcite, in which case *SIcc* = 0. Negative *SIcc* values indicate that the solution is undersaturated with respect to calcite, and there is therefore a chemical potential for this mineral to dissolve in the presence of the groundwater. Positive values indicate that the solution is supersaturated with respect to calcite, and calcite should therefore precipitate. As can be seen in the figures, calculated differences in log $P_{CO2(g)}$ and *SIcc* can be rather large, but most fall within a narrow range of about ± 0.8 log units. These differences are important, however, because they are similar in magnitude to uncertainties inherent in the calculation of *SIcc*, and to uncertainties in related constraints on the $P_{CO2(g)}$ - pH evolution of shallow and deep groundwaters in the Tono region (Section 4).

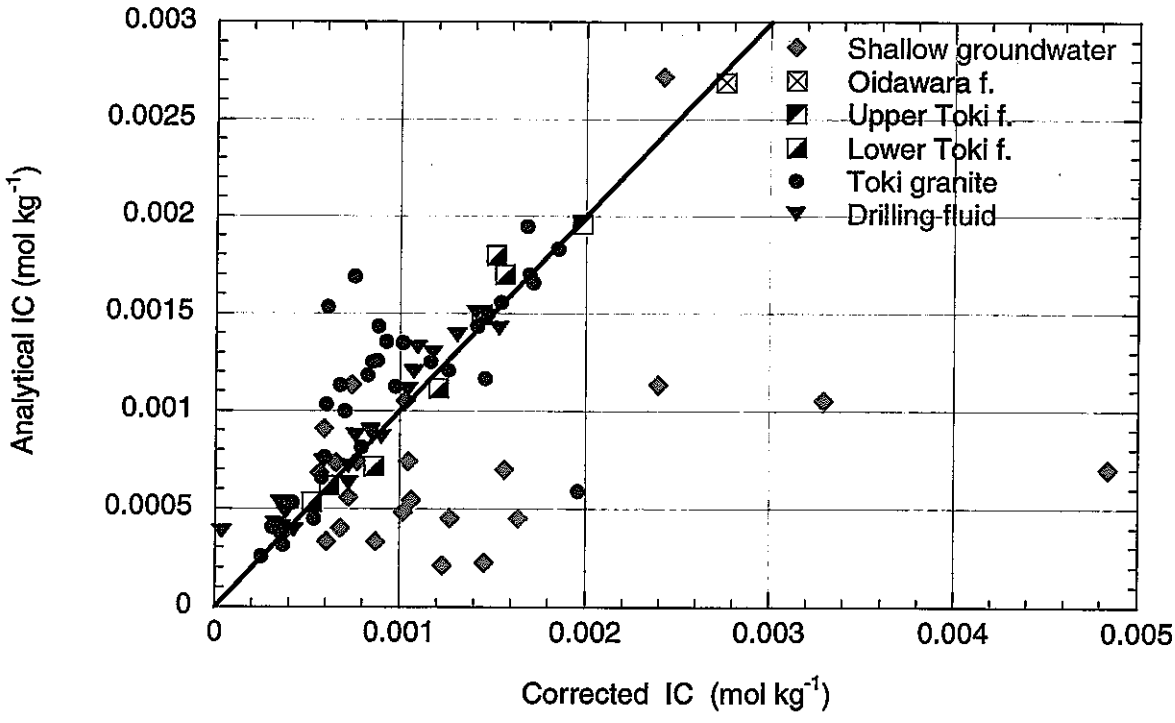

Figure 2.4.2_3. Comparison of analyzed carbonate concentrations (IC) and corresponding "corrected" values, calculated assuming charge balance on the basis species HCO_3^-.

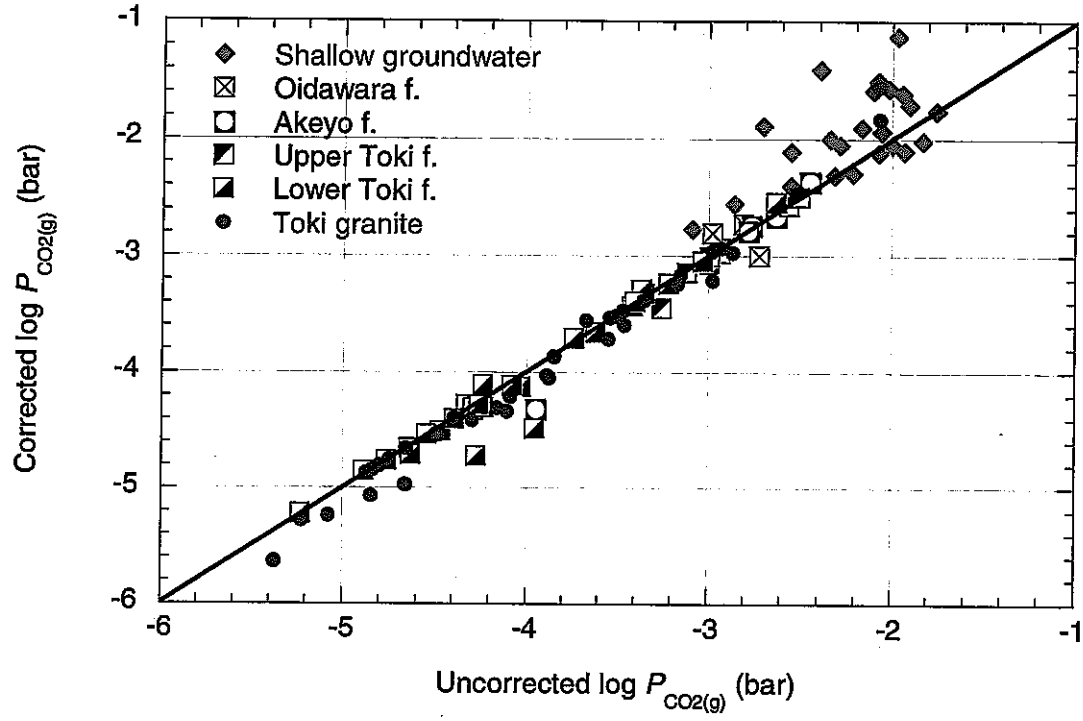

Figure 2.4.2_4. Plot comparing log $P_{CO2(g)}$ values calculated using corrected and uncorrected groundwater analyses.

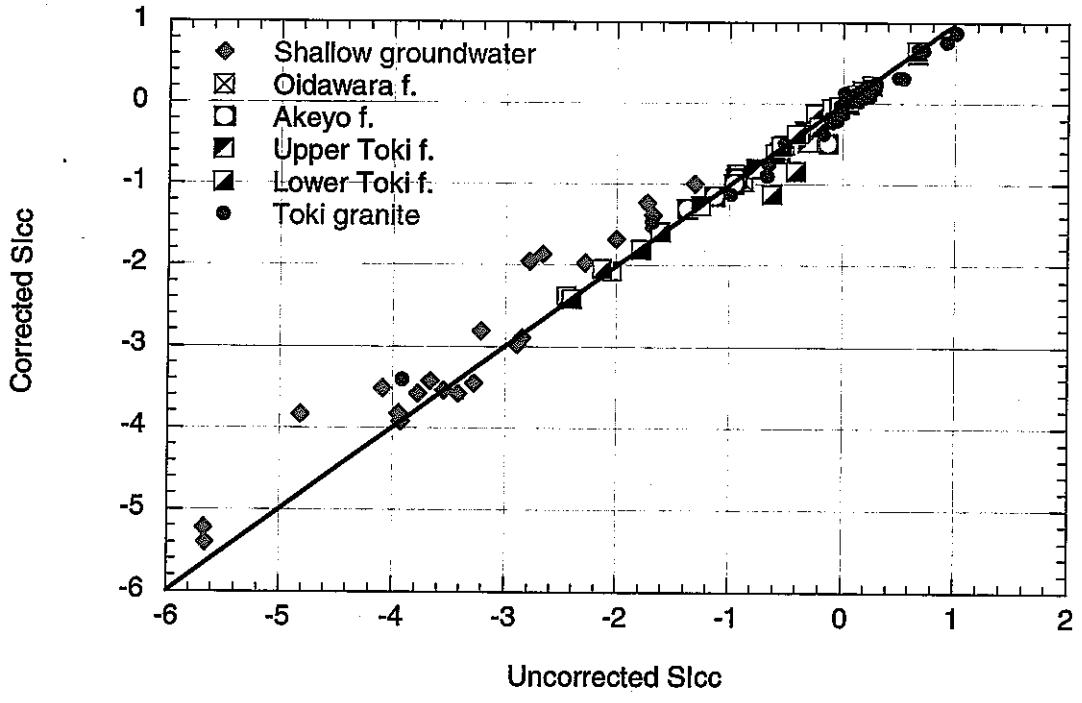

Figure 2.4.2_5. Plot comparing saturation indices for calcite (SIcc) calculated using corrected and uncorrected groundwater analyses.

3 Empirical hydrochemical trends

Hydrochemical trends in groundwaters may be viewed from two perspectives. The first is geographic and seeks trends in chemistry that are related to the location of the sampling point. The location can be simply the surface coordinates and depth or it can be the geologic or hydrologic context of the sample.

The second perspective is evolutionary and seeks in the chemistry to discern the origin of the groundwater and the processes leading to its observed chemistry. Trends of this type reflect the mineral environment and extent of water-rock interaction, relative residence times and flow paths, and the types of water-conducting features. Identification and interpretation of such trends is facilitated by comparisons with the behavior of other, similar groundwater systems.

This section considers the evidence of evolutionary trends in groundwaters of the Tono area. It examines the general chemistry of the water for evidence of chemical evolution (Section 3.1). It also makes use of information about the chemistry of waters from the crystalline rock in northern Switzerland, the Black Forest region of Germany and the Stripa region of Sweden as examples of well-understood evolutionary trends in groundwaters of crystalline rock (Sections 3.2).

3.1 Chemical character of groundwaters

Variations in the concentrations of major cations (Na^+, K^+, Ca^{2+}, Mg^{2+}) and major anions (HCO_3^- + CO_3^{2-}, SO_4^{2-}, Cl^-) can be used to help define the general chemical characteristics of most natural waters (*e.g.*, Laaksoharju, 1999). The approach is used here to define these characteristics for groundwaters in three geologic domains of the Tono region:

- shallow groundwaters in alluvium and in sedimentary formations of the Seto group,
- deeper groundwaters in sedimentary formations of the underlying Mizunami group, and
- groundwaters in the Toki granite.

These domains are related to shallow groundwater flow systems in the area by local topography, which causes meteoric recharge to infiltrate through shallow alluvium or surface exposures of the Seto group into underlying sedimentary formations of the Mizunami group, and then along channel structures in the unconformity between the sedimentary cover and basement granite (Yanagizawa *et al.*, 1995; Koide *et al.*, 1996; JNC, 2000; Iwatsuki *et al.*, 2000). The domains are also related to the deeper regional flow system in the area, where groundwaters that are recharged in high ground to the N and NE flow in fractures in the basement granite toward the Toki River valley in the S. The hydraulic interconnectivity of these domains suggests that the groundwaters within them may be genetically related, and, if so, this should be revealed by trends in their general chemical characteristics. The analytical data used in the following evaluation of these characteristics are summarized in Table 3.1_1. The data are taken mainly from Table 2.1_1, but concentrations of HCO_3^- and CO_3^{2-} are calculated, for reasons discussed in Section 2.2, assuming dissolved inorganic carbon concentrations are fixed by charge balance.

Table 3.1_1. Concentrations of major cations and anions in Tono groundwaters (ppm)[1].

No.[2]	bhl.[3]	Na^+	K^+	Ca^{2+}	Mg^{2+}	Cl^-	HCO_3^-	CO_3^{2-}	SO_4^{2-}
SHALLOW GROUNDWATER (SETO GROUP/ QUATERNARY ALLUVIUM)									
MC-8		4.8	1.7	4.0	0.4	1.2	18.2	0.0	7.2
MC-9		12.8	1.6	9.5	1.1	1.5	57.9	0.05	5.7
MC-12		9.5	5.3	3.1	0.5	5.1	33.0	0.0	2.4
MC-13		5.2	1.8	1.5	0.2	3.3	10.0	0.0	4.7
MC-14		4.7	1.9	2.2	0.5	0.7	20.2	0.0	1.9
MC-15		10.4	1.5	13.7	1.1	1.3	68.9	0.02	5.2
MC-16		4.7	1.3	6.0	0.4	2.3	20.1	0.0	7.6
MC-17		6.3	2.7	6.7	1.0	1.1	20.3	0.0	18.9
MC-18		4.8	1.4	5.1	0.6	1.3	23.0	0.0	4.8
MC-19		8.0	8.2	26.1	4.2	6.1	102.0	0.0	19.1
MC-20		4.6	2.1	3.6	0.7	3.3	12.7	0.0	2.7
MC-21		1.7	1.3	0.8	0.2	1.4	7.1	0.0	1.1
MC-24		3.5	1.8	15.2	1.5	1.0	57.6	0.08	3.9
MC-25		4.1	1.2	2.5	0.3	0.7	18.6	0.0	1.2
MC-26		3.3	1.2	1.9	0.2	0.7	14.9	0.0	0.8
MC-27		3.5	1.1	2.1	0.3	0.9	15.7	0.0	1.1
MC-28		26.5	1.4	25.4	1.2	2.5	123.5	0.07	21.0
MC-29		21.5	1.7	24.9	3.2	3.0	141.6	0.03	4.7
MC-30		20.0	1.5	11.8	1.5	2.0	83.0	0.01	9.7
MC-31		9.5	1.7	18.0	2.1	4.1	55.4	0.01	24.1
MC-35		3.8	2.0	12.0	2.5	0.7	53.5	0.03	6.1
MC-36		2.6	3.3	3.2	1.5	1.9	21.2	0.0	3.7
MC-37		1.4	0.8	0.5	0.2	0.8	5.1	0.0	0.7
OIDAWARA FORMATION									
13	TH-6	27.9	2.2	7.5	0.4	3.0	76.7	0.2	12.2
14	TH-8	30.5	2.0	7.4	0.5	1	101.5	0.2	0.3
94	TH-8	30.8	1.9	7.1	0.5	1.1	102.9	0.2	0.3
95	TH-6	27.1	1.8	6.9	0.4	2.6	78.4	0.2	9.2
dh11c	DH-11	67.3	1.7	2.8	0.2	2.5	158.6	7.6	4.2
AKEYO FORMATION									
15	TH-1	18.0	1.6	12.1	1.1	1.0	83.3	0.1	4.2
16	TH-2	13.7	1.5	12.1	1.3	0.9	74.5	0.05	4.9
17	TH-3	16.3	1.1	12.5	1.2	1.9	76.3	0.1	5.8
18	TH-4	32.3	1.3	6.6	0.5	2.8	60.3	0.1	5.4
19	TH-6	42.7	1.1	4.7	0.1	3.7	32.8	1.0	35.0
20	TH-8	44.7	1.6	5.0	0.1	1.3	123.1	0.7	1.2
97	TH-8	47.7	1.2	4.5	0.2	1.3	135.5	0.5	0.4
21	AN-6	29.7	0.8	4.6	0.2	0.9	89.0	0.2	1.6
96	AN-6	43.7	1.1	6.3	0.4	1.3	129.5	0.3	2.6
UPPER TOKI FORMATION									
22	TH-1	50.5	1.8	4.3	0.2	3.3	118.9	0.5	10.7
23	TH-2	65.0	1.4	5.2	0.2	1.1	172.1	1.3	1.1
24	TH-3	62.0	1.3	4.1	0.2	1.5	99.9	1.1	1.3
25	TH-4	46.7	1.4	3.6	0.2	3.7	119.2	0.2	4.7
26	TH-6	73.0	1.6	6.2	0.1	8.4	52.1	1.3	51.0
27	TH-8	13.3	1.0	1.8	0.1	1.9	30.8	0.05	4.8
152	DH-13	19.9	0.7	27.3	0.6	1.6	111.4	0.2	18.4
LOWER TOKI FORMATION									
28	TH-1	38.7	0.3	1.5	0.03	1.9	48.3	6.9	12.2
29	TH-2	45.0	0.5	1.9	0.04	2.0	95.3	1.7	9.7
30	TH-3	40.7	0.4	1.5	0.03	3.9	22.3	0.6	17.1
31	TH-4	55.3	0.4	2.9	0.03	4.2	85.3	3.9	29.8
98	TH-4	56.5	0.3	2.6	<0.02	4.6	81.9	3.1	38.8
32	TH-6	45.0	0.4	2.1	0.02	4.3	20.4	1.0	41.0
33	TH-8	21.3	0.3	1.1	0.04	0.9	49.0	0.2	3.6
1	KNA-6	45.5	0.4	1.7	0.03	1.0	76.0	10.9	0.9
2	KNA-6	42.5	0.3	2.3	0.02	0.9	85.6	6.1	0.1
2a	KNA-6	46.5	0.2	1.9	0.02	0.7	84.8	9.7	0.2
46	KNA-2	45.0	0.3	2.0	0.02	1.1	89.1	6.5	1.3

No.[2]	bhl.[3]	Na^+	K^+	Ca^{2+}	Mg^{2+}	Cl^-	HCO_3^-	CO_3^{2-}	SO_4^{2-}
52	TFA-1	49.9	<1.0	0.8	0.3	6.3	71.7	0.5	7.4
53	TFA-1	31.9	<1.0	0.3	0.3	2.6	50.5	0.2	10.4
54	TFA-1	62.9	<1.7	1.4	0.6	3.7	29.5	0.04	97.5
150	DH-12	72.5	0.4	2.1	<0.2	53.3	28.7	8.2	<0.4
TOKI GRANITE									
3	KNA-6	29.3	0.4	12.3	0.2	1.1	99.4	0.7	0.2
3a	KNA-6	31.5	0.5	11.7	0.2	0.6	101.6	1.5	0.1
34	TH-1	36.3	0.9	7.0	0.3	2.5	90.8	0.3	14.7
35	TH-6	46.0	1.3	15.1	0.4	12.1	41.9	0.8	82.0
105	TH-8	23.6	1.2	16.4	0.5	1.5	98.7	0.3	4.2
51	DH-3	12.3	10.1	1.4	0.2	1.4	47.0	0.01	2.9
6	DH-3	8.2	3.5	16.0	0.1	2.3	32.7	6.7	2.3
7	DH-3	11.6	0.9	12.2	0.1	3.7	34.0	1.1	6.7
8	DH-3	19.5	1.6	9.6	0.03	4.2	26.4	6.5	12.7
9	DH-3	36.5	1.2	4.1	0.03	3.5	33.0	7.0	9.1
10	DH-3	36.0	1.2	4.7	0.2	3.9	57.7	3.2	6.8
11	DH-3	39.5	0.8	3.7	0.1	3.1	52.3	6.1	6.2
106	DH-5	10.3	3.0	19.0	0.8	1.4	73.1	0.2	7.8
107	DH-6	21.4	0.6	3.2	0.1	3.4	34.9	1.4	5.5
dh7d	DH-7	7.7	1.6	11.9	0.7	4.3	38.5	1.6	5.6
dh7e	DH-7	13.3	2.5	13.7	0.2	4.5	6.7	7.1	6.8
dh7f	DH-7	18.6	2.4	9.3	0.03	3.9	14.4	6.0	5.7
108	DH-7	25.4	2.3	5.4	0.3	4.4	20.8	14.0	4.6
dh7g	DH-7	20.4	3.7	13.0	0.01	4.2	0.8	1.1	6.5
dh7h	DH-7	19.0	2.4	10.6	0.01	3.5	4.7	3.2	6.3
dh7i	DH-7	27.2	3.4	20.3	0.01	5.9	1.3	4.4	4.5
dh7j	DH-7	28.8	2.8	18.2	<0.01	5.7	1.2	4.1	4.2
dh7k	DH-7	18.6	1.6	13.5	0.3	4.2	12.7	8.5	5.0
dh7l	DH-7	30.8	1.0	10.2	0.01	2.8	38.5	8.3	4.6
109	DH-7	31.3	9.1	3.2	0.6	3.1	36.2	8.3	5.6
dh7o	DH-7	40.6	1.9	8.2	0.04	4.3	1.7	4.8	4.2
110	DH-7	48.0	22.0	5.4	0.7	5.1	88.2	13.6	5.4
dh7p	DH-7	46.0	4.2	9.7	0.1	6.5	3.3	6.4	2.8
dh7q	DH-7	49.0	3.7	10.0	0.07	5.8	2.8	8.5	2.0
111	DH-8	23.2	5.1	2.8	0.04	3.8	47.1	2.5	n.d.
112	DH-8	22.1	0.5	6.9	0.09	3.8	52.0	0.9	4.2
113	DH-8	28.0	4.5	1.0	0.09	3.9	55.0	0.8	3.7
114	DH-8	39.1	11.0	4.3	0.7	19.2	50.8	1.9	3.1
115	DH-8	25.8	0.9	6.8	0.7	6.4	49.0	1.9	1.7
dh9a	DH-9	24.0	7.3	12.0	0.4	2.9	87.1	1.1	1.8
dh9b	DH-9	20.0	6.6	12.0	0.4	2.2	86.1	1.3	1.8
dh9c	DH-9	15.0	4.0	14.0	0.7	1.8	68.7	0.9	3.1
dh10a	DH-10	5.7	2.1	9.7	0.5	2.4	46.6	0.7	1.4
dh10b	DH-10	5.6	2.0	8.8	0.4	1.9	40.1	0.06	1.4
dh10c	DH-10	12.9	1.6	18.2	0.3	6.9	37.8	0.04	15.6
dh11a	DH-11	38.2	5.3	6.5	0.05	6.0	87.6	0.1	5.5
dh11b	DH-11	38.0	6.9	7.6	0.06	5.4	91.2	0.2	6.4
151	DH-12	55.2	<0.2	6.5	<0.2	52.6	22.2	2.4	<0.4
154	DH-12	71.7	0.4	13.1	<0.2	99.9	16.9	1.4	<0.4
155	DH-12	81.5	0.9	25.6	<0.2	137.0	20.6	0.9	<0.4
156	DH-12	94.9	0.9	32.4	<0.2	175.0	13.7	0.6	<0.4
157	DH-12	66.0	0.4	10.4	<0.2	72.1	28.8	2.6	<0.4
153	DH-13	16.1	0.9	22.2	0.7	1.6	90.8	0.6	6.9
158	DH-13	15.4	1.1	20.6	0.5	1.4	83.3	1.0	5.5

[1]- Piper diagrams discussed in this section are constructed assuming that ionic concentrations are equal to the detection limit if values reported in this table are less than the detection limit.

[2]- Sample numbers correspond to those in Table 2.1_1.

[3]- Borehole (bhl.) locations shown in Figs. 2.1_1 – 2.1_3.

3.1.1 Groundwaters in sedimentary rocks

The Piper diagram in Fig. 3.1.1_1 provides a visual summary of the chemical characteristics of groundwaters in sedimentary formations of the Tono area[4]. As can be seen, there are distinct chemical differences among groundwaters from the "shallow" and "deep" sedimentary domains discussed in the preceding section.

The relative abundance of Ca in the shallow groundwaters is highly variable, ranging from about

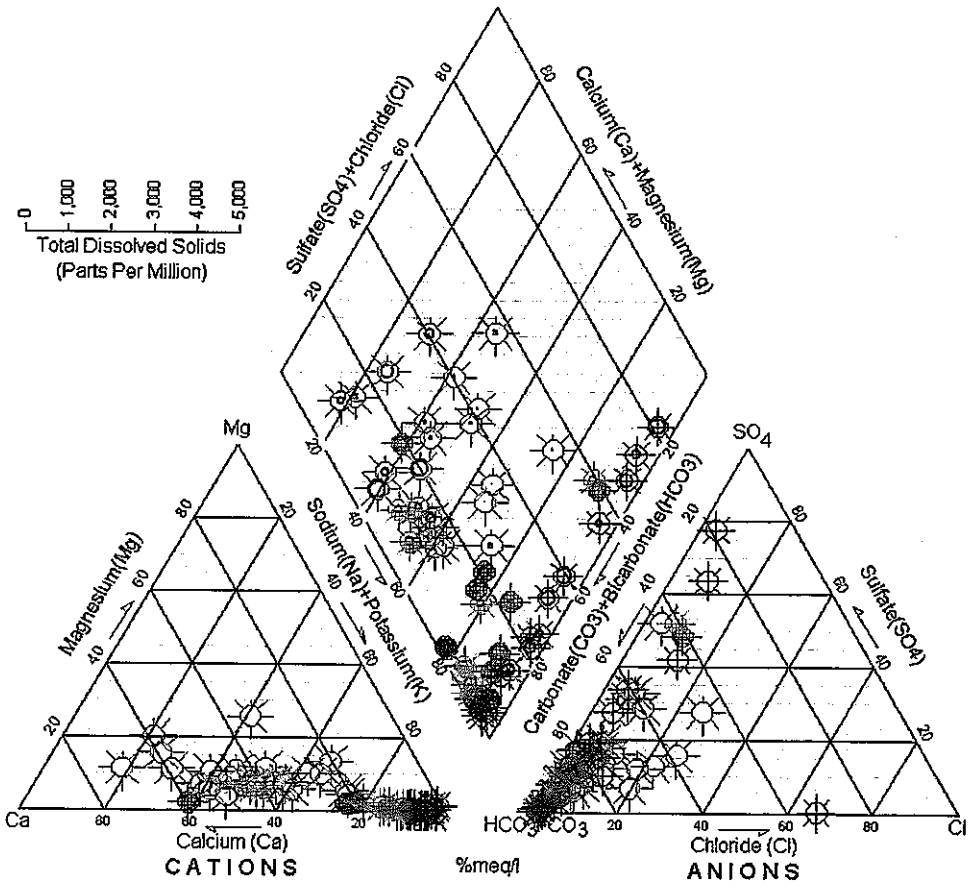

Figure 3.1.1_1. Piper diagram illustrating general chemical characteristics of shallow groundwaters (red symbols) and of deeper groundwaters in sedimentary formations of the Mizunami group (Oidawara f. – purple symbols; Akeyo f. – gold symbols; upper Toki f. – green symbols; lower Toki f. – blue symbols).

[4] Piper (1944) and Hem (1985) describe procedures used to construct such diagrams, and limitations in their use. The limitations stem mainly from the fact that groundwater systems are generally too complex to justify an exacting geochemical and hydrologic interpretation of trends that might be revealed by such diagrams. The diagrams are useful, however, as a source of supporting evidence for conclusions regarding trends in groundwater characteristics that also have other bases of support.

20 to 80 equ. %. The variations in Ca concentration are balanced mainly by Na (+ K). Magnesium concentrations span a much narrower range from about 5 to 20 equ. %, and are slightly, but consistently, higher than most of the deeper groundwaters. The anionic character of the shallow groundwaters is dominated by HCO_3 + CO_3 (carbonate alkalinity), but several samples also include significant contributions from SO_4 (up to 53 equ. %) and (or) Cl (up to 27 equ. %).

In comparison, the deep sedimentary groundwaters are distinctly richer in Na than the shallow groundwaters. As can be seen in Fig. 3.1.1_1, Na comprises more than 75 equ. % of total cations in all but 4 of the deep groundwater samples [samples 15, 16, 17 (Akeyo formation) and 152 (upper Toki formation, Table 3.1_1][5]. The deep groundwaters tend to become more Na rich with increasing depth in the stratigraphic sequence and Mg concentrations are uniformly low. The anionic composition of these waters is dominated in most cases by carbonate alkalinity (ranging from about 80 to almost 100 equ. % HCO_3 + CO_3), but several samples, most notably from the lower Toki formation, contain significant, if not dominant, SO_4. One groundwater sample from this formation in borehole DH-12 (sample 150, Table 3.1_1) is unusual in that it contains a relatively high concentration of Cl, low carbonate alkalinity and low SO_4 concentration. This apparently unique high-Cl groundwater type is discussed further in Section 3.1.2.

As noted earlier, it is possible that deep groundwaters in the Mizunami group have evolved chemically from shallow groundwaters infiltrating downward through the overlying alluvium or sediments of the Seto group by coupled processes of fluid flow and water-rock interaction. The differences in chemical characteristics of these two groundwater types discussed above suggest that these processes result mainly in the progressive enrichment of Na relative to Ca and, to a lesser extent, Mg (see also Yusa *et al.*, 1993; Iwatsuki *et al.*, 1995). Groundwater evolution does not appear to involve any significant change in the dominant contribution of carbonate alkalinity to the overall anionic character of the fluids. Although SO_4 is an important anion in some samples, the range in relative and absolute concentrations of SO_4 between the shallow and deep groundwaters is similar, which may suggest that SO_4 is a conservative constituent of these solutions. It is also possible, however, that the similar spread in SO_4 concentrations alternatively reflects an approximate steady state involving a number of complex and possibly related processes (*e.g.*, dissolution/precipitation of sulfate minerals, oxidation/reduction of sulfides, mixing with formation fluids, *etc.*).

3.1.2 Groundwater in the Toki granite

The general chemical character of groundwater in the Toki granite is shown in the Piper diagram in Fig. 3.1.2_1. For reasons discussed below, this figure includes data for all relevant boreholes in the region except DH-7. Remarks addressing the DH-7 data are summarized separately at the end of this section.

As can be seen in Fig. 3.1.2_1, the chemical character of most granite groundwaters is grossly

[5] It is noteworthy that these four samples are all from the shallowest sampling horizons in their respective boreholes (see Table 2.1_1), and contain similar Ca concentrations as observed in shallow groundwaters.

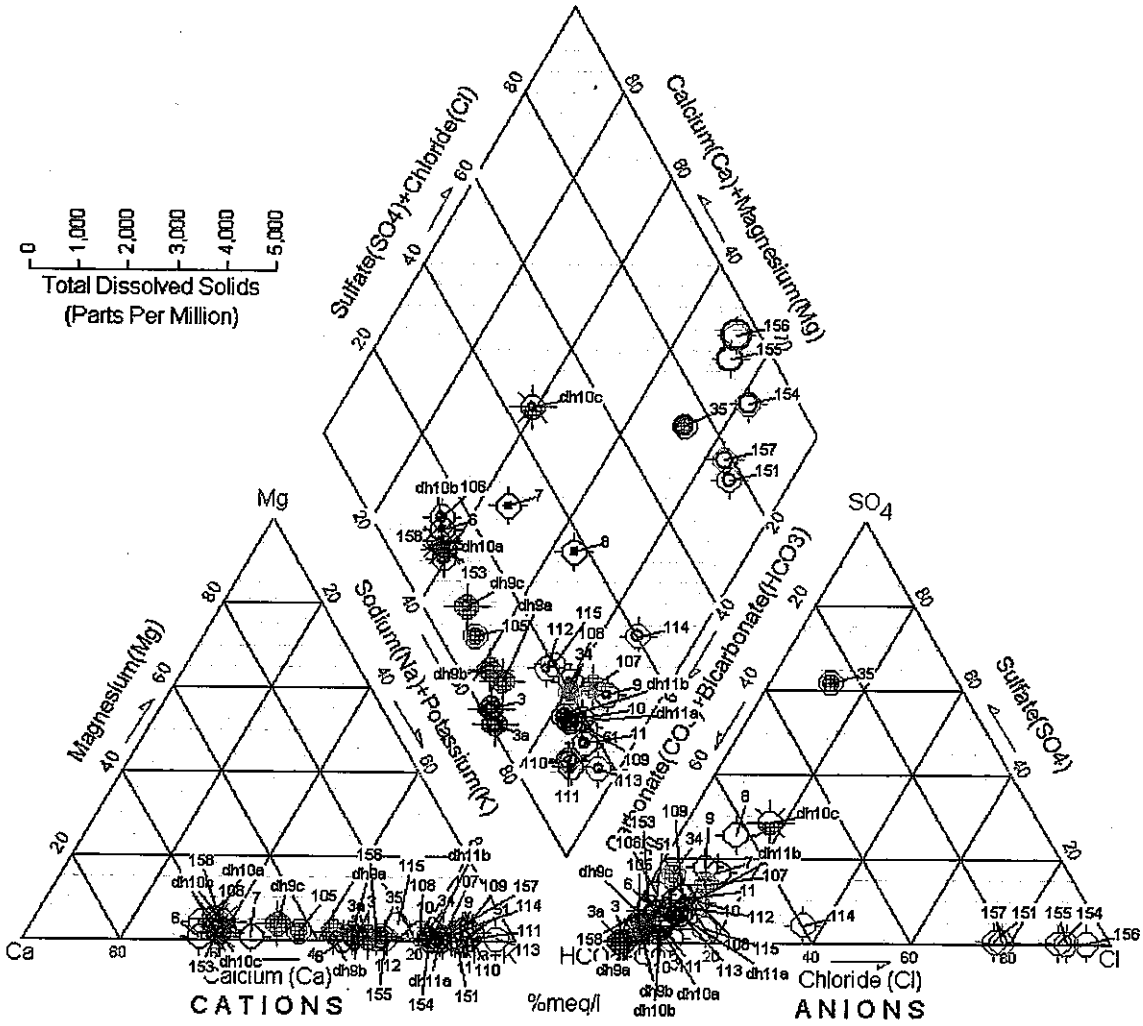

Figure 3.1.2_1. Piper diagram illustrating general chemical characteristics of groundwaters in the Toki granite. The labeled sample numbers correspond to those in Table 3.1_1.

similar to that of the sedimentary fluids discussed in Section 3.1.1. Cations in the granite waters range from about 65 equ. % Ca to nearly 100 equ. % Na with no sample containing more than about 5 equ. % Mg. The anions for all but nine samples are greater than 70 equ. % $HCO_3 + CO_3$. Five of these exceptional samples (Samples 151 and 154 – 157, Table 2.1_1) are from the DH-12 borehole. They have from 75 to over 90 equ. % Cl and are similar in this respect to the DH-12 water noted in Section 3.1.1 from the lower Toki formation (Sample 150, Table 2.1_1). One of the other exceptional granite groundwaters (Sample 114) contains moderate Cl (35 equ. %), two others (samples 8 and dh10c) contain significant SO_4 (25 – 30 equ. %) and one (sample 35) contains nearly 65 equ.% SO_4. The SO_4 content of the latter sample is similar to that in groundwaters from sedimentary formations penetrated by the same borehole (TH-6; see Table 2.1_1). The highest Cl sample, Sample 156, has more than 70 equ. % Na while the other high Cl samples have from 75 to 90 equ. % Na.

The hydrologic context of the granite groundwaters may provide some insight into processes controlling their chemical evolution. For example, water at a depth of about 1000 m in the center of the region around DH-9 and DH-11 (see Fig. 2.1_1) is thought to have been recharged about 2.5 km to the N-NW near DH-3 (Iwatsuki *et al.,* 2001). As can be seen in Fig. 3.1.2_1, the chemistry of groundwaters along a flow path defined by these boreholes appears to evolve from a Ca-HCO_3 type solution in upper sections of borehole DH-3 (*e.g.,* Samples 6 and 7) to a Na-Ca-HCO_3 water in DH-9 and then to a Na-HCO_3 solution in DH-11. Similarly, granite groundwaters in other boreholes located in northern recharge areas (*i.e.,* DH-10 and DH-13) are similar to the Ca-HCO_3 recharge waters in upper sections of DH-3, whereas other groundwaters to the south (boreholes TH-1, TH-8, KNA-6 and DH-8) are similar to the evolved groundwaters in DH-9 and DH-11. These observations suggest that the chemical evolution of groundwaters in the Toki granite is characterized mainly by the transition from a Ca-HCO_3 type solution to a progressively more Na-HCO_3 type water as the solutions migrate from recharge to discharge areas along the regional flow path.

There are notable exceptions to this apparent evolutionary trend, however. For example, groundwaters in deeper sections of borehole DH-3 (Samples 9 – 11, see Fig. 3.1.2_1) are chemically similar to the relatively evolved Na-HCO_3 groundwaters found in southern regions of the area. This suggests that evolved groundwaters may exist at depth in the northern recharge areas. Moreover, a clear exception to the regional evolutionary trend is that the shallowest groundwater in DH-3 (Sample 51, Table 3.1_1) is similar to the relatively evolved groundwaters in DH-11. Conversely, a moderately deep groundwater from borehole DH-5 (Sample 106), which lies about as far south from DH-3 as do DH-9 and DH-11, is similar to the Ca-HCO_3 type water in upper sections of DH-3. Thus, although groundwaters in the Toki granite appear to evolve generally from Ca-HCO_3 to Na-HCO_3 type solutions, exceptions to this trend are rather common.

It is unclear whether the relatively saline waters sampled in borehole DH-12 are related to the hydrochemical trends observed in the Toki granite and in the overlying sedimentary formations discussed in Section 3.1.1. This is because there are at least two possible explanations for the origin of these high Cl waters, both of which appear to be consistent with the regional hydrogeology of the Tono area.

The two alternative explanations differ according to the extent to which it is assumed that the composition of fresh meteoric recharge in the area is influenced by residual, connate formation fluids. If the effects are negligible, Cl concentrations will increase only in proportion to the extent of leaching of fluid inclusions, intergranular salts and Cl-bearing minerals (*e.g.,* fluorapatite, biotite) in the host rock, and thus in proportion to increasing residence time of the groundwater. Borehole DH-12 is located near the Toki River, which represents the main groundwater discharge zone in the Tono region (Yanagizawa *et al.,* 1995; Iwatsuki *et al.,* 2000). In contrast, the other boreholes considered above are located well to the north of this river, and thus apparently lie further upstream along the regional groundwater flow path. The relatively high Cl waters in DH-12 may thus reflect the greater extent of water-rock interaction associated with the longer residence time of this groundwater in the regional hydrologic system.

Alternatively, the elevated Cl concentration in DH-12 groundwater could result from mixing of fresh meteoric recharge and trace amounts of saline formation fluids that have been partially retained in the host rocks following the most recent period of marine regression during the middle-to-late Miocene. Preliminary results based on a numerical model of the regional hydrogeology of the Tono area suggest that the effects of such mixing, if any, should be most evident in groundwaters from DH-12, again because this borehole is close to the regional groundwater discharge zone represented by the Toki River (Inaba and Saegusa, *pers. comm.).* If so, the influence of connate fluids on present day groundwater chemistry must be small because the concentration of Cl in DH-12 groundwater, though high regionally, is extremely low compared to that of modern seawater (*i.e.,* about 19,800 ppm). In summary, the DH-12 groundwaters are chemically distinct based on their high Cl content, but it is unclear whether this chloride comes from mixing with residual, saline formation fluids or represents an advanced stage of chemical evolution resulting from water-rock interaction. This question is considered further in Section 3.2.1.

Some of the groundwater samples from borehole DH-7 are similar to the Na-HCO_3 type waters discussed above. Other samples are, however, distinctly richer in Ca and poorer in carbonate alkalinity relative to the Na-HCO_3 waters, and also differ significantly compared to the high-Cl waters from DH-12. These unusual DH-7 waters were in some cases sampled from a position in the borehole that had previously yielded a Na-HCO_3 type groundwater using a different sampling technique. This suggests that the differences in groundwater chemistry may be related to differences in sampling methodology.

These observations are summarized in the Piper diagram in Fig. 3.1.2_2, which takes into account all the DH-7 water analyses in Table 2.1_1. The black symbols in the figure refer to samples obtained using JNC's 1000 m groundwater sampler (1000GS). The red symbols represent samples obtained using a multi-piezometer (MP) sampling apparatus (see Table 2.1_3 and Iwatsuki *et al.,* 2001). For reference, MP samples dh7g and dh7h were collected from the same position in the borehole as 1000GS Sample 108, MP sample dh7o was taken from the same sampling horizon as 1000GS Sample 109, and MP samples dh7p and dh7q were obtained from the same borehole position as 1000GS Sample 110 (Table 2.1_1). As can be seen in the figure, the chemical character of the MP samples is more strongly influenced by Ca than the 1000GS samples. Although the anionic character of the MP waters appears to be more strongly influenced by SO_4 and (or) Cl compared to the 1000GS waters, this apparent shift in chemical character arises mainly from the extremely low concentrations of $HCO_3 + CO_3$ in these samples rather than to any actual increases in SO_4 or Cl (see Table 2.1_1).

By comparing Figs. 3.1.2_2 and 3.1.2_1 it can also be seen that the MP samples from DH-7 differ chemically from other granite groundwaters in the Tono area, and that the 1000GS samples are essentially identical to the Na-HCO_3 type granite groundwaters discussed above. Referring to Table 3.1_1 and the corresponding detailed analyses in Table 2.1_1, it is apparent that the MP samples are more alkaline, have generally higher concentrations of Ca and Si and have much lower $HCO_3 + CO_3$ concentrations than do samples obtained using 1000GS system.

It is unclear whether the unusual MP samples from DH-7 are representative of a distinct groundwater type in the Tono region or are the result of perturbations to *in-situ* groundwater

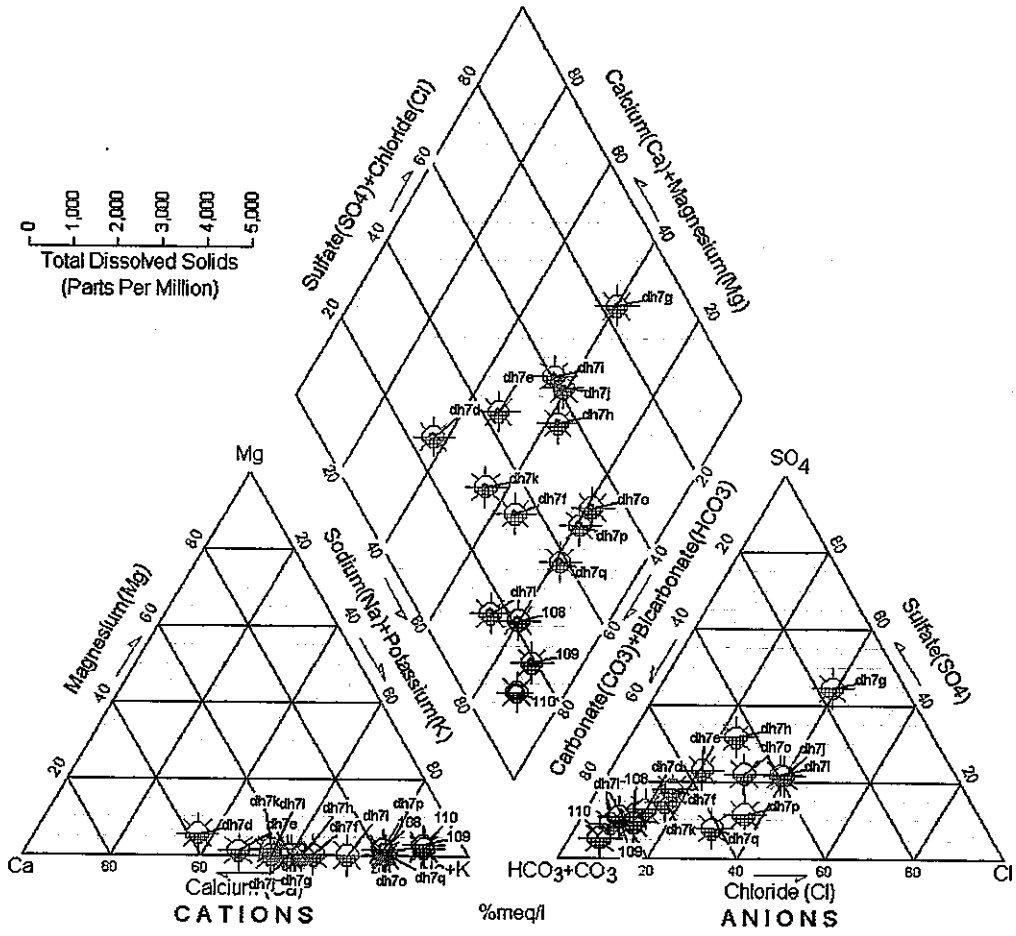

Figure 4.1.2_2. Piper diagram illustrating general chemical characteristics of groundwaters sampled in borehole DH-7 (see text).

compositions arising from deficiencies in this sampling technique. It is important to note in this regard that groundwaters sampled using the MP system in other boreholes in the Tono region (see Table 3.1_1) are all chemically dissimilar to the unusual DH-7 samples, which suggests that the anomalous chemistry of these waters cannot be attributed to any deficiencies in the MP sampling method alone. Borehole records indicate that the 1000GS samples were each collected immediately after a period of hydrotesting, during which time several hundred liters of groundwater were pumped to the surface over a period of several days (JNC 1999). In contrast, the MP samples were collected a year or two after the 1000GS samples, and sampling was apparently not preceded by a similar period of hydrotesting. The 1000GS samples may thus represent groundwater that has been induced to flow, possibly over a considerable distance, toward the borehole during the hydrotesting period. The MP samples may on the other hand represent groundwaters residing more locally in the granite nearer the borehole. If so, the differences in chemical character observed between the 1000GS and MP samples from DH-7 may reflect real differences in the respective chemistry of granite groundwaters flowing in conductive features of the regional flow system versus less mobile waters in the granite matrix and local fractures.

3.2 Comparison of hydrochemical trends in granitic rocks

Hydrochemical trends observed in groundwaters of the Toki granite are compared in this section with those observed in other, similar deep groundwater systems in crystalline rocks of the Stripa area of Sweden (Nordstrom *et al.*, 1989) and those of northern Switzerland and the Black Forest region of Germany (Grimaud *et al.*, 1989; Michard *et al.*, 1996). Common features in the trends observed among all these systems may be attributable to similarities in the mineral environment and extent of water-rock interaction, relative residence times and flow paths, and the types of water-conducting features. Trends in Cl concentration and Na/K ratio are particularly useful as general indicators of both the direction and extent of chemical evolution.

3.2.1 Chloride

The ratios of all major solutes except Cl can be explained by water-mineral equilibria. Chloride as well as Br, and in some cases SO_4, are called free or mobile elements because their concentrations are determined by factors other than local chemical equilibrium. The remaining elements are called controlled or inert elements because their concentrations do result from local chemical equilibrium reactions (Michard, 1987).

The chloride and other mobile anions in groundwaters in crystalline rock have several sources. They may have been present in recharge to the groundwater system, added to the groundwater by mixing with higher chloride waters from adjacent formations, or leached from the host rock itself from fluid inclusions or intergranular salts.

Chloride concentrations resulting from host-rock leaching indicate the extent of water-rock interaction that has occurred and increase with the residence time of the groundwater. Figure 3.2.1_1 illustrates this point using data for the crystalline and adjacent sedimentary rocks of northern Switzerland. The figure shows dissolved helium concentrations plotted against the Cl concentrations of groundwater[6]. Helium accumulates in groundwater from subsurface production of alpha particles during the decay of Th and U-series isotopes disseminated throughout the rock. To interpret helium concentrations in terms of residence time requires knowledge of the U and Th contents of the rock, the porosity, and the proportion of He that is able to leave the minerals in which it is produced and enters the groundwater. Generally these factors are not known with great precision, particularly the last. Thus, the ages of groundwaters from helium concentrations are at best only order of magnitude estimates. Because helium concentrations are proportional to residence times, the corresponding increases in chloride contents shown in Fig. 3.2.1_1 demonstrate that chloride is also an indicator of residence time.

Figure 3.2.1_2 shows the relationship between the sodium and chloride contents of water from crystalline rock of northern Switzerland and adjacent southern Germany, from the Stripa region

[6] Balderer and Lehmann (1991) describe the general behavior of helium in groundwaters of northern Switzerland.

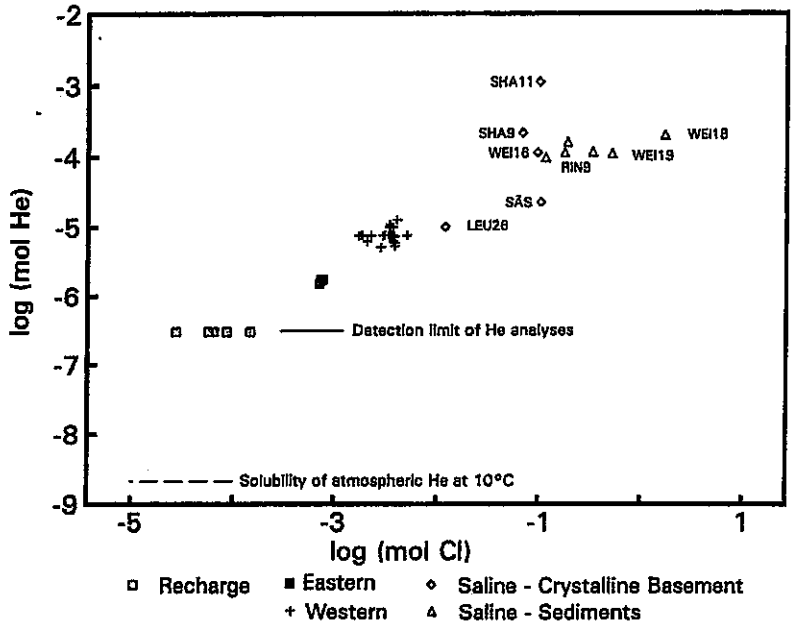

Figure 3.2.1_1. He vs. Cl contents of groundwaters from crystalline and adjacent sedimentary rock of northern Switzerland and southern Germany (Michard et al., 1996).

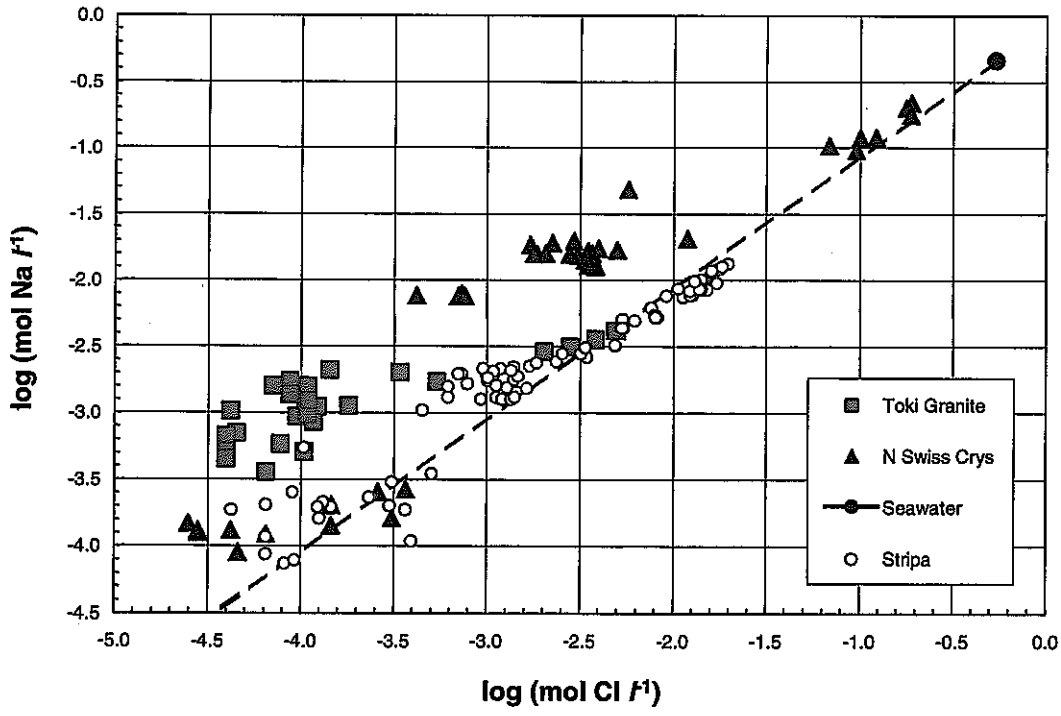

Figure 3.2.1_2. Na vs. Cl content of groundwaters from northern Switzerland, the Stripa region and the Toki granite. Data are from Michard et al. (1996), Nordstrom et al. (1985) and Iwatsuki et al. (2000a), respectively. Seawater and its path of dilution with pure water are also shown.

of Sweden and from the Toki granite. Waters from the Swiss crystalline span a range of concentrations from about $10^{-4.6}$ to $10^{-0.8}$ mol l^{-1} Cl. Michard *et al.* (1996) describe their evolution in detail. Waters from Stripa range from $10^{-4.4}$ to $10^{-1.7}$ mol l^{-1} Cl, and are discussed by Nordstrom *et al.* (1989) and Grimaud *et al.* (1990). The Toki granite waters range from $10^{-4.4}$ to $10^{-2.3}$ mol l^{-1} Cl and appear to have a similar pattern of evolution. For reference, seawater and a line representing its dilution by pure water are also shown in Fig 3.2.1_2. This line is virtually the same as a line representing mol l^{-1} Na = mol l^{-1} Cl.

Waters from the recharge area of the Swiss and Stripa flow systems have Cl contents between about $10^{-4.5}$ to $10^{-3.4}$ mol l^{-1} and Na/Cl ratios from about 0.5 to 6. There is a group of Toki granite samples with similar low Cl contents, but with much higher Na/Cl ratios from 6 to 25.

Northern Swiss and Stripa waters have similar patterns with increasing Cl contents as well. As Cl increases beyond the low recharge-water concentrations, there is at first a relatively much greater increase in Na. Na/Cl ratios in the northern Swiss reach values from 10 to 18 in the samples with Cl contents from $10^{-3.1}$ to $10^{-3.4}$ mol l^{-1}. Stripa samples with Cl contents in this range have Na/Cl ratios that reach only 3, but, with one exception, all are greater than 2.

At still higher Cl contents, the Na/Cl ratios of both northern Swiss and Stripa samples decrease to or below that of seawater (0.85). The northern Swiss samples do not reach their lowest Na/Cl ratios until they have attained Cl concentrations greater then 10^{-1} mol l^{-1}. The Stripa waters reach this Na/Cl ratio at much lower Cl contents.

Groundwater samples of relatively high Cl content from the Toki granite follow the same trend of decreasing Na/Cl with increasing Cl. Their pattern is virtually identical with that of the Stripa samples in that they reach a low Na/Cl ratio at a relatively low Cl content. Other water chemical properties suggest that the seawater Na/Cl ratios of Sample 156 and the other high-Cl samples (Table 3.1_1) are not a result of seawater dilution. One of these is that the Na/K ratio of this sample may be consistent with water-rock equilibrium but not consistent with residual seawater. This is discussed in more detail in the following section. The other is that data from samples from the Stripa granite have a similar excess of Na at low salinities but when they reach Cl concentrations of about $10^{-2.4}$ mol l^{-1} there is no longer an Na excess, and at higher chlorides Na is slightly depleted relative to seawater (see Fig. 3.2.1_2, and Nordstrom *et al.*, 1989, Fig. 5).

Although increasing chloride has been treated as an indicator of the extent of water-rock interaction, it is important to rule out other sources of Cl. For example, the Cl could be diffusing or flowing into the granite from higher-Cl adjacent sediments. Or, the solutes present could, in part, be remnants of a higher Cl water that is only now being replaced by waters of low solute contents. In the case of the northern Swiss and Stripa systems, these sources can be ruled out by the geographic pattern of water chemistry and internal evidence based on the geochemistry of the samples themselves, as described in the studies cited above. The Na/K ratios suggest this is also true of the Toki granite water (Section 3.2.2).

The pattern of hydrochemical trends with depth as displayed in several boreholes from which a number of samples were taken also supports this conclusion. Figure 3.2.1_3, for example, is a

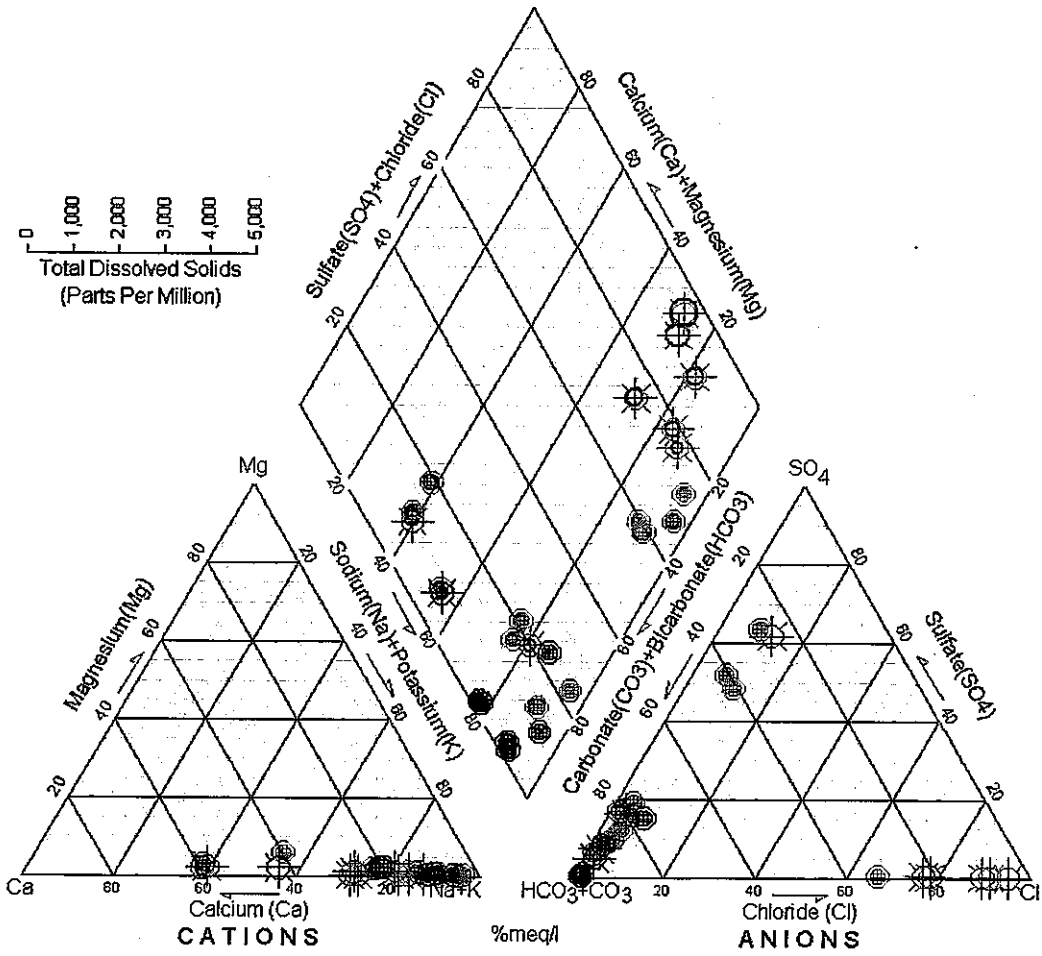

Figure 3.2.1_3. Piper diagram of samples comprising vertical profiles through both sediments (filled symbols) and granite (open symbols). TH-1: Red symbols; TH-6: Green symbols; TH-8: Black symbols; DH-12: Magenta symbols; DH-13: Blue symbols.

Piper diagram showing the chemistry of waters from both the Toki granite and overlying sediments from several boreholes in the Tono area. Wide ranges of water types are evident in the DH-12 and TH-6 waters, moderate ranges in the TH-1 and TH-6 samples, and only a small range in the DH-13 samples. The basis for the variation is an increase in the proportion of Cl from the sediments into the granite in the DH-12 borehole, and of SO_4 in the other samples, particularly in TH-6.

Figure 3.2.1_4 shows the variation of Cl with depth for the same five boreholes. The greatest range is in samples from DH-12. The four deepest samples from this borehole are granite waters. There is also a noticeable increase of Cl in the TH-6 samples, although the reason for the major shift apparent in Fig. 3.2.1_3 is an increase of SO_4. Only the deepest sample from TH-6 is from the granite. The Cl contents of all samples from the TH-1, TH-8 and DH-13 boreholes are very low and show no regular trend with depth.

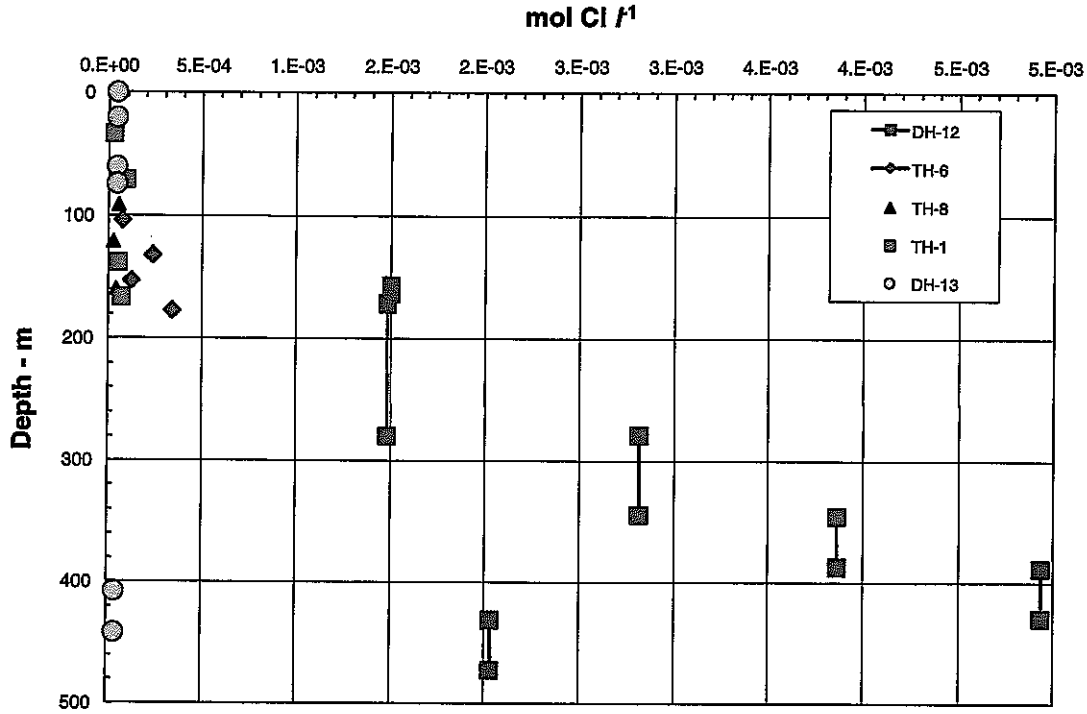

Figure 3.2.1_4. Variation of Cl with depth in the Toki granite and overlying formations in selected boreholes.

Two other boreholes, not included in Figs. 3.2.1_3 or 3.2.1_4, provide additional information on the variation of Cl with depth. These are DH-3, from which seven samples of water were taken from granite to a depth of nearly 500 m., and DH-8 from which five samples of granite water are available to nearly 1000 m. Except for one sample from DH-8, all waters from these boreholes have Cl contents below 2.0×10^{-4} mol l^{-1} and show no regular pattern with depth.

The pattern of decreasing Cl upwards from the granite into the sediments in DH-12 and TH-6 indicates that the Cl in the Toki granite has not been carried in from overlying sediments. The deepest sample from DH-12 has a lower Cl content than the more shallow samples from granite in this borehole. This, plus the low Cl contents of deeper water from the other boreholes suggests that there is also no deep source of Cl.

3.2.2 Na / K Ratios

The change of the Na/K ratio with sample temperature has also been used to indicate progress toward water-rock equilibrium in a flowing groundwater. A plot of Na/K ratios against the reciprocal temperature is shown in Fig. 3.2.2_1. This type of plot is used because equilibrium reactions such as

$$\text{Na-feldspar} + K^+ = \text{K-feldspar} + Na^+$$

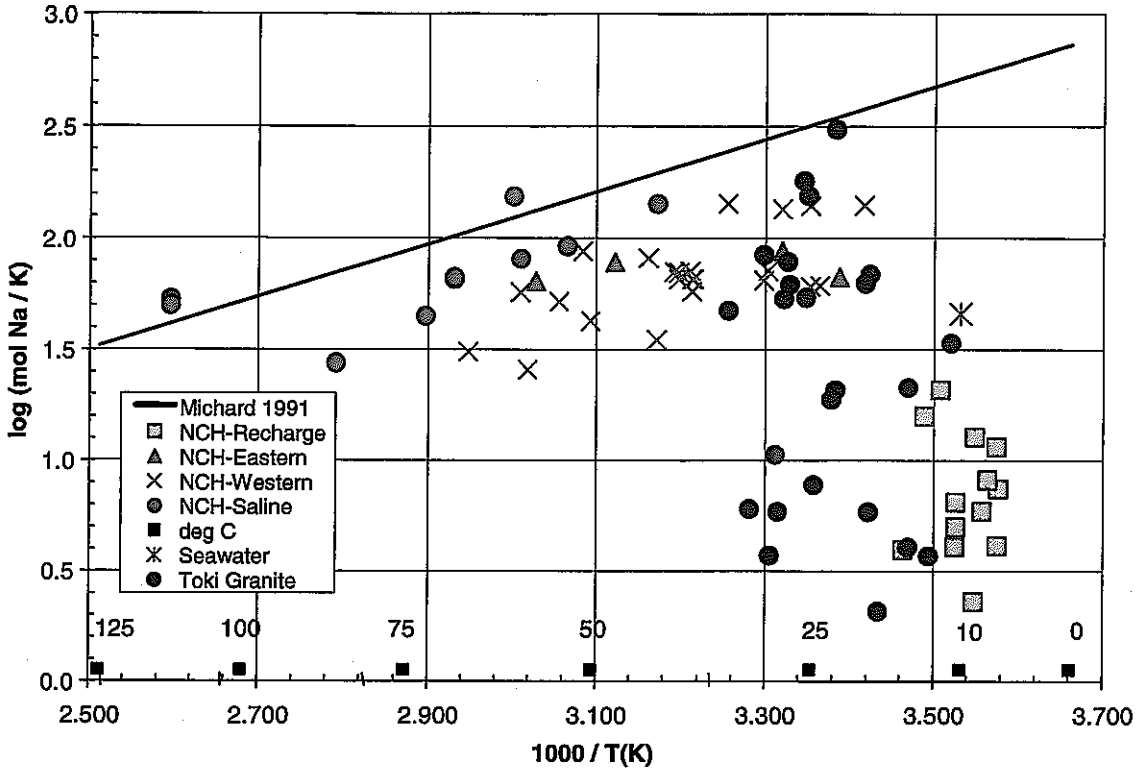

Figure 3.2.2_1. Na/K ratios vs. *reciprocal temperature for groundwaters from northern Switzerland and the Toki granite.*

can be represented by equations of the form:

$$\log\left(\frac{Na^+}{K^+}\right) = \frac{1170}{T(K)} - 1.42.$$

A line representing this equation is given in Fig. 3.2.2_1. It is based on observations of the temperature dependence of groundwater chemistry in geothermal areas as described by Michard *et al.* (1996). A similar line derived from thermodynamic data for feldspars from, for example, SUPCRT (Johnson *et al.*, 1992) would lie to the upper left of Michard's line.

Figure 3.2.2_1 shows that the Na/K ratio in recharge waters of both northern Switzerland and the Toki granite are relatively low and far below the equilibrium lines. The northern Swiss samples in Fig. 3.2.2_1 are shown in groups corresponding to their stage of evolution, as described by Michard *et al.* (1996), and illustrate that with increasing Cl content and residence time, the Na/K ratio increases and reaches equilibrium in several of the samples. These samples are of the most evolved waters, as indicated by their Cl and He contents.

The Na/K ratios of the highest Cl samples from the Toki granite also reach the equilibrium Na/K ratio but at much lower Cl contents and lower temperatures than any of the Swiss waters. Because of this low Cl, it seems unlikely the residence time of the water could have been long

enough for Na/K equilibrium to be achieved at such a low temperature. However, an alternate explanation - that the Na/K ratio is residual from a previous groundwater - also seems unlikely. As mentioned in the previous section, the Na/Cl ratio of the highest Cl samples is like that of seawater but as can be seen in Fig. 3.2.2_1 the Na/K ratio of seawater is quite different from any of the high Cl samples. Thus, for the moment, the Na/K ratio is tentatively accepted as indicating an advanced stage of water-rock interaction evolution in the high-Cl waters from DH-12.

3.3 Summary

The present study confirms the observations of Yusa *et al.* (1993), Iwatsuki and Yoshida (1999) and others that the basic chemical character of most groundwaters in the Tono region lies within a continuous compositional range bounded by Ca-HCO_3 and Na-HCO_3 type solutions. Magnesium concentrations in all the groundwaters are low. The anionic character of the waters is dominated generally by carbonate alkalinity, but SO_4 may also be important mainly in shallow groundwaters and in deeper sedimentary waters of the lower Toki formation.

Iwatsuki *et al.* (1995) and Iwatsuki and Yoshida (1999) point out that Na is enriched in Tono groundwaters relative to Ca as sampling depth increases. This observed trend implies a genetic relationship among the waters if depth and residence time are directly related. This appears to be the case for shallow flow systems in sedimentary formations of the Tono region because depth and residence time are related in these systems by local topography (Yanagizawa *et al.*, 1995; Iwatsuki *et al.*, 2000), and because Ca-rich groundwaters in alluvium and sediments of the Seto group are observed to become progressively enriched in Na and depleted in Ca as they migrate deeper into underlying formations of the Mizunami group. There is also evidence that the relative concentrations of Na and Ca are genetically related in the deeper regional flow system in the basement Toki granite, where Na contents are observed to increase at the expense of Ca as the apparent residence time of the groundwater increases. Other evidence directly contradicts this latter trend, however, which may indicate that depth and residence time are not simply correlated in the regional flow system.

The high-chloride waters sampled in borehole DH-12 are chemically distinct compared to the Ca-Na-HCO_3 waters discussed above. There are at least two possible explanations for the origin of these solutions: 1) they may evolve chemically from the Ca-Na-HCO_3 waters by water-rock interaction, or 2) they may be the product of mixing of Ca-Na-HCO_3 solutions with residual, connate formation fluids. Both possibilities are consistent with the regional hydrogeology of the area because DH-12 lies near the main discharge zone of the Toki River. The Na/K ratios of the high-Cl waters differ from that in seawater, which may suggest that these fluids either did not result from mixing with residual seawater or that their Na/K ratios are determined not only by mixing but also by water-rock interaction.

Granite groundwaters sampled using a multi-piezometer sampling apparatus in borehole DH-7 are also chemically distinct compared to both the Ca-Na-HCO_3 waters and high-Cl waters discussed above. These unusual solutions tend to be richer in Ca and poorer in carbonate alkalinity than other granite groundwaters. Although the possibility cannot be ruled out that these

differences in composition are sampling artifacts, it is possible that they reflect real differences in the respective chemistry of granite groundwaters flowing in conductive features of the regional flow system versus less mobile waters in the granite matrix and local fractures.

4 Empirical constraints on geochemical models

A number of groundwater chemical and isotopic parameters discussed in Sections 2 and 3 appear to be strongly correlated. Correlations involving two key parameters, the "master variables" Eh and pH, are examined in this section to deduce quantitative constraints on models of the evolution of these parameters in Tono groundwaters.

4.1 pH and the carbonate system

The pH of Tono groundwaters is strongly correlated with variations in the partial pressure of $CO_2(g)$. The correlation is shown in Fig. 4.1_1 for all shallow and deep groundwaters in the regional database (Table 2.1_1), and, for reasons discussed below, in Fig. 4.1_2 for groundwaters in the Toki granite. The data in the figures indicate that pH variations are closely correlated with variations in $P_{CO2(g)}$, and that this correlation holds over the entire range of measured pH and calculated $P_{CO2(g)}$ values. The likely explanation for this behavior is that primary minerals in the sedimentary rocks and granite are weathered by carbonate-bearing solutions, which thus tend to lose carbonate and become more alkaline as weathering progresses. If so, the extremely close correlation between pH and $P_{CO2(g)}$ shown in the figures suggests that the complex and possibly strongly coupled processes governing fluid flow and water-rock interaction in the Tono region are remarkably uniform on a regional scale.

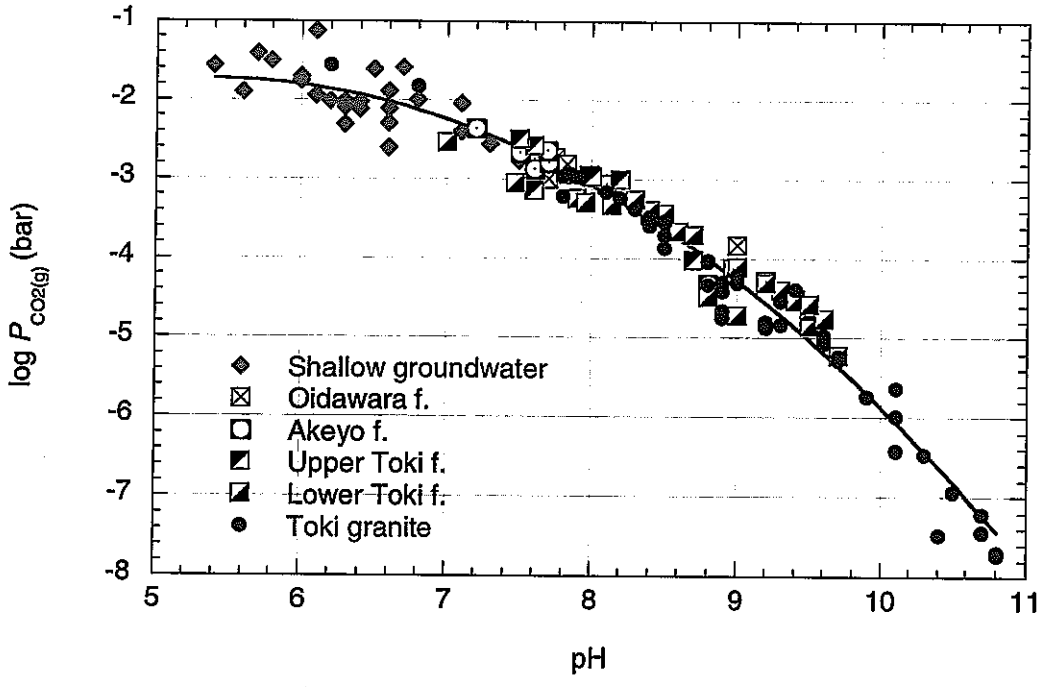

Figure 4.1_1. Plot showing the covariance of pH and $P_{CO2(g)}$ in groundwaters of sedimentary and granitic rocks of the Tono region. Best fit curve through the data is shown by the solid line.

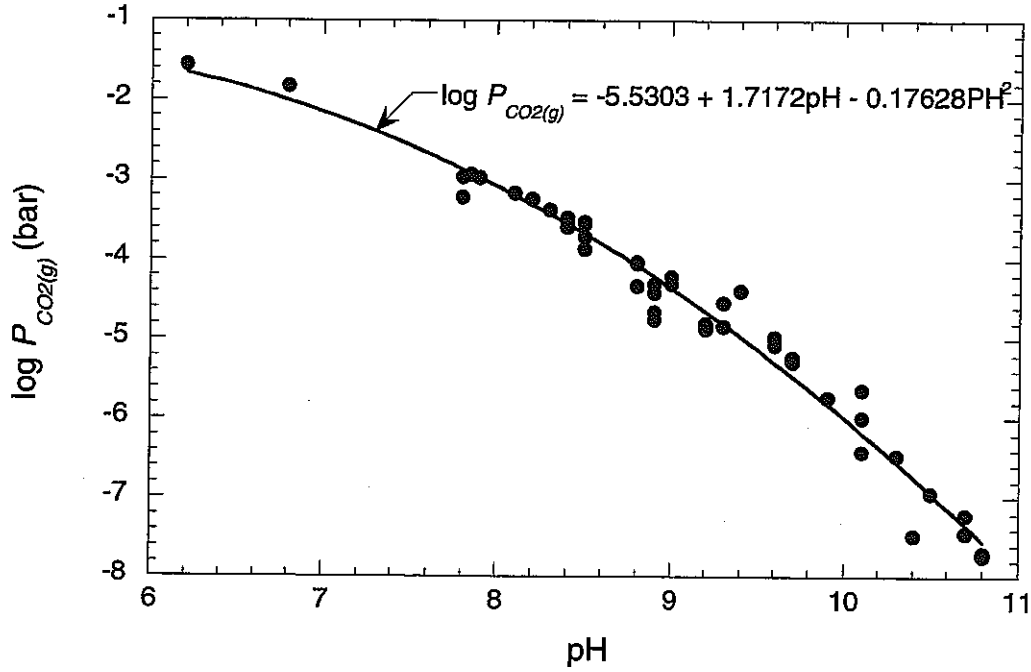

Figure 4.1_2. Correlation between pH and $P_{CO2(g)}$ in groundwaters of the Toki granite.

Figures 4.1_1 and 4.1_2 provide a framework for testing various hypotheses of processes controlling the pH-$P_{CO2(g)}$ evolution of Tono groundwaters. It appears, for example, that much of the covariance in the pH and $P_{CO2(g)}$ data can be explained using a highly simplified model of buffering by calcite. Calcite is a common equilibrium phase in most deep groundwater systems. The model assumes as a first approximation that calcite equilibrates with water at 25°C over a pH range from 6 to 11. Total dissolved carbonate concentrations are fixed by solubility equilibrium. Calcium concentrations are fixed by charge balance.

Figure 4.1_3 compares variations in pH and $P_{CO2(g)}$ calculated using the simple buffer model with measured pH and $P_{CO2(g)}$ values and the empirical best-fit curve shown in Fig 4.1_2. As can be seen, the model closely agrees with the analytical data if the pH is greater than about 7.9, but significantly overestimates $P_{CO2(g)}$ in two groundwater samples at lower pH. It is possible that calcite has not equilibrated with these relatively acidic groundwaters.

Corresponding Ca concentrations calculated using the model are compared with their analytical counterparts in Fig. 4.1_4. Although there is considerable scatter in the analytical data, most of these data agree with model predictions to within about an order of magnitude.

The good overall agreement between model predictions and analytical data suggests that even this highly simplified buffer model adequately captures much of the complex evolutionary processes controlling pH, $P_{CO2(g)}$ and Ca variations in the granite groundwaters. As can be seen by comparing Figs. 4.1_1 and 4.1_2, this preliminary conclusion also appears to be valid for many of the deep groundwaters in sedimentary formations of the Mizunami group.

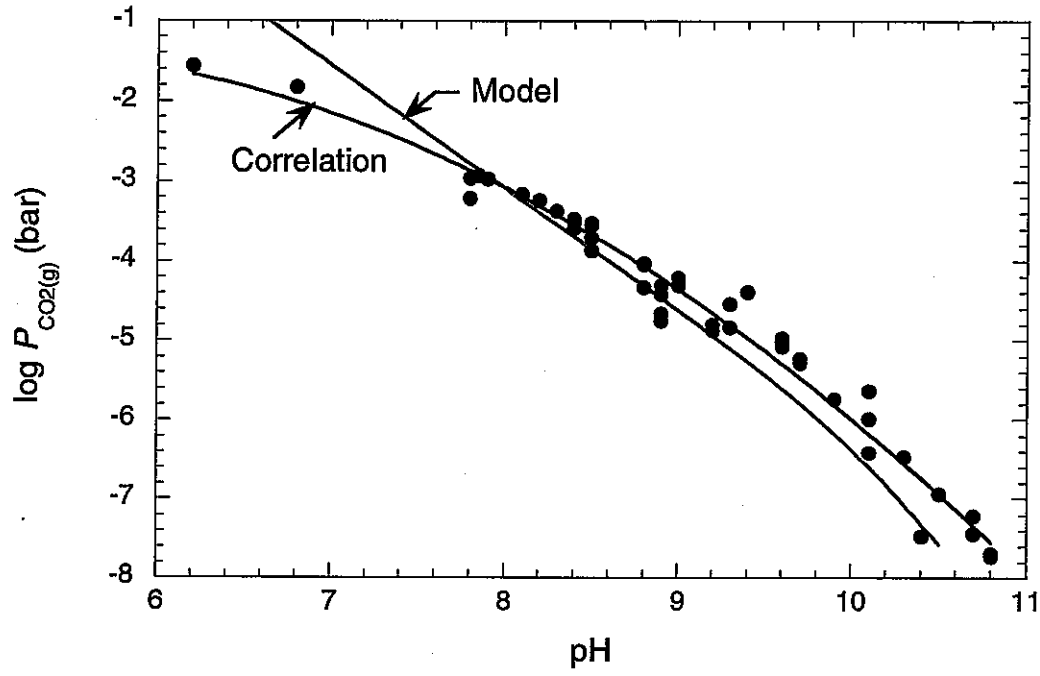

Figure 4.1_3. Comparison of modeled versus analytical pH and $P_{CO2(g)}$ values in granite groundwaters.

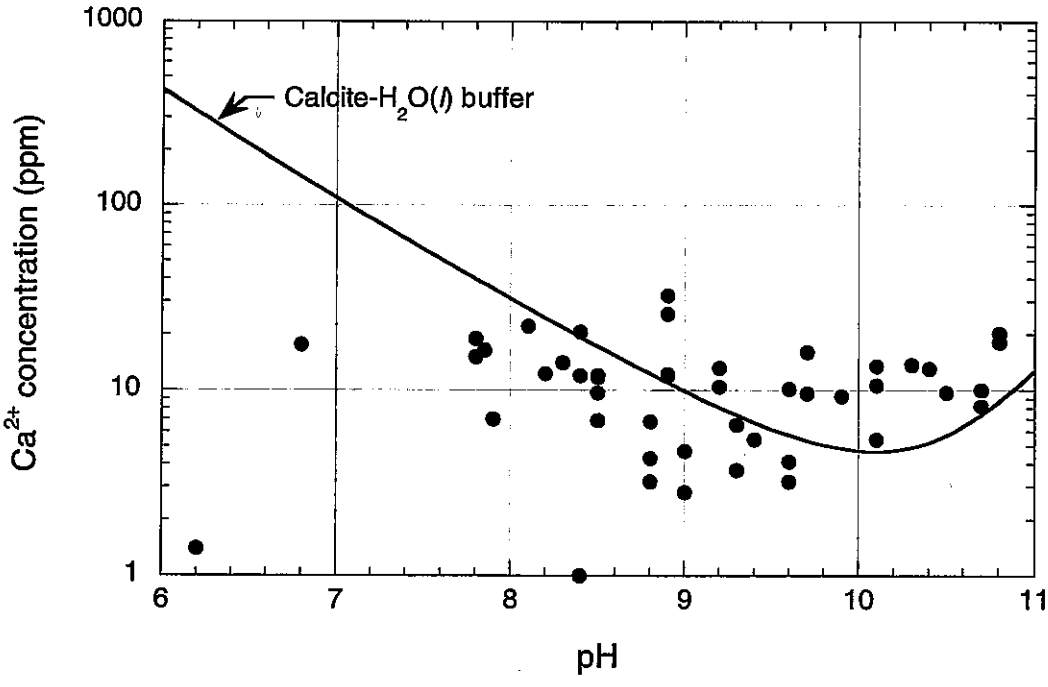

Figure 4.1_4. Comparison of modeled versus analytical Ca concentrations in granite groundwaters.

The preliminary conclusion that simple calcite buffering can explain much of the covariance in pH and $P_{CO2(g)}$ values observed in modern groundwaters of the Tono region suggests that the empirical correlations and best-fit curves shown in Figs. 4.1_1 and 4.1_2 may also be valid for paleo-groundwaters in this region. This is because the basic assumption of calcite equilibrium is as reasonable for the paleo-groundwater systems as it is for their modern counterparts. The implications of this key conclusion are examined in the following section.

5 Summary and conclusions

The long-term goal of the Tono Geochemical Research Project (TGRP) is to develop a quantitative geochemical modeling approach that can be used to help improve our understanding of groundwater evolution in the Tono area, and to evaluate the effects of human-induced disturbances on groundwater chemistry. Work carried out during FY02 includes efforts to establish quantitative constraints on the modeling approach that are consistent with empirical observations of hydrochemical conditions in the Tono region.

Three tasks were set up in FY 02 for this purpose. In the first task, the regional hydrochemical database for the Tono area was first updated and critically evaluated. The evaluation indicates that although the analytical quality of many of the groundwater samples is good, the quality of many other samples is rather poor(*i.e.,* exceeding the strictly acceptable range of 0 ± 5 %). A number of factors are apparently responsible for the poor charge balances. They include: 1) analytical errors (*e.g.,* of alkalinity), 2) errors arising from the use of IC values that are unrepresentative because CO_2 was gained by or lost from the sample during storage and (or) analysis, and 3) errors arising from the invalid assumption that non-carbonate contributions to the alkalinity of Tono groundwaters are always negligible.

The second task includes an examination of empircal trends among the chemical and isotopic parameters comprising the regional hydrochemical database. Results confirm previous observations that the basic chemical character of most groundwaters in the Tono region lies within a continuous compositional range bounded by Ca-HCO_3 and Na-HCO_3 type solutions. The trend of increasing Na relative to Ca with increasing sampling depth implies a genetic relationship among the waters if depth and residence time are directly related. This appears to be the case for shallow flow systems in sedimentary formations of the Tono region because depth and residence time are related in these systems by local topography, and because Ca-rich groundwaters in alluvium and sediments of the Seto group are observed to become progressively enriched in Na and depleted in Ca as they migrate deeper into underlying formations of the Mizunami group. There is also evidence that the relative concentrations of Na and Ca are genetically related in the deeper regional flow system in the basement Toki granite, where Na contents are observed to increase at the expense of Ca as the apparent residence time of the groundwater increases. Other evidence directly contradicts this latter trend, however, which may indicate that depth and residence time are not simply correlated in the regional flow system. The high-chloride waters sampled in borehole DH-12 are chemically distinct compared to the Ca-Na-HCO_3 waters discussed above. There are at least two possible explanations for the origin of these solutions: 1) they may evolve chemically from the Ca-Na-HCO_3 waters by water-rock interaction, or 2) they may be the product of mixing of Ca-Na-HCO_3 solutions with residual, connate formation fluids. Both possibilities are consistent with the regional hydrogeology of the area because DH-12 lies near the main discharge zone of the Toki River. The Na/K ratios of the high-Cl waters differ from that in seawater, which may suggest that these fluids either did not result from mixing with residual seawater or that their Na/K ratios are determined not only by mixing but also by water-rock interaction.

The third task involves an initial evaluation of geochemical models that are consistent with the identified empirical trends. Work on this task during FY02 examines two critically important parameters, Eh and pH, and also considers mineral indicators of Eh-pH conditions in paleo-groundwater. Results suggest that a co-precipitation approach used to deduce paleo-redox conditions based on the Fe(II) and U(VI) contents of late-stage fracture calcites is a promising tool, but results must be interpreted with caution. The main conclusions of the preliminary FY02 study, which is limited to deep groundwaters in the Toki granite, are that the inferred range of Eh-pH conditions for paleogroundwaters in the granite is nearly identical to that presently observed in deep, moderately reducing groundwaters. The deep redox chemistry of the regional hydrochemical system thus appears to be remarkably stable over time scales that are at least as long as the time required to flush moderately saline fluids, apparently present at the time of initial calcite precipitation, out of the granite. This consistency between paleo-redox and modern redox conditions constitutes a rigid constraint on regional hydrochemical models.

6 References

Balderer, W. and Lehmann, B. E. 1991. ^{3}He and ^{4}He. In: *Applied isotope hydrogeology - A case study in northern Switzerland* [F. J. Pearson, Jr., W. Balderer, H. H. Loosli, B. E. Lehmann, A. Matter, Tj. Peters, H. Schmassmann and A. Gautschi (eds.)]. Nagra TR 88-01, Nagra, Baden, Switzerland, 276-287.

Grimaud, D., Beaucaire, C. and Michard, G. 1990. Modelling of the evolution of ground waters in a granite system at low temperature: The Stripa ground waters, Sweden: *Appl. Geochem.*, 5, 515-525.

Hem, J. D. 1985. Study and interpretation of the chemical characteristics of natural water. 3rd ed., U. S. Geol. Survey Water-Supply Paper 2254.

Iwatsuki, T. and Yoshida, H. 1999. Groundwater chemistry and fracture mineralogy in the basement granitic rock in the Tono uranium mine area, Gifu Prefecture, Japan – Groundwater composition, Eh evolution analysis by fracture filling minerals. *Geochem. J.*, 33, 19 – 32.

Iwatsuki, T., Xu, S., Itoh, S., Abe, M. and Watanabe, M. 2000. Estimation of groundwater age in in the Tono research site, central Japan. *Nucl. Instr. Meth. Phys. Res., B*, 172, 524 – 529.

Iwatsuki, T., Metcalfe, R., Amano, K., Hama, K., Noda, N., Arthur, R. C. and Sasamoto, H. 2001a. Data book on groundwater chemistry in the Tono area. JNC TN 7450 2001-003, Japan Nuclear Cycle Development Institute, Tono Geoscience Center, Toki, Japan (draft report).

Iwatsuki, T., Xu, S., Mizutani, Y., Hama, K., Saegusa, H. and Nakano, K. 2001b. Carbon-14 study of groundwater in the sedimentary rocks at the Tono study site, central Japan. *Applied Geochem.*, 16, 849 – 859.

JNC, 2000. H12: Project to establish the scientific and technical basis for HLW disposal in Japan – Supporting report 1: Geological environment in Japan. JNC TN 1400 2000-002, Japan Nuclear Cycle Development Institute, Tokai-Mura, Ibaraki, Japan.

JNC, 1999. DH-7 borehole report. JNC TJ744 99-025 vol. I. Japan Nuclear Cycle Development Institute, Tono Geoscience Center, Toki, Japan (in Japanese).

Johnson, J. W., Oelkers, E. H. and Helgeson, H. C. 1992. SUPCRT92 - A software package for calculating the standard molal thermodynamic properties of minerals, gases, aqueous species, and reactions from 1-bar to 5000-bar and 0 to 1000-degrees-C: *Computers & Geosciences*, 18, 899-947.

Koide, K., Sugihara, K., Yoshida, H., Seo, T. and Yanagizawa, K. 1996. Current state of geoscientific studies in and around the Tono mine in Japan. Proc. Internat. Conf. Deep Geological Disposal of Radioactive Waste, Winnipeg, Manitoba. 7-19 – 7-29.

Lampén, P. and Snellman, M. 1993. Summary report on groundwater chemistry. Report YJT 93-14. Nuclear Waste Commission of Finnish Power Companies, Helsinki, Finland.

Laaksoharju, M. 1999 Groundwater characterization and modelling: problems, facts and possibilities. SKB TR 99-42, Swedish Nuclear Fuel and Waste Management Co., Stockholm, Sweden.

Langmuir, D. 1997. *Aqueous Environmental Geochemistry.* Prentice-Hall, New Jersey, 600p.

McEwen, T. and Äikäs, T. 2000. The site selection process for a spent fuel repository in Finland – Summary report. Report Posiva 2000-15, Posiva Oy, Helsinki, Finland.

Michard, G. 1987. Controls of the chemical composition of geothermal waters. In: *Chemical transport in metasomatic processes* [H. C. Helgeson (*ed.*)]: Proceedings of the NATO Advanced Study Institute on Chemical Transport in Metasomatic Processes, Corinthia and the Cycladic Islands, Greece, Dordrecht, Holland, D. Reidel Publishing Co., NATO Advanced Study Institutes Series. Series C; Mathematical and Physical Sciences, 218, 323-353.

Michard, G., Pearson, F. J. Jr. and Gautschi, A. 1996. Chemical evolution of waters during long term interaction with granitic rocks in northern Switzerland. *Appl. Geochem.*, 11, 757-774

Nordstrom, D. K., Smellie, J. A. T and Wolf, M. 1990. Chemical and isotopic composition of groundwaters and their seasonal variability at the Osamu Utsumi mine and Morro do Ferro analogue study sites, Poços de Caldas, Brazil. NTB 90-24, Nagra, Baden, Switzerland.

Nordstrom, D. K., Andrews, J. N., Carlsson, L., Fontes, J. Ch., Fritz, P., Moser, H. and Olsson, T. 1985. Hydrogeological and hydrogeochemical investigations in boreholes: Final report of the phase I geochemical investigations of the Stripa groundwaters: Nagra TR 85-56, Nagra, Baden, Switzerland.

Nordstrom, D. K., Ball, J. W., Donahoe, R. J. and Whittemore, D. 1989. Groundwater chemistry and water-rock interactions at Stripa: *Geochim. Cosmochim. Acta*, 53, 1727-1740.

Pitkänen, P., Snellman, M., Vuorinen, U., Leino-Forsman, H. 1996. Geochemical modelling study of the age and evolution of the groundwater at the Romuvaara site. Report Posiva 96-06, Posiva Oy, Helsinki, Finland.

Pitkänen, P., Luukkonen, A., Ruotsalainen, P. Leino-Forsman, H. and Vuorinen, U. 1999. Geochemical modelling of groundwater evolution and residence time at the Olkiluoto site. Report Posiva 98-10, Posiva Oy, Helsinki, Finland.

Pitkänen, P., Luukkonen, A., Ruotsalainen, P. Leino-Forsman, H. and Vuorinen, U. 2001. Geochemical modelling of groundwater evolution and residence time at the Hästholmen site. Report Posiva 2001-01, Posiva Oy, Helsinki, Finland.

Piper, A. M. 1944. A graphic procedure in the geochemical interpretation of water analyses. *Am. Geophys. Union Trans.*, 25, 914 – 923.

Saegusa, H., Inaba, H., Koide, K. and Ogata, N. 1997. Simulation of regional scale groundwater flow in the Tono area. Proceedings of the annual meeting of the Chubu branch of the Japan Society of Engineering Geology, 1-4, (in Japanese).

Smellie, J. and Laaksoharju, M. 1992. The Äspö hard rock laboratory: final evaluation of the hydrogeochemical pre-investigations in relation to existing geologic and hydraulic conditions. SKB TR 92-31, Swedish Nuclear Fuel and Waste Management Co., Stockholm, Sweden.

Stumm, W. and Morgan, J. J. 1996. *Aquatic Chemistry.* 3rd ed. John Wiley & Sons, New York, 1022p.

Wittwer, C. 1986. Probenahmen und chemische analysen von grundwässern aus den sondierbohrungen. NTB 85-49, Nagra, Baden, Switzerland.

Wolery, T. 1992. EQ3NR, A computer program for geochemical aqueous speciation-solubility calculations: Theoretical manual, user's guide, and related documentation. UCRL-MA-110662 PT III, Lawerence Livermore National Laboratory, Livermore, CA.

Yusa, Y., Ishimaru, K., Ota, K. and Umeda, K. 1993. Geological and geochemical indicators of paleohydrogeology in Tono uranium deposits, Japan. In: *Paleohydrogeological methods and their applications.* Proc. NEA Workshop, Paris, 9 – 10 November 1992. OECD, Paris, 117 – 146.